2015-06

# Analysis of graphite oxide and graphene as enhancers for NATO F-76 diesel fuel

Carroll, Benjamin O.

Monterey, California: Naval Postgraduate School


# NAVAL POSTGRADUATE SCHOOL

**MONTEREY, CALIFORNIA**

# THESIS

**ANALYSIS OF GRAPHITE OXIDE AND GRAPHENE AS ENHANCERS FOR NATO F-76 DIESEL FUEL**

by

Benjamin O. Carroll

June 2015

Thesis Advisor: Claudia Luhrs
Thesis Co-Advisor: Douglas Seivwright

THIS PAGE INTENTIONALLY LEFT BLANK

# REPORT DOCUMENTATION PAGE

*Form Approved OMB No. 0704–0188*



| **1. AGENCY USE ONLY** *(Leave blank)* | **2. REPORT DATE** June 2015 | **3. REPORT TYPE AND DATES COVERED** Master's Thesis |
|---|---|---|

**4. TITLE AND SUBTITLE**
ANALYSIS OF GRAPHITE OXIDE AND GRAPHENE AS ENHANCERS FOR NATO F-76 DIESEL FUEL

**5. FUNDING NUMBERS**

**6. AUTHOR(S)** Benjamin O. Carroll

**7. PERFORMING ORGANIZATION NAME(S) AND ADDRESS(ES)**
Naval Postgraduate School
Monterey, CA 93943-5000

**8. PERFORMING ORGANIZATION REPORT NUMBER**

**9. SPONSORING /MONITORING AGENCY NAME(S) AND ADDRESS(ES)**
N/A

**10. SPONSORING/MONITORING AGENCY REPORT NUMBER**

**11. SUPPLEMENTARY NOTES** The views expressed in this thesis are those of the author and do not reflect the official policy or position of the Department of Defense or the U.S. Government. IRB Protocol number ____N/A____.

**12a. DISTRIBUTION / AVAILABILITY STATEMENT**
Approved for public release; distribution is unlimited

**12b. DISTRIBUTION CODE**

**13. ABSTRACT (maximum 200 words)**

The aim of this thesis was to test the performance of graphite oxide (GO) and graphene (G) as fuel additives. Both compounds are variations of the honeycomb structure found in graphite but possess higher surface areas and different amounts of oxygen functional groups. The use of graphite oxide was considered due to its ability to release the oxygen species at moderate temperatures, while graphene could be readily dispersed and completely burned off during the combustion process. Graphite oxide was fabricated by chemical routes and graphene by thermal exfoliation. X-ray powder diffraction was used to characterize the crystal structure of the initial powders and the particulate sizes were studied by scanning electron microscopy. The additives were mixed with NATO F-76 diesel fuel in 0.1 to 3% weight ratios. The mixtures were then analyzed by differential scanning calorimetry and thermogravimetry to determine heat flows and mass changes, respectively, as the samples were heated, then compared with bare F-76. The evolved gases from all the processes were identified by mass spectroscopy. The fuel-additive mixtures were tested in a diesel engine to determine ignition delays and the cetane numbers for each composition are reported.

**14. SUBJECT TERMS**
graphite oxide, graphitic oxide, graphene, F-76, diesel, diesel engine, cetane, combustion, and propellant.

**15. NUMBER OF PAGES**
115

**16. PRICE CODE**

| **17. SECURITY CLASSIFICATION OF REPORT** | **18. SECURITY CLASSIFICATION OF THIS PAGE** | **19. SECURITY CLASSIFICATION OF ABSTRACT** | **20. LIMITATION OF ABSTRACT** |
|---|---|---|---|
| Unclassified | Unclassified | Unclassified | UU |

NSN 7540–01-280-5500

Standard Form 298 (Rev. 2–89)
Prescribed by ANSI Std. 239–18

THIS PAGE INTENTIONALLY LEFT BLANK

**Approved for public release; distribution is unlimited**

# ANALYSIS OF GRAPHITE OXIDE AND GRAPHENE AS ENHANCERS FOR NATO F-76 DIESEL FUEL

Benjamin O. Carroll
Lieutenant, United States Navy
B.S., The Citadel, 2009

Submitted in partial fulfillment of the
requirements for the degree of

**MASTER OF SCIENCE IN MECHANICAL ENGINEERING**

from the

**NAVAL POSTGRADUATE SCHOOL**
**June 2015**

Author: Benjamin O. Carroll

Approved by: Claudia Luhrs
Thesis Advisor

Douglas Seivwright
Thesis Co-Advisor

Garth Hobson
Chair, Mechanical and Aerospace Engineering Department

THIS PAGE INTENTIONALLY LEFT BLANK

# ABSTRACT

The aim of this thesis was to test the performance of graphite oxide (GO) and graphene (G) as fuel additives. Both compounds are variations of the honeycomb structure found in graphite but possess higher surface areas and different amounts of oxygen functional groups. The use of graphite oxide was considered due to its ability to release the oxygen species at moderate temperatures, while graphene could be readily dispersed and completely burned off during the combustion process. Graphite oxide was fabricated by chemical routes and graphene by thermal exfoliation. X-ray powder diffraction was used to characterize the crystal structure of the initial powders and the particulate sizes were studied by scanning electron microscopy. The additives were mixed with NATO F-76 diesel fuel in 0.1 to 3% weight ratios. The mixtures were then analyzed by differential scanning calorimetry and thermogravimetry to determine heat flows and mass changes, respectively, as the samples were heated, then compared with bare F-76. The evolved gases from all the processes were identified by mass spectroscopy. The fuel-additive mixtures were tested in a diesel engine to determine ignition delays and the cetane numbers for each composition are reported.

THIS PAGE INTENTIONALLY LEFT BLANK

# TABLE OF CONTENTS

# LIST OF FIGURES

# LIST OF TABLES

THIS PAGE INTENTIONALLY LEFT BLANK

# LIST OF ACRONYMS AND ABBREVIATIONS

| | |
|---|---|
| ° C | degrees Celsius |
| ° F | degrees Fahrenheit |
| AOP | angle of peak pressure |
| BTC | before top dead center |
| CAD | crank angle degrees |
| CNT | carbon nanotubes |
| CO | carbon monoxide |
| CO2 | carbon dioxide |
| DI | deionized |
| DSC | differential scanning calorimetry |
| DOD | Department of Defense |
| DON | Department of the Navy |
| G | graphene |
| GO | graphite oxide |
| FGS | functionalized graphene sheets |
| H2O | water |
| H2O2 | hydrogen peroxide |
| H2SO4 | sulfuric acid |
| H3PO4 | phosphoric acid |
| HCl | hydrochloric acid |
| inHg | inches of mercury |
| JCPDS | Joint Committee on Powder Diffraction Standards |
| KMnO4 | potassium permanganate |
| LHV | lower heating value |
| MnO2 | manganese oxide |
| MS | mass spectrometry |
| MSDS | Material Safety Data Sheet |
| NATO | North Atlantic Treaty Organization |
| NO | nitric oxide |

| | |
|---|---|
| NO2 | nitrogen dioxide |
| NPS | Naval Postgraduate School |
| PP | peak pressure |
| SO2 | sulfur dioxide |
| SO3 | sulfur trioxide |
| QMS | quadrupole mass spectrometer |
| RPM | revolutions per minute |
| SCCM | standard cubic centimeters per minute |
| SECNAV | Secretary of the Navy |
| SEM | scanning electron microscopy |
| STA | simultaneous thermal analysis |
| TDC | top dead center |
| TGA | thermogravimetric analysis |
| XRD | x-ray diffraction |

# ACKNOWLEDGMENTS

Completion of this thesis research would have been impossible without the help of several NPS professors. First, and foremost, to Professor Claudia Luhrs: your guidance and patience were extremely helpful when I was in the tight spots, and I appreciate your willingness to drop everything you were doing to provide direction for this research. To my co-advisor, Professor Doug Seivwright: your countless hours during and after the work day, as well as the many weekends spent working on the diesel engine to make the meat of this research possible, is very appreciated. To Professor Sarath Menon: You gave so much time to setting up the lab equipment and to helping me characterize my samples. Without your knowledge and guidance, my research would have been impossible. Lastly, to Professor Sanjeev Sathe: You taught me to fail early, to step outside the box, and to ask the hard questions. Your guidance granted me the ability to believe that nothing is impossible with perseverance and seeing success beforehand.

I would also like to thank many of my colleagues who contributed in many ways to the completion of my thesis: LTs Ryan Bohning and Robert “Bob” Riley, who provided their knowledge of thermodynamics where mine was lacking; LCDR Jonathan Gandy, LT Natalie Jenkins, and LT Eid “Eddie” Fakhouri, who listened to my many frustrations and provided YouTube videos to give me a good laugh; and, lastly, our Materials Science cohort, MAJ Rene Delafuente, and LTs Karima Greenaway, Ervin “Erv” Mercado, and William “Will” Curtin. You guys were the best group of friends to work with throughout our materials theses.

Finally, I would like to thank my wonderful wife, Lisa. As a naval officer here at NPS who also finished her thesis at the same time as I, she never complained about my many hours spent working on my thesis after our daughter, Emmy, went to bed, or the many late nights and weekends spent at school while she cared for the home front. We juggled our time to allow each other the opportunity to complete our research for our theses while also raising our lovely daughter. I could not have asked for a better wife or mother to our children (our second daughter, Autumn, is due this September)!

THIS PAGE INTENTIONALLY LEFT BLANK

# I. INTRODUCTION AND MOTIVATION

The Department of the Navy (DON) recognizes its heavy reliance on petroleum [1]. In order to move toward a more energy-efficient organization, the United States Navy and Marine Corps have initiated its efforts to improve their energy conservation [1]–[4]. This study provides propulsion research and analysis that brings insight into possibilities to make such improvements. This gave motivation to study drop-in additives as enhancers to NATO F-76 diesel fuel, specifically two additives: graphite oxide (GO) and graphene (G). These materials have been shown to experience exothermic reactions during heating, which then begs the answer to the question: What effects will these additives in F-76 have on the performance and characteristics of the fuel?

Through experimentation, GO and G were mixed in various ratios with F-76 to analyze and compare the exothermic reactions against F-76 alone. Complete characterization of the additives was conducted, while the fuel mixtures' energy and mass changes were studied through calorimetry and thermogravimetric analysis (TGA), respectively.

Further research to determine combustive characteristics and cetane number was conducted on the fuel mixtures through outside contracting and via onsite diesel engine testing. Large quantities of several fuel mixtures were prepared to study such parameters as cetane number and energy output during combustion, to name a couple. These tests allowed the comparison of standard and modified diesel fuels to be tested in an actual setting for which these fuels were meant to operate.

## A. DEPARTMENT OF THE NAVY JUSTIFICATION

Secretary of the Navy (SECNAV), the Honorable Ray Mabus, set forth five DON energy goals in 2009 to reach by year 2020; the goals aim to reduce the DON's environmental fingerprint and increase its energy independence [5]:

- Energy Efficient Acquisition: Evaluation of energy factors will be mandatory when awarding contracts for systems and buildings.
- Sail the "Great Green Fleet" [6]: DON will demonstrate a Green Strike Group capable of using advanced biofuel blends, nuclear power, and employing energy saving methods in local operations by 2012 and sail it by 2016.
- Reduce Non-Tactical Petroleum Use: By 2015, DON will reduce petroleum use in the commercial fleet by 50%.
- Increase Alternative Energy Ashore: By 2020, DON will produce at least 50 % of shore-based energy requirements from alternative sources. These include, but not limited to, such sources as wind, solar, geothermal, wave energy, tidal currents, nuclear energy, and biofuels derived from algae, camelina, and other feedstocks [7].
- Increase Alternative Energy Use DON-Wide: By 2020, 50% of total DON energy consumption will come from alternative sources [7].

Regarding the production and use of "alternative sources" stated in the last two energy goal bullets previously mentioned; such alternative sources "must be 'drop in' replacements, able to mix with traditional petroleum products with no adverse effects to the fuel quality." Furthermore, the DON mandates alternatives have lower life cycle greenhouse gas emissions than conventional petroleum-based fuels. These requirements added to the motivation to study GO and G as drop-in additives to F-76.

## B. ALTERNATIVE SOURCE CONSIDERATIONS

While the SECNAV mandates that alternative sources must be drop-in replacements, there are considerations that the DON must overcome in order to transition into a more energy efficient entity amongst petroleum users in the world. Among these considerations include technology maturity, resource availability, and alternative fuel availability. As technology matures, the DON must leverage leading-edge advances in technology and deploy them in the tactical and shore arenas [7].

Thus, far, research into alternatives has included the Green Hornet flight [7], [8], the Great Green Fleet demonstration [6], and studies involving additives in thermite mixtures [9]. Earth Day 2010 marked a significant milestone in fuel alternative studies as the DON successfully launched a F/A-18 Super Hornet using a 50/50 blend of conventional jet fuel and a biofuel derived from camelina (a hardly U.S.-grown plant that

can thrive in the harshest of soils). The 50/50 blend made absolutely no difference in performance of the fighter, which displayed its capabilities at speeds including supersonic. During the July 2012 Rim of the Pacific exercise, the largest international maritime exercise, United States participants including an aircraft carrier and its air wing, a cruiser, two destroyers, and an oiler, nicknamed the 2012 Great Green Fleet, demonstrated successful performance of drop-in replacement advanced biofuel blends (50/50 blends made from cooking oils or algae mixed with petroleum: HRD-76 and HRJ-5) and other energy efficient technologies in an operational setting. All systems performed at full capacity. Lastly, the Mechanical Engineering Department at the Naval Postgraduate School (NPS) has researched drop-in additives (graphite oxide [GO] and graphene [G]) in solid propellants to study thermite reactions. Conclusions from research showed significant increases in exothermic reactions when compared to the solid propellants without the additives [9]. The next step is to consider these two additives in liquid fuels used by the DON.

## C. GRAPHITE OXIDE

GO, seen in Figure 1, is a carbonaceous, solid material with approximately half its weight composition containing two-dimensional sheets of carbon atoms arranged in a hexagonal pattern while the other half contains oxygen groups such as epoxy, carboxyl, and hydroxyl (see Figure 2). It is light brown initially, but due to its hydrophilic nature it often absorbs moisture and becomes dark brown in color. It can also be described as having a powdery consistency and texture.

GO has interesting properties[10]–[16], namely that it acts as an insulator, like a semiconductor [17], it is a candidate for reverse osmosis water purification because of its permeability to water and water vapor and impermeability to other substances [15], and it has the ability to readily release its oxygen groups [9], [18]. For these characteristics, but also because it is easy to be generated from graphite nanopowder, it proves to be a cost-effective and convenient method for graphene synthesis (which is the second material studied) [19]. For its energy releasing potential in inert atmospheres as shown through research conducted at the NPS by LT Nicholas Vilardi [9], GO was selected as the first

material to research as an enhancer to F-76. GO's structure contains roughly 50% oxygen groups; when introduced to heat, it is believed to release these groups from its structure. This could enhance combustion of F-76 by increasing burn rates and lower ignition temperatures, as Sabourin *et al.* suggest with the use of colloidal dispersions to facilitate enhanced ignition and combustion [20]. They also suggest the use of other similar colloidal particles to enhance cetane numbers and fuel economy of automotive diesel fuels, only further justifying the use of GO as a drop-in additive to NATO F-76 diesel fuel.

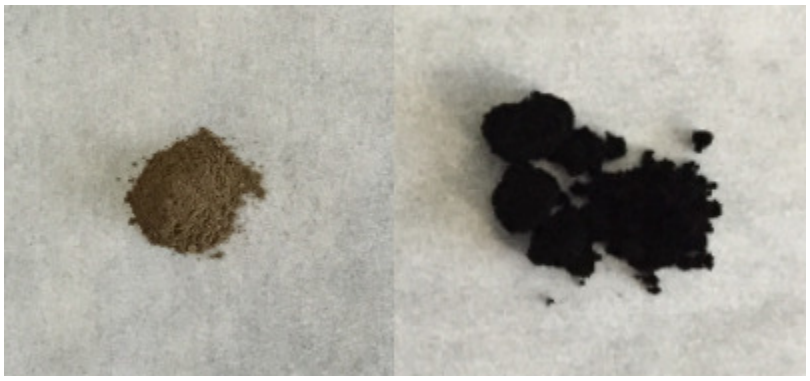

Figure 1. Graphite Oxide Nanopowder (Left Side), Graphene Nanopowder (Right Side)

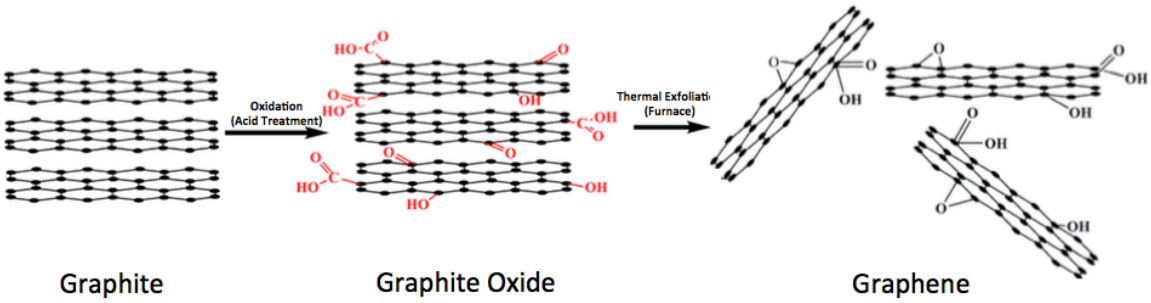


Figure 2. Process of Oxidation of Graphite to Synthesize GO, and of Thermal Exfoliation of GO to Synthesize G, after [21].

## D. GRAPHENE

Graphene, pictured right in Figure 1, is a very light and fluffy black powder and is carbonaceous as it is synthesized through thermal exfoliation of GO (see Figure 2). As with GO, G contains sheets of honeycomb-structured carbon atoms. These sheets, unlike GO, are not arranged on top of each other such that they run parallel, but seem to have no order in their arrangement.

There have been numerous studies of G due to its extensive electrical, optical and mechanical properties [22]–[29]. Moreover, there have been recent studies of the thermal properties of G as an additive to enhance thermite reactions [9] and of a graphene-like material known as functionalized graphene sheets (FGS) as colloidal dispersions in liquid propellant combustion [20]. These studies, as well as those of A. Balandin [30], suggest that G has a high thermal conductivity, which directly relates to increased combustion reactions, which makes G a prime candidate as and enhancer for F-76.

## E. NATO F-76 (PROPELLANT)

As the medium for which GO and G would be dispersed, NATO F-76 diesel fuel was chosen because many systems that operate within the DON use it. It only made sense to use F-76 such that the additives could simply be “dropped into” the fuel and be used in existing systems without further expenses past the cost of the additive.

F-76, a bright, transparent-yellow diesel fuel that is free of visual particulates (see Figure 3), is characterized by parameters distributed for use by all departments and agencies in the Department of Defense (DOD) [31], as well as safety parameters provided in a Material Safety Data Sheet (MSDS) [32]. Of those parameters, F-76 should have a minimum cetane number of 42 on a scale from 0 to 100 [31]. Cetane number relates to the ignition delay of diesel fuel. This ignition delay is determined by the time it takes between fuel injection into the cylinder and the first identifiable pressure increase due to combustion. It is believed that increasing the cetane number can reduce pollutant emissions, provide a more complete combustion, avoid difficulties in an engine, such as cold-starting, and increased combustions characteristics at large loads [33]–[36].

Figure 3. NATO F-76 Diesel Fuel

## F. INDICATIONS OF ADDITIVE REACTIONS IN PROPELLANT

Characterization of the additives and fuel/additive mixtures is necessary in order to determine the effectiveness they may or may not have when combined with the F-76. This research studies parameters such as energy output from calorimetric research and mass reduction from thermogravimetric analysis in the lab, cetane number characteristic of select fuel mixtures, and raw data from our onsite diesel engine which allows calculations of ignition delay, cylinder crank angle, pressure, and heat of release during combustion. To elaborate on a few of these parameters, cetane number is an indication of the combustion speed of a diesel fuel. The higher the number, the faster the fuel will ignite, which brings up ignition delay. Ignition delay is the time duration between the start of ignition of the fuel and the start of combustion of the fuel. By raising the cetane number, it is likely that ignition delay is shortened, thereby creating quicker and more complete combustion. In order to determine this parameter, we will have to collect data directly from the diesel engine such as the pressure and strain inside the cylinder during a complete cycle. A complete cycle, while referring to crank angle degrees of each cylinder of a two-stroke engine, evident in Figure 4, begins with the compression stroke as exhaust from a previous cycle is released while in taking new air (180° and -180°, respectively), and as it travels upward, the air is compressed and super heated. Before top dead center (0°), fuel is injected and mixed and combustion begins thereafter, and the power stroke begins and ends with the start of the next compression cycle. During this

travel, heat of release data, which in turn relates to energy output of the fuel combustion, is collected to study the effects the fuels will have on the engine.

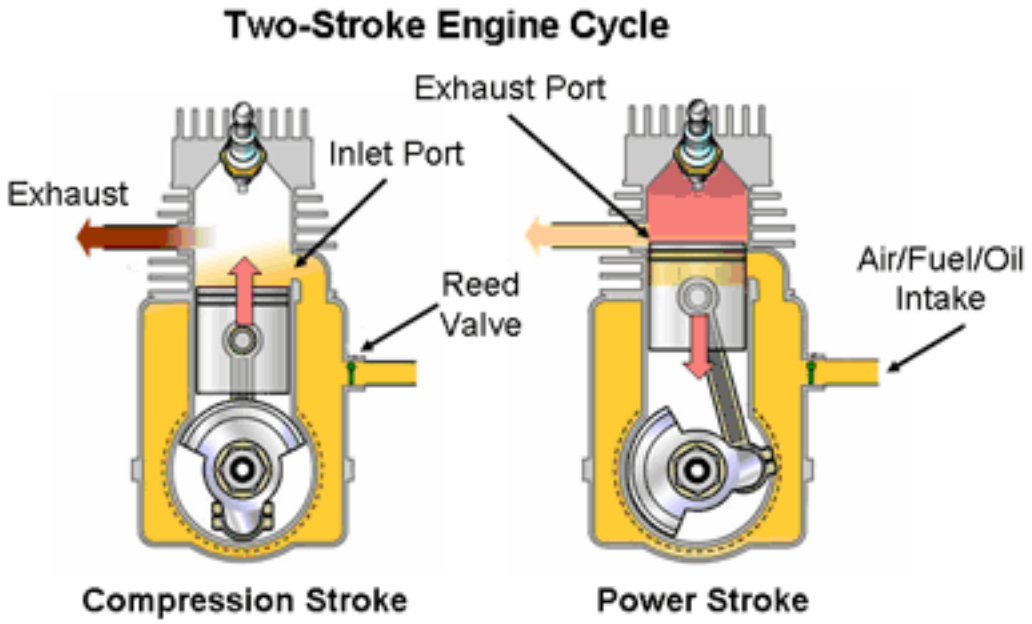


Figure 4. Cylinder Cycle of Two-Stroke Diesel Engine, from [37]

## G. SUMMARIZED HYPOTHESIS

The use of GO and G as additives in NATO F-76 allowed for several hypotheses:

- GO: Given that GO contains oxygen groups, it might enhance F-76 by increasing the oxygen in the fuel/air mixture for a more complete combustion. GO/F-76 mixtures might have the potential to decrease ignition delays, which would increase cetane number.
- G: Adding G to F-76 might increase cetane number of F-76 by increasing the amounts of gases released during the combustion reactions.
- Both Additives: GO and G introduced in F-76 have potential as to increase energy output (in the form of heat) during combustion compared to F-76 with no additives.

## H. THESIS OUTLINE

The body of this thesis describes in detail the experimental methods, analysis, and results conducted in order to prove/disprove the hypotheses stated in Section E.

Chapter II explains the experimental methods used to study F-76, GO and G. These include conditions for laboratory analysis such as the synthesis of GO and G, as well as, X-Ray diffraction (XRD), scanning electron microscopy (SEM), differential scanning calorimetry (DSC), thermogravimetric analysis (TGA), and mass spectrometry (MS) of fuel mixtures of F-76 with GO and with G in various quantities. Also explained are the methods used to study large quantities of select GO and G fuel mixtures in a diesel engine and their characteristic properties compared to F-76 without additives.

Chapter III lists and explains the results gathered from each of the laboratory experiments conducted and from tests used to characterize the fuel mixtures in a diesel engine.

The conclusion is Chapter IV, which provides a summary of the work conducted, the findings and the outcomes of the hypotheses, and recommendations for future research.

# II. EXPERIMENTAL METHODS

This chapter discusses the equipment and methods used to fabricate and analyze graphite oxide and graphene as enhancers in NATO F-76. It will also introduce the protocols employed to characterize the materials and test the diesel mixtures.

## A. GENERATION OF ADDITIVES AND FUEL MIXTURES

In order to test the hypotheses stated in Chapter I, Section 3, the precursors, graphite oxide and graphene, needed to be generated in our NPS laboratories. The costs of commercial GO and G are much higher than the cost of producing them from graphite flakes. In fact, ACS Material sells GO in 1.0-gram batches for $180 and 500-mg batches of graphene for $360 [38], [39]. To produce GO in-situ, 1.0 gram of GO only costs approximately $75 and no additional costs related to reactants are ensued to produce graphene (see Table 7 in Appendix A). Moreover, those products when provided by a commercial firm are commonly delivered as a solid dispersed in liquid media (approximately 2mg/ml of GO in water per ACS Material) requiring further drying or separation steps to be taken, making our process seem as a more viable start point [38], [39]. Fabricating GO and G directly also allowed us to control their quality.

### 1. Graphite Oxide

This section describes the method used to synthesize GO, which is based on the original synthesis of GO by Hummers' Method [40] and on modifications to the method reported by Marcano *et al.* [41]. The GO production was performed by the oxidation of graphite using a mixture of acids, potassium permanganate and hydrogen peroxide. The resulting GO solid was then washed to remove other byproducts. Table 1 lists the chemicals used for the synthesis of GO, as stated in the following paragraphs.

Table 1. Chemicals/Materials Used for GO Synthesis

| Chemical/Material | Specifics | Catalog # | Quantity Required |
|---|---|---|---|
| Graphite Nanopowder | Sigma-Aldrich, <20μm, synthetic | 282863-25G | 0.75g |
| H2SO4 | Sigma-Aldrich, 95.0-98.0% ACS Reagent | 258105-500ML | 90ml |
| H3PO4 | Sigma-Aldrich, >85.0wt% ACS Reagent | 438081-500ML | 10ml |
| KMnO4 | Mallinckrodt Baker Inc., ACS Reagent | 3227-01 | 4.5g |
| H2O2 | Sigma-Aldrich, 30.0wt% in H2O, ACS Reagent | 216763-500ML | 1.5ml |
| DI Water * | Essential Wholesale | 100713KF | 270ml |
| HCl * | Sigma-Aldrich, 37.0% ACS Reagent | 320331-500ML | 360ml |
| Ethanol * | Sigma-Aldrich, >99.5% ACS Reagent, 200 proof absolute | 459844-500ML | 360ml |
| * The amounts used were dependent on the transparency of supernatant liquid. | | | |

The graphite nanopowder was treated with 90 mL $H_2SO_4$ and 10 mL $H_3PO_4$. The mixture was then sonicated for one minute to create homogenous dispersion using an ultrasonic cleaner (see Figure 5, left-side) at room temperature. Placing the mixture on a magnetic stirrer and hotplate, a Spinbar magnetic stir bar was gently placed inside the mixture and set at 240 RPMs to allow continuous homogenous dispersion (see Figure 6, left-side). The $KMnO_4$ was added next, which caused an exothermic reaction to take place. At this point, it was necessary to allow the mixture to continually stir for a five-and-a-half-hour period under a vent hood. Once the required time period had elapsed, ice cubes frozen from 150 mL of distilled water were added to the mixture and allowed to dissolve. Once the cubes were fully dissolved, the $H_2O_2$ was added drop-wise. As the drops were added, bubbles were observed and increased as more drops were added due to an exothermic reaction of the mixing. Once all drops were added, the mixture was allowed to continue stirring for an additional hour, and then the mixture was left to settle

overnight. The GO particulates settled at the bottom of the beaker (an olive drab-type color), separated from the supernatant liquid on top (a deep purple-black color). The excess liquid was carefully pipetted and properly discarded, while the remaining solid material, still dispersed in small amounts of liquid, was divided into six 50 mL centrifuge tubes. Using the centrifuge in Figure 5 (right side), the tubes were rotated at 2200 RPMs for five minutes, the excess liquid was carefully removed and the remaining solid (GO) washed as described below.

The solid GO was sequentially dispersed and washed in three reagents (DI water, HCl and ethanol), each time sonicating it to disperse the particulates and then using the centrifuge to separate the supernatant liquid with dissolved byproducts from the solid GO. The first washing required adding 20 mL of deionized water to the particulates left over in each tube. After being sonicated for approximately one minute for homogenous mixing, the tubes were placed into the centrifuge at the same settings as in the previous procedure. This was only done once, and the excess liquid was drained. The second reagent was HCl. We added 20 mL of HCl solution to the particulates and followed the same steps as with DI water. The particulates were bathed three times with the HCl solution, in which the supernatant liquid was observed to be nearly clear with all particulates settled at the bottom (see Figure 6, middle). This would indicate no remnant acids, permanganate, or peroxides in the solution. 20 mL of ethanol was used as the last washing reagent, using the same process three times. As with the HCl solution, a clear liquid was observed with the solid material settled at the bottom.

With the GO thoroughly washed, the final step was simply to dry the remaining material (GO). The GO was carefully removed from each centrifuge tube and placed into a small dish (see Figure 6, right-side). The dish was placed into a vacuum environment using a Nalgene vacuum desiccator. Once completely dry, the solid GO was crushed thoroughly in a mortar and then dried inside a ThermoScientific Barnstead Lab-Line oven at 50 °C for fifteen minutes in preparation for analysis by XRD and SEM techniques.


Figure 5. MIDMARK M150 Soniclean Ultrasonic Cleaner (Left) and HERMLE Labnet Z206A Centrifuge (Right)

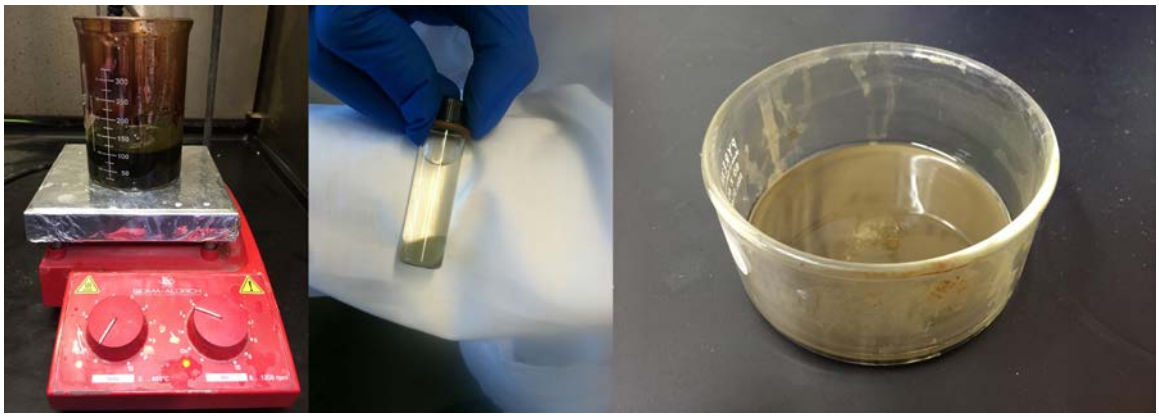

Figure 6. Mixture of Graphite Nanopowder, $H_2SO_4$, and $H_3PO_4$ on a Sigma-Aldrich Magnetic Stirrer/Hotplate (Left), GO Particulates Settled with Clear Supernatant After Being Centrifuged (Middle), and GO Prior to Vacuum (Right)

## 2. Graphene

Graphene was produced from GO through thermal exfoliation. The brown GO powder was spread evenly in an alumina crucible and placed inside a one-inch diameter quartz tube (see Figure 7, left side). The tube was sealed with stainless steel fittings to allow the flow of nitrogen to pass through. Using a Matheson Tri Gas flow meter in conjunction with flow tables specified by Matheson [42], we displaced the air atmosphere

at 100 SCCM (98.0 scale reading) for a half-hour period to remove any oxygen that might exist inside the tube. Afterwards, the flow was reduced to about 8 SCCM (15.0 scale reading), and the tube was placed inside a ThermoScientific Linberg/Blue M furnace (see Figure 7, right side) at 1000 °C for ten minutes. The process left behind a black, seemingly weightless but high volume powder, roughly half the weight of the GO from which it was produced (see Figure 7, middle and right).

Figure 7. (Left to Right) GO in Quartz Tube Prior to Thermal Exfoliation, Graphene just after Thermal Exfoliation, ThermoScientific Furnace with Graphene in Quartz Tube

## 3. Fuel Mixtures

This section covers the production of fuel mixtures using both GO and G in different quantities.

### *a. Graphite Oxide-F76 Fuel Mixture*

The amount of GO to be mixed with F-76 was measured by weight percentage. The quantities analyzed were 0.1 wt%, 1.0 wt%, 2.0 wt%, and 3.0 wt% measured using an OHAUS Adventurer Pro scale. To create the enhanced fuel mixture, we weighed a sample of F-76 using the scale, then we measured the appropriate weight percent of GO to be used, and afterwards, we combined the fuel and additive and sonicated it for five minutes to ensure a homogenous mixture. The left image in Figure 8 is a sample of an enhanced fuel mixture using 0.1wt% GO. Once there were no suspended GO particles visible, the fuel mixture was pipetted and dripped into a crucible and placed into our simultaneous thermal analyzer for calorimetric, thermogravimetric, and mass spectral analysis (see Figures 9 and 13).

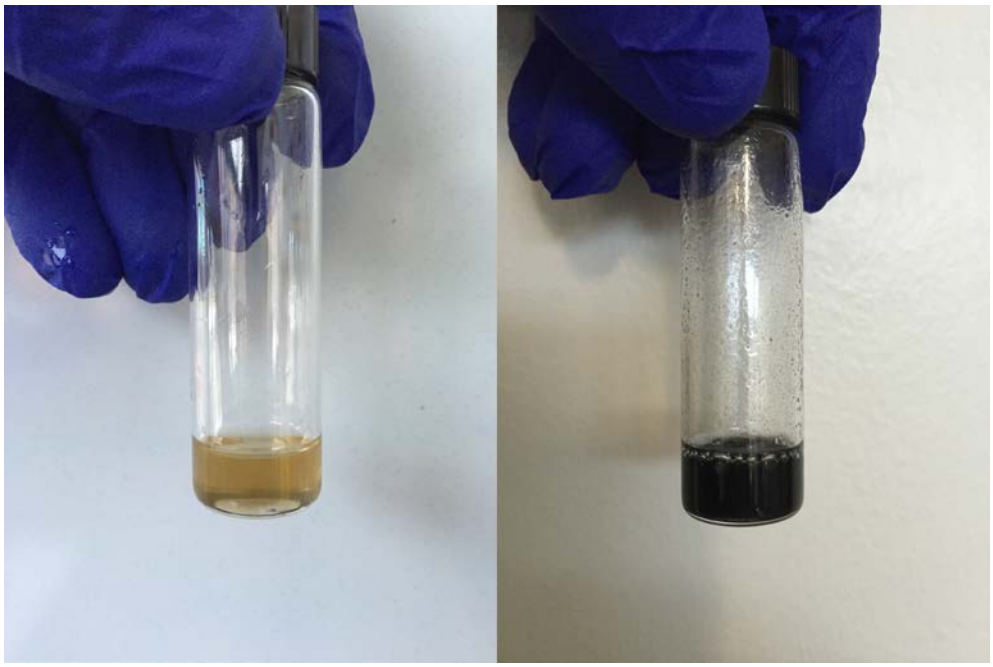

Figure 8. Sample of 0.1wt% GO/F-76 Mixture (Left) and Sample of 1.0 wt% Graphene/F-76 Mixture (Right)

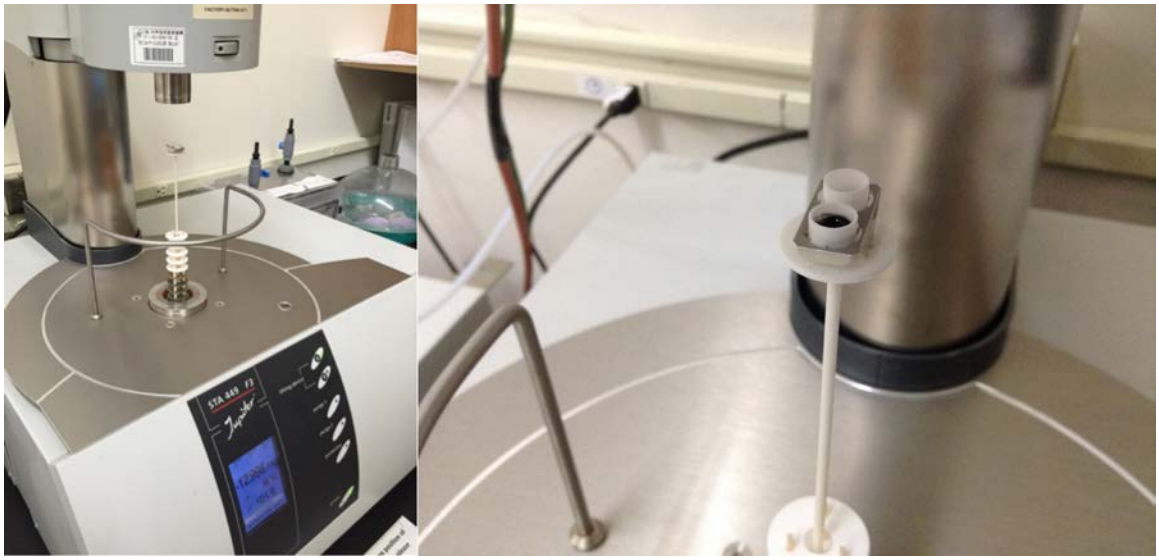

Figure 9. Crucible Ready for Analysis in STA

### *b. Graphene-F76 Fuel Mixture*

Similar to the previous section, graphene was measured by weight percentage and analyzed in the same quantities. The same procedure to mix the solutions and place them in a simultaneous thermal analyzer was also followed. The right image of Figure 8 is an example of 1.0 wt% G/F-76 fuel.

## B. CHARACTERIZATION TECHNIQUES

In the following sections, various characteristic techniques were used to analyze the GO and G nanopowders, as well as the fuel mixtures. These include XRD, SEM, and Simultaneous Thermal Analysis (STA).

### 1. X-Ray Diffraction

XRD was performed on GO, for it was a solid powder with a crystalline structure, but also because it was necessary to determine if there were trace amounts of manganese oxide ($MnO_2$) from the $KMnO_4$ that could contaminate the mixtures or affect the other analysis. Moreover, a peak close to $9°–13°$ (2-theta) distinguishes the structure of GO from the one shown in G. We also performed XRD on the G we synthesized. To do this, a Rigaku Miniflex 600, using Copper $K\alpha$ radiation, was used to analyze the crystalline structure.

GO samples and a G sample were prepared by mounting the nanopowders on a zero-background silicon plate such that each sample was leveled with the surface of the holder, as can be viewed in Figure 10. We carefully inserted the silicon slides into the holders of the Rigaku, seen in Figure 11. It should be noted that GO was required to be finely ground before mounting and all samples to be leveled with a silicon plate to avoid fluctuations in intensity and spottiness in retrieved data, while also aiding a good signal-to-noise ratio.

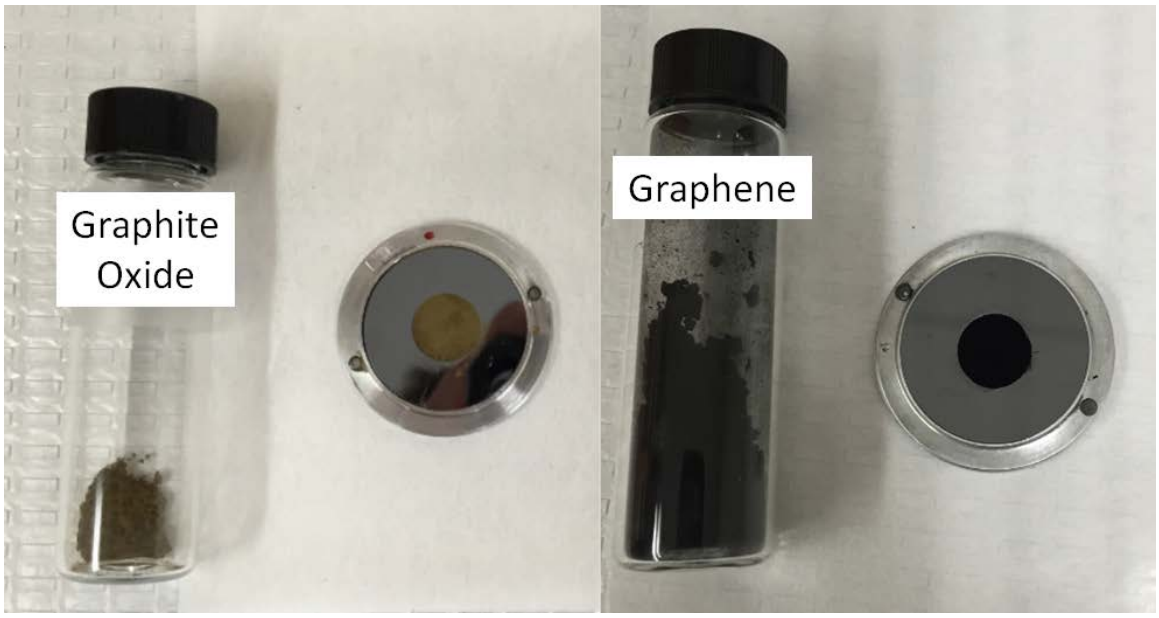


Figure 10. GO and Graphene in Zero-Background Silicon Plates


Figure 11. Rigaku Miniflex 600 XRD

XRD of the GO was performed before G was created via thermal exfoliation and before any mixture of fuel and additives could be produced. This only made experimentation easier for the future to know that the GO produced in-situ was of sound quality.

## 2. Scanning Electron Microscopy

SEM images of GO and G were captured in order to study their particle sizes and distribution. To do this, an electron beam from a Zeiss Neon 40 Field Emission Scanning Electron Microscope (see Figure 12) interacted with the surfaces of the samples, producing a purely topographical image. Multiple images were captured that enabled us to determine if the particle sizes and distribution of the ground GO and G were uniform or not. This was necessary in order to determine two things: 1.) If the GO or G might easily mix and distribute in fuel, and 2.) If the particles would be small enough such that injection of a fuel mixture might be possible.


Figure 12. Zeiss Neon 40 Field Emission Scanning Electron Microscope

## 3. Simultaneous Thermal Analysis of Fuel Mixtures

Much of the groundwork was accomplished using STA, specifically, DSC, TGA, and MS. All three methods were performed using the NETZSCH Simultaneous Thermal Analyzer 449 F3 Jupiter and NETZSCH Quadrupole Mass Spectrometer 403 C Aëolos setup in Figure 13.


Figure 13. Setup of NETZSCH Simultaneous Thermal Analyzer 449 F3 Jupiter (Right) and Quadrupole Mass Spectrometer 403 C Aëolos (Left)

### *a. Differential Scanning Calorimetry*

DSC is a technique in which the difference in energy input into a substance and a reference material is measured as a function of temperature, while the substance and reference material are subjected to a controlled temperature program [43]. Essentially, by referring back to Figure 9 and to a diagram of the two furnaces in which the sample and reference are placed, one can understand as the temperature changes in the sample material (left of Figure 14), power, or energy, is either applied to or removed from the calorimeter (the reference crucible, right of Figure 14) to compensate for the energy change of the sample. Thus, at all times, the system remains in a thermal “null” state, and

therefore, the amount of power required to maintain this state of equilibrium is directly proportional to the energy changes occurring in the sample [43]. These energy changes are recorded as exothermic reactions when heat is released or as endothermic reactions when heat is required of the material to compensate for its surroundings.

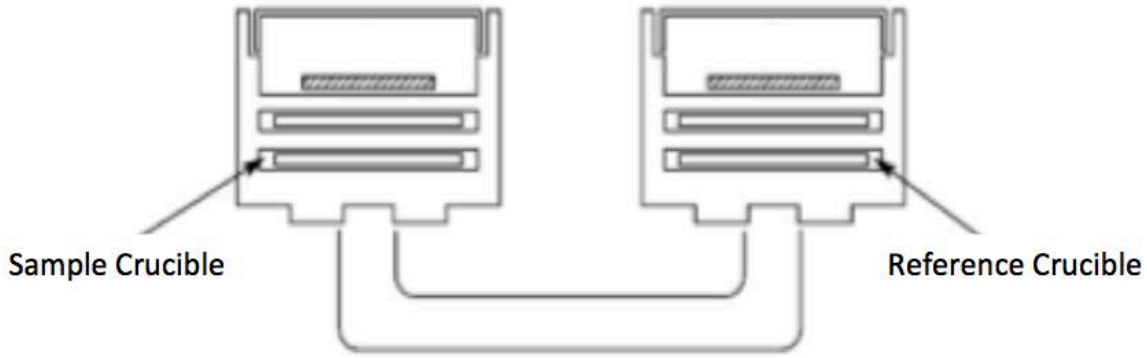


Figure 14. Sample and Reference Furnaces inside STA, after [43]

We exposed each sample to the settings inside the STA that are shown in Table 2.

Table 2. DSC/TGA System Settings

| Environment Gases | Flow Rate (mL/min) | Temperature Rate (°C/min) | Temperature Range (°C) |
|---|---|---|---|
| **Nitrogen** | 80 | 2 | 30 - 1050 |
| **Oxygen** | 20 | | |
| **Nitrogen (Protective)** | 50 | | |

### *b. Thermogravimetric Analysis*

TGA is a technique in which the mass of a substance is monitored as a function of temperature or time as the sample specimen is subjected to a controlled temperature program in a controlled atmosphere [43]. That is to say, TGA relies upon a high degree of precision in three measurements: mass change, temperature, and the change in temperature. We utilized TGA while simultaneously collecting DSC data. Inside the

settings, we tare the weight of the crucible in which the sample is set in, and we only record the weight of the sample itself. As TGA is conducted, the program can be set to record its weight change by milligrams and by percentage. We chose percentage, set at 100% weight initially.

### *c. Mass Spectral Data Analysis*

MS is an analytical technique that helps identify the type of chemicals present in a sample by measuring the mass-to-charge ratio and abundance of gas-phase ions [43]. With DSC and TGA simultaneously being analyzed, the QMS is controlled separately but records and analyzes data concurrently. The settings for the transfer line, inlet system and adapter head were all set at 250 °C.

## C. CETANE NUMBER AND LOWER HEATING VALUE TEST ON FUEL MIXTURES

As part of our goals with this research, we needed to test the cetane number and the lower heating value of several enhanced fuel mixtures to compare against F-76. Increasing the cetane number would decrease the ignition delay after injection resulting in less unburned fuel and the possibility of increasing fuel efficiency. Determining the lower heating value (LHV) would be necessary for the next test, running the fuel mixtures through our on-site diesel engine. So, we prepared the following propellants in 1050-milliter quantities and contracted them out to Southwest Research Institute (located at 6220 Culebra Road, San Antonio, Texas, 78238-5166): F-76, F-76/0.1wt% GO, and F-76/0.1wt% graphene.

Just as we created the fuel mixtures described in Section 3, paragraphs a and b, we created the two fuel/additive mixtures and poured them into the containers in the left image of Figure 15. A courier for Southwest Research Institute Inspected them prior to sealing the containers (middle image of Figure 15), and once approved for transportation, he placed them inside the box in the right image of Figure 15.

Figure 15. Containers Used to Transport F-76, 0.1wt% GO/F-76 Mixture, and 0.1wt% G/F-76 Mixture

## D. DIESEL ENGINE TESTS ON FUEL MIXTURES

To test the performance of the fuels in a practical application, a marine diesel engine located in the marine propulsion laboratory, Naval Postgraduate School was utilized (see Figure 16). The engine used is an in-line, three-cylinder, direct-injected, two-stroke Detroit Diesel 3-53. Table 3 lists the key specifications of the engine. The control setup for the engine can be seen in Figure 17, while a detailed description of the engine controls, instrumentation, and data acquisition systems used can be found in Peterson *et al.* [44]. It is a representative platform in applications currently in use by the United States Navy.

Figure 16. Detroit 3-53 Diesel Engine

Table 3. Specifications for Detroit 3-53 Diesel Engine

| | |
|---|---|
| Model Number | 5033-5001N |
| Number of Cylinders | 3 |
| Bore and Stroke | 0.0984 x 0.1143 meters (3.875 x 4.5 inches) |
| Engine Displacement | 0.0026 cubic meters (159 cubic inches) |
| Compression Ratio | 21:1 |
| Maximum Power Output | 75.3157 kW (101 hp) at 2,800 RPM |
| Peak Torque | 277.9427 N-m (205 ft-lbf) at 1,560 RPM |
| Brake Mean Effective Pressure | 668791.4571 Pa (97 psi) |


Figure 17. Diesel Engine Test Stations (Left to Right): Engine Speed/Load Console, Engine Speed/Load Analyzer, Engine Cylinder Analyzer

### *a. Testing Procedures*

1.5-liter quantities of F-76, 0.1 wt% GO/F-76, and 0.1% wt G/F-76 were formulated, with F-76 neat to be used as the base reference. With limited test fuel quantities available, it was estimated that, at most, two speed lines with four torque settings each (for a total of 8 speed load points) could be recorded and available for analysis. A test matrix for those points was developed and is illustrated in Table 4. The numbers represent the order of testing.

It should be noted that at the time of testing, the full range of operating torque for the engine was not available due to mechanical issues associated with the governor. A maximum of 120 ft-lbfs represented the upper end of the torque range and the remaining points were chosen to best represent this limited operating range.

Table 4. Test Matrix, Engine Speed and Load

| Torque [ft-lbf] | Engine Speed [RPM] | |
|---|---|---|
| | 1100 | 1700 |
| 50 | 5 | 4 |
| 75 | 6 | 3 |
| 95 | 7 | 2 |
| 120 | 8 | 1 |

All tests were performed on the same day with temperature, humidity and pressure in the test cell recorded.

### *b. Analysis*

Figure 18 is representative of a pressure trace (top image) and a cumulative energy release (bottom image) trace from the operation of the engine. The figure shows several important characteristics used to compare the fuel samples. Some of these features include: the start of injection (SOI), which is nominally 14° before top-center (BTC) and combustion duration (CD) which is determined from the cumulative sum of the heat release and is indicated below. For this thesis CD was defined as the CAD from when 10% of the fuel was consumed to when 90% of the fuel was consumed (CAD90-CAD10). CAD10 and CAD90 are determined using the cumulative sum of the heat release rate [44] .

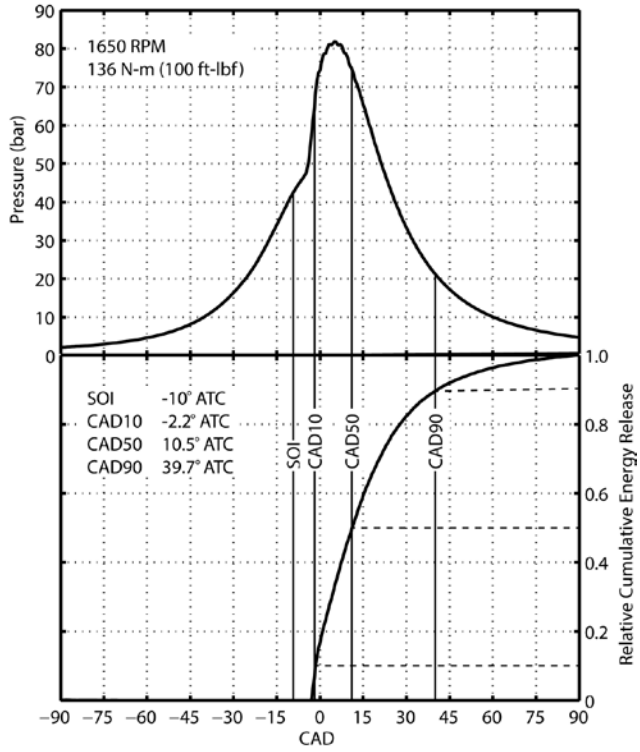


Figure 18. Pressure Trace and Cumulative Energy Release for Operating Point at 1650 RPM and 100 ft-lbf Indicating the Measured Values for SOI, CAD10, CAD50, and CAD90, from [44].

Additionally, MRR, PP, and AOP were all determined from the pressure trace. MRR is the maximum slope of the pressure trace in bar/CAD. PP is the maximum pressure and AOP is the CAD corresponding to the PP.

Energy or heat of release is calculated from the pressure-volume data measured during test runs using the first law energy balance:

$$\frac{\delta Q_{ch}}{dt} = p\frac{dV}{dt} + m c_v \frac{dT}{dt} + \frac{\delta Q_H}{dt}$$

A detailed explanation of the derivation of this equation can be found in Peterson *et al.* [44]. This analysis allows for the important metric of start of combustion (SOC) to be ascertained which in turn is utilized, in conjunction with SOI, in calculating the ignition delay (IGD), a characteristic associated with the delay before auto-ignition occurs in a Diesel engine. Comparison of relative differences in IGD between F-76 and GO and graphene additive mixtures at the same speed and load points can then be determined. Ignition delay is defined as follows:

$$\text{IGD} = \text{SOC} - \text{SOI}$$

$$\Delta\text{IGD} = \text{IGD}_1 - \text{IGD}_2 = (\text{SOC} - \text{SOI})_1 - (\text{SOC} - \text{SOI})_2$$

where the subscripts 1 and 2 indicate different fuel types.

THIS PAGE INTENTIONALLY LEFT BLANK

# III. RESULTS AND DISCUSSION

This chapter will present and analyze the results generated by the characterization methods described in the previous chapter. The first discussions introduce XRD and SEM data of the precursor powder (GO and G). Such section will be followed by studying the calorimetric (DSC), thermogravimetric (TGA), and compositional (MS) data retrieved from each of the fuel mixtures. The cetane number and net heat of combustion for the fuel and fuel/additives mixtures will be presented. Finally, we present information generated during the diesel engine tests.

## A. XRD

XRD analysis of GO and G was the first characterization step after their synthesis. Such data allowed us to analyze their crystal structures and aided in determination of their quality.

### 1. GO

The GO signatures in Figure 19 show an intense peak located near 10° (2-theta), which is characteristic of GO. Two other peaks, located close to 20° and 42° (2-theta), were also observed. This is consistent with data presented by Titelman *et al.*, Vilardi, and Maxson [9], [14], [18]. Since, GO research is relatively recent, its pattern is not found in the ICDD 2014–2015 JCPDS database [45].

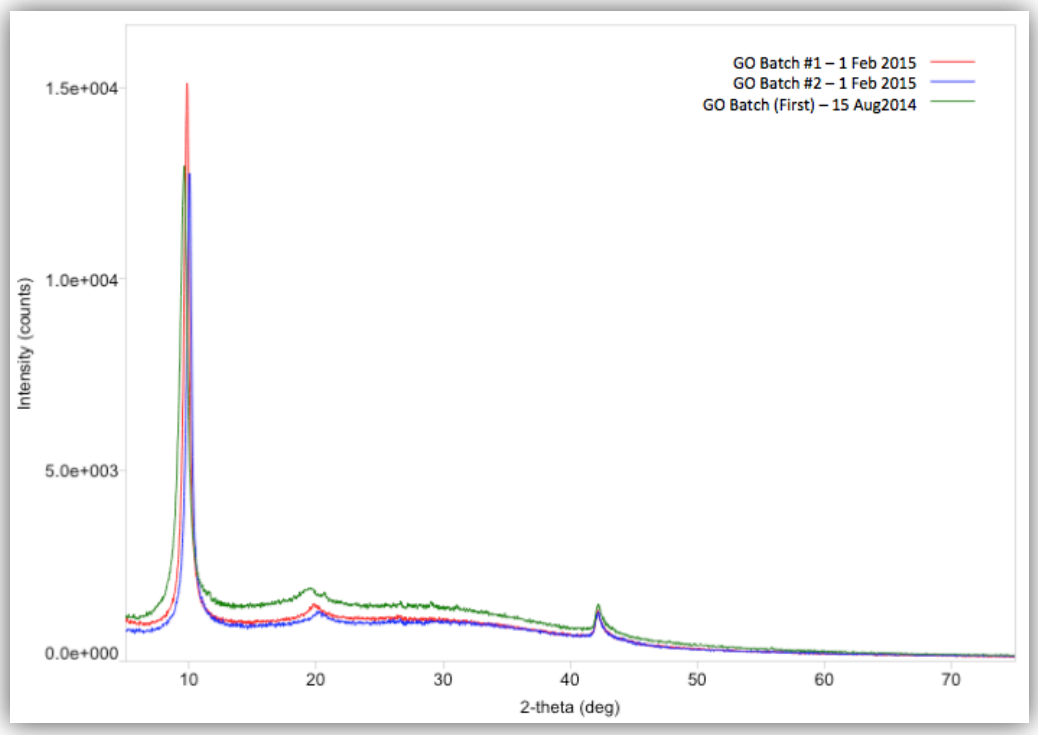


Figure 19. XRD Data for Three GO Batches

## 2. Graphene

As of the May, there does not appear to be any XRD analysis of graphene in the 2014–2015 JCPDS database. However, our analysis does show consistency with Titelman *et al.*, Mowry *et al.*, and Wakeland *et al.* [14], [46], [47] and closely resembles that of data generated in the past by our research group at NPS (Vilardi and Maxson) [9], [18]. In Figure 20, the large peak located near 25° and smaller peak located around 43° are characteristic of G.

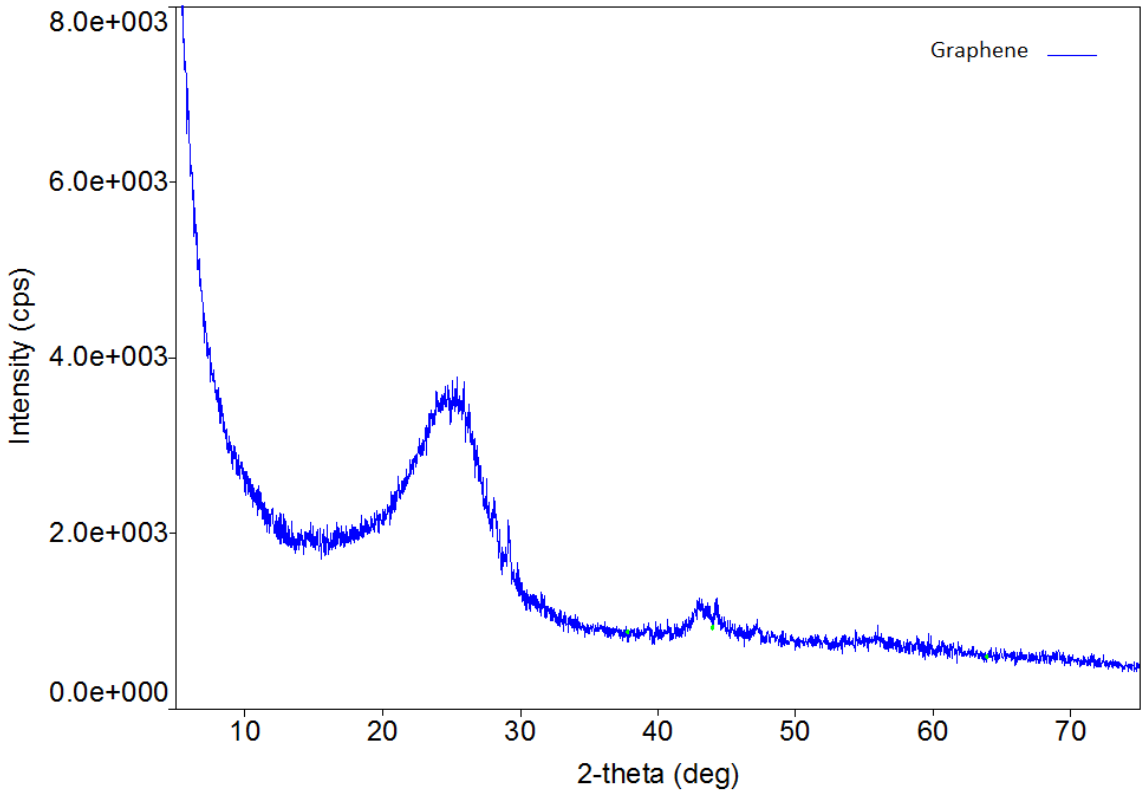


Figure 20. XRD Data for Graphene

## B. SEM

SEM images of the particulate shape, size and distribution were captured for GO and G. These images enabled us to answer whether these materials will have an adequate size (less than 10 microns) to be used with the diesel engine filters. If sizes were larger than the filter's pore dimensions, the particles would become trapped by the filters and we would not be able to study their effect. For the calorimetric and thermogravimetric analysis there were no size limitations.

### 1. GO

Figure 21 and 22 are the same GO sample, however, there were differences in the preparation for SEM imaging. Figure 21 is an image of GO that had been ground in a mortar for five minutes, and several of the particles measured are clearly over 10 microns in length. Because this would definitely present problems passing through the filters and fuel injectors in the diesel, we took the sample and ground it for an additional ten minutes

(for a total of fifteen minutes of grinding). We replaced the GO in the SEM, and the image in Figure 22 shows that the particle sizes were mostly under the 10-micron restriction. So, we were able to ascertain that GO would most likely be injected successfully into the diesel engine.

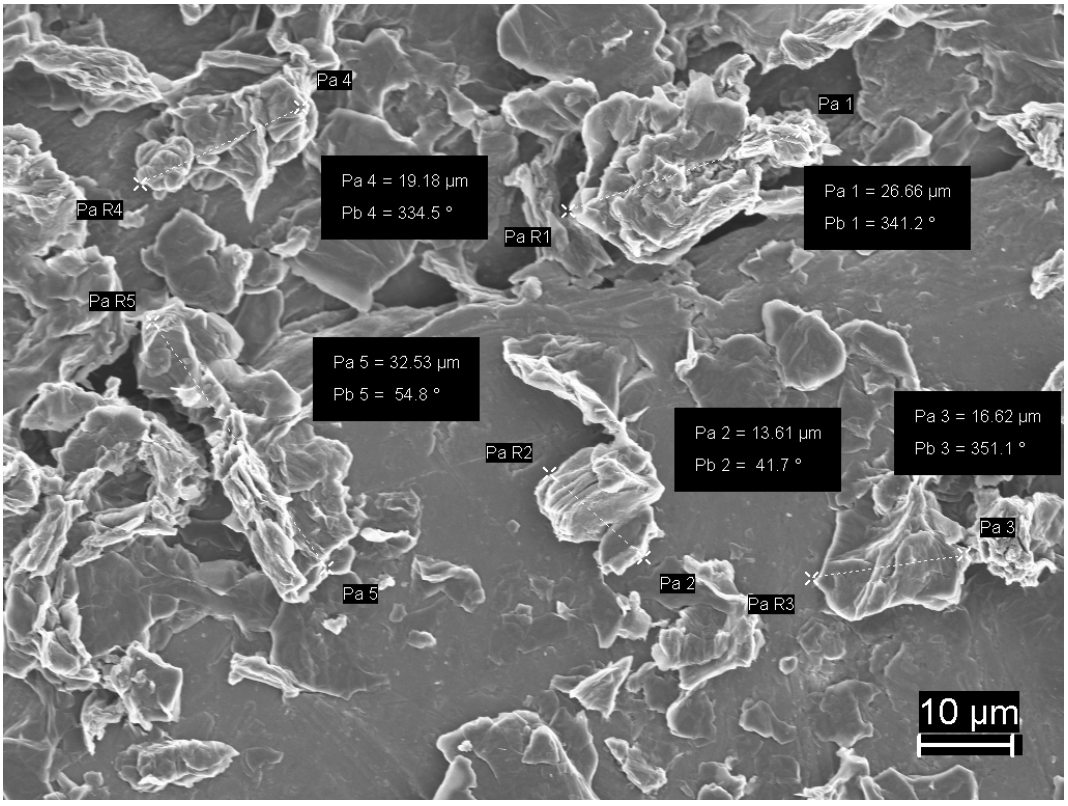


Figure 21. Graphite Oxide Particles Measuring Greater than 10 Microns after Five Minutes of Grinding

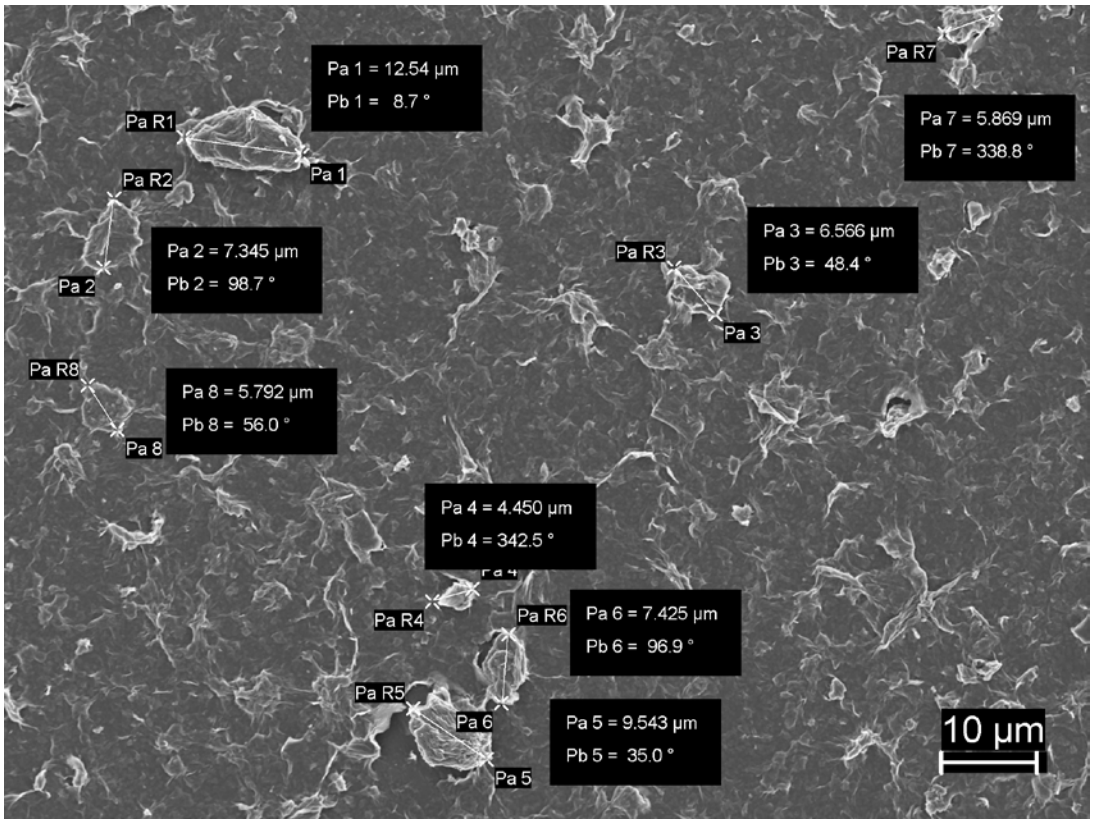


Figure 22. Graphite Oxide Particles Measuring Less than 10 Microns after Fifteen Minutes of Grinding

### 2. Graphene

Referring back to Figure 2, the structure of G after the thermal exfoliation of GO should be that of single sheets of carbon arranged in no particular orientation to other sheets with extremely low amounts (if any) of oxygen groups from GO. After mounting G in the SEM, images revealed that particulates were mostly under the 10-micron restriction, as seen in Figure 23. However, in order to further study the structure, namely the single sheets of carbon, we needed to magnify this image. In Figure 24, images of the G taken at 5000X and 25000X magnification show individual sheets, but also present are sheets that exfoliated, creating a honeycomb structure where some sheets were still linked to others. Therefore, we decided that G was a contender for research as a drop-in additive for F-76.

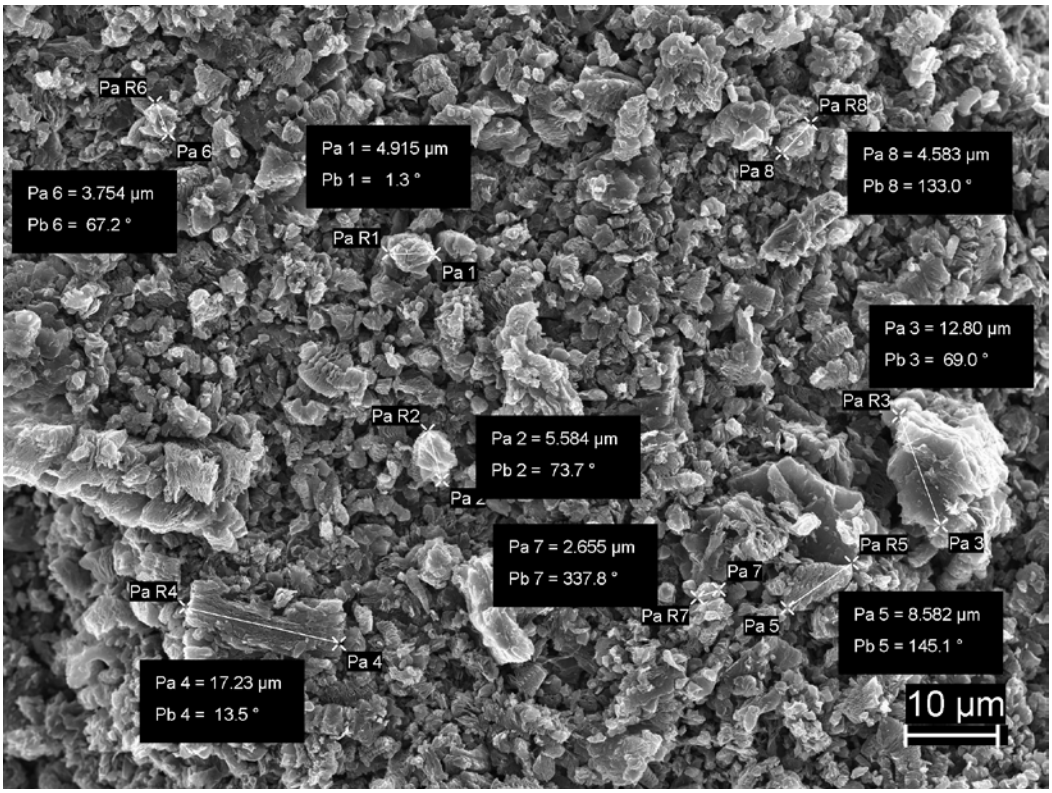


Figure 23. Graphene Particles Measuring Less than 10 Microns

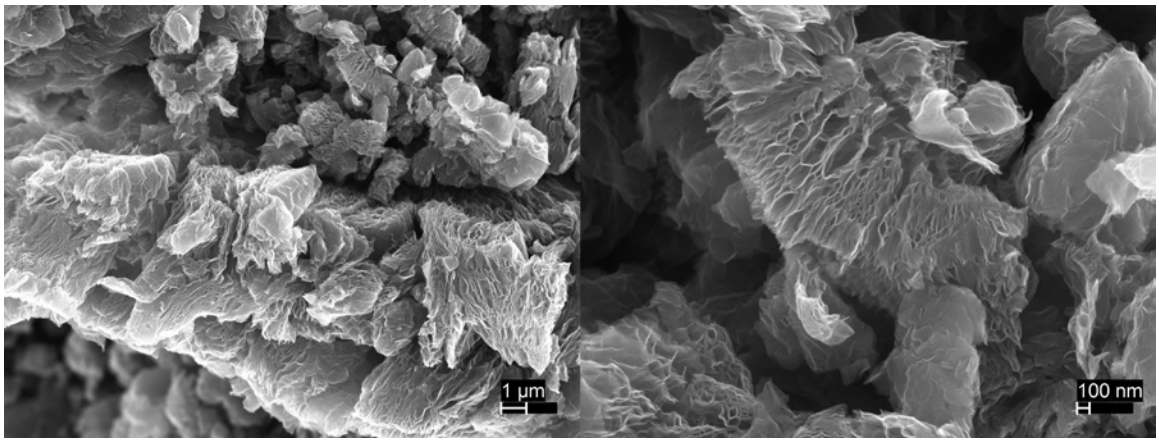


Figure 24. Graphene at 5000X (Left) and at 25000X Magnification (Right)

## C. STA

Further research to determine whether GO or G would be good candidates as fuel enhancers involved studying the temperature programmed oxidation of F-76 and the fuel mixtures. The outcome of such experiments includes: curves of heat flows in mW/mg versus temperature (DSC) and weight loss as percentage of initial mass versus temperature (TGA). We compared the behavior of the GO/F-76 and G/F-76 mixtures against neat F-76 to decide which mixtures might be eligible for diesel engine testing.

### 1. F-76 DSC/TGA Analysis

F-76 neat was analyzed to study its calorimetric and thermogravimetric characteristics in order to set forth a basis of comparison to the characteristics of GO-mixed and G-mixed fuels. Figure 25 shows that the temperature range of combustion (shaded region) occurred between 110°C and 190°. The shaded region shows an exothermic reaction as the fuel combusts, and the area is equivalent to the reaction energy output in J/gram. Energy output for F-76 was calculated to be 16.805 J/g, value included in Tables 5 and 6 to compare with the energy outputs of the GO and G fuels.

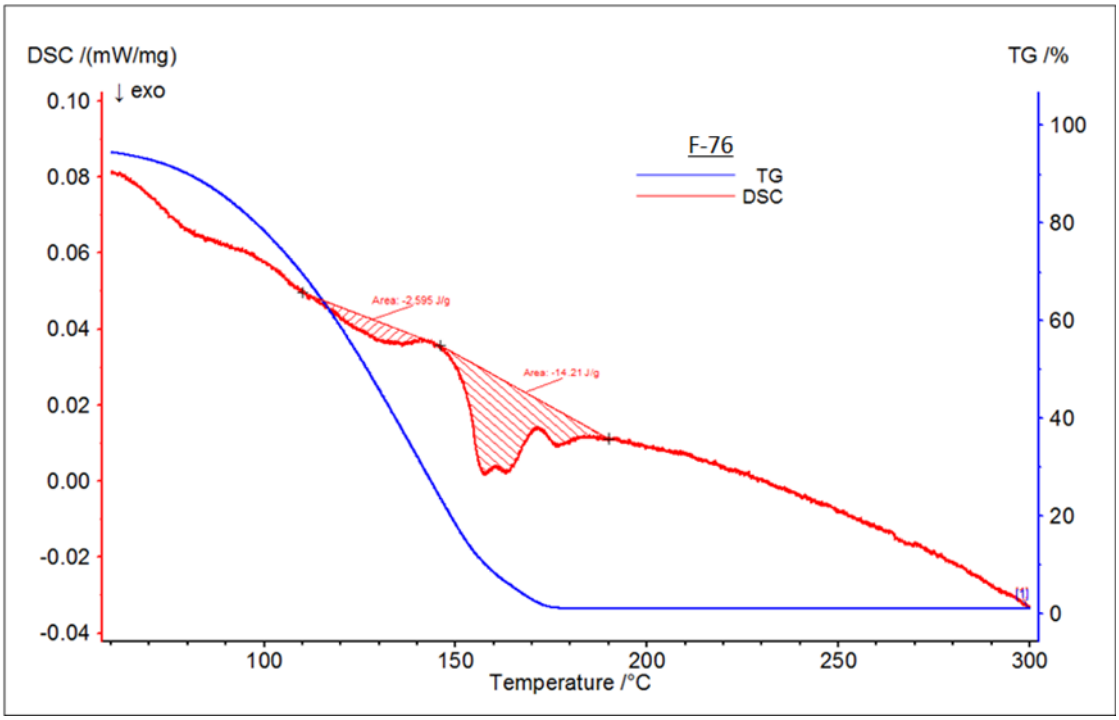


Figure 25. DSC/TGA for F-76 Fuel

TGA showed the mass change (by percentage) collected as the F-76 was heated per Table 2 settings. It is apparent that the fuel's decrease in mass occurs over similar temperature ranges that coincide with the ranges analyzed in Figure 25. After approximately 180 ° C, the fuel's mass is reduced to zero.

It is worth noting that all of the F-76 has reacted with the oxygen in the reaction environment by the time the sample reaches ~190 ° C. The reaction completion temperature is dependent on the nature of substance analyzed and the heating rates. All DSC/TGA experiments were conducted at 2 ° C/min. The results are used as guidance in terms of the use of diverse amounts of additives and helped determine the minimum amount of additive measurements, presented in Sections 6 and 7. Those results were taken using much faster heating rates than the results presented in this section, which are then not comparable.

## 2. DSC/TGA for GO and G Powders

In order to understand possible reactions that might occur due to increases in temperature of GO-mixed and G-mixed F-76 fuels, we first studied the GO and G powders in the STA using DSC and TGA. For the former, Figure 26 shows that GO and G both have exothermal characteristics when subjected to an air environment and constantly heated. Comparing the exothermal reactions with F-76 in Figure 25, GO has a reaction that occurs inside the analyzed temperature range apparent in Figure 25 (between ~50 °C and 260 °C) while both GO and G present a much larger reaction occurring at temperatures between 200 °C and 650 °C.

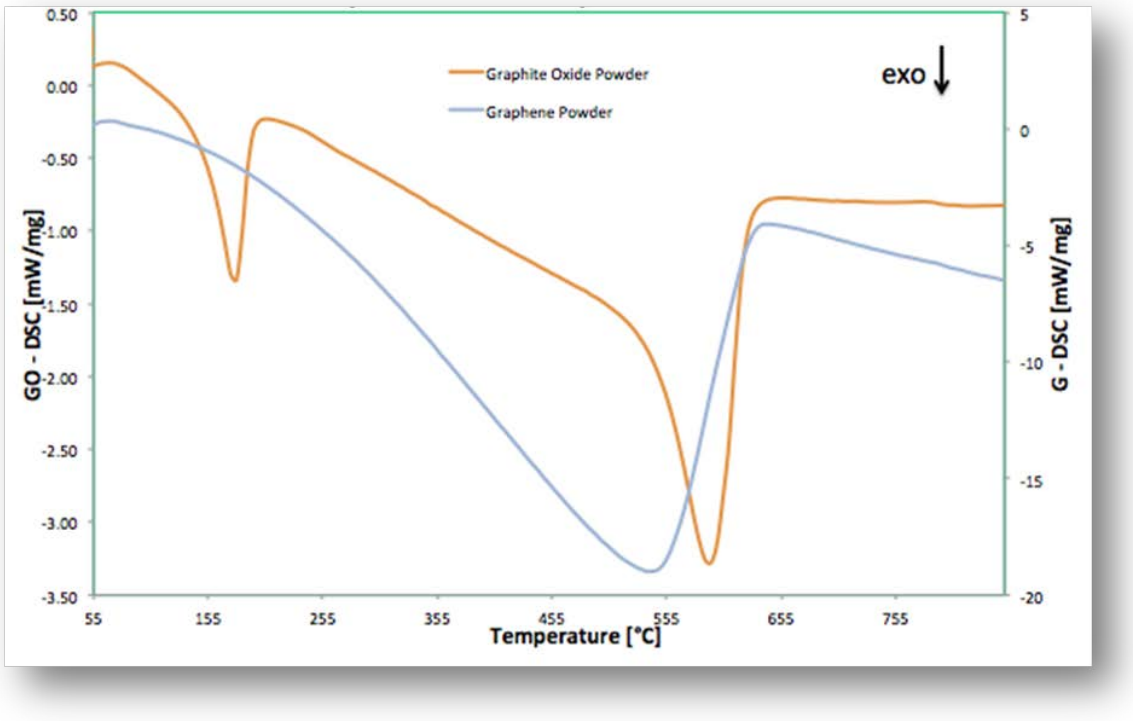


Figure 26. DSC Data for GO and G Powders

The first process identified in the GO corresponds to the loss of absorbed water and the oxygen species contained on its structure. The peak for both GO and G, which maximums are at ~610°C and 660°C respectively, correlates with the complete transformation of the solid carbon byproducts into $CO_2$. That is, the burn off of graphene.

We can make several observations studying the TGA data in Figure 27 for GO and G powders. For GO, we see rapid decreases in mass percentage at 180°C, 260°C, and 610°C. Water, carbon monoxide, and carbon dioxide are given off at the first two temperature points, while the solid byproduct, graphene, is burned off at the highest temperature. For G, we only see the rapid decrease around 660°C, which corresponds to G turning into $CO_2$. These characteristics are expected in GO and G and are the first indication of their possible capabilities for enhancing F-76 by producing extra gases. The diverse processes observed here at diverse stages, at low heating rates, are expected to occur instantaneously when those heating rates increase.

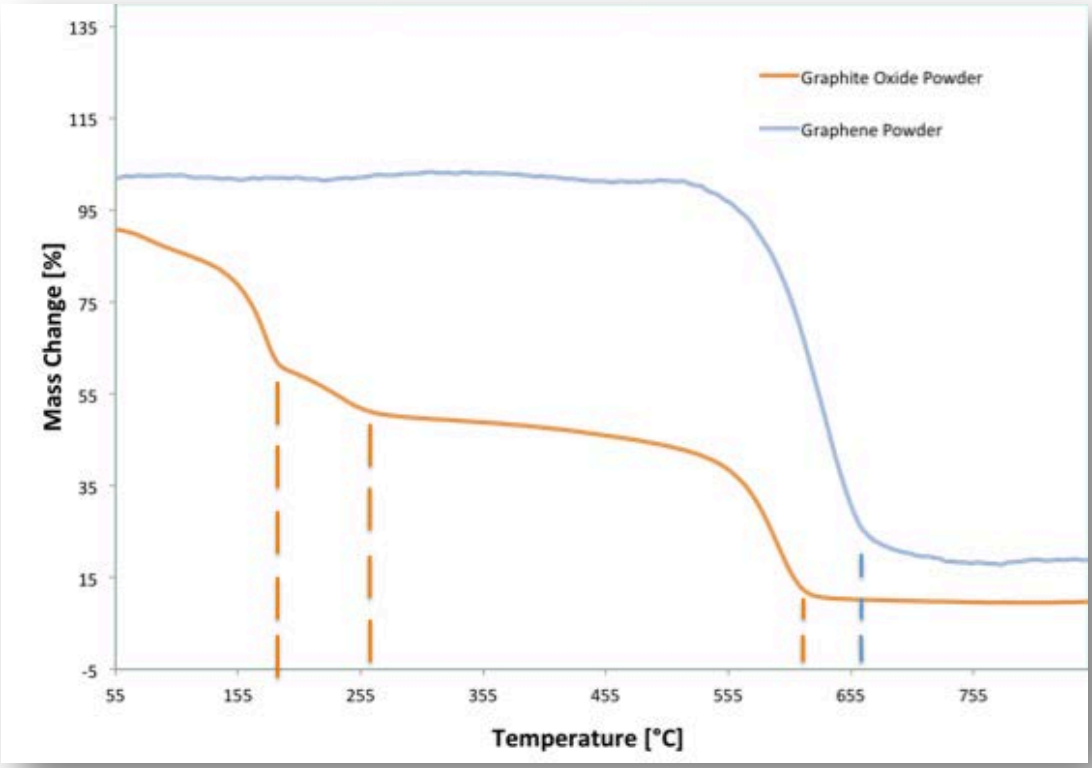


Figure 27. TGA Data for GO and G Powders

### 3. DSC/TGA for GO Mixtures

GO fuel/additive mixtures were analyzed under the same conditions as F-76 presented in Table 2. Figure 28 plots the DSC and TGA curves for each mixture, and it can be seen that the mixtures in quantities of 1.0 wt% to 3.0 wt% showed dramatic endothermic reactions later in their analysis (indicative of absorption of heat), while the lowest quantity of 0.1 wt% GO/F-76 fuel was similar to that of F-76 with the exothermic reaction early in the analysis and no endothermic spike. This lead to the decision later on in this study to further use this quantity (0.1 wt%).

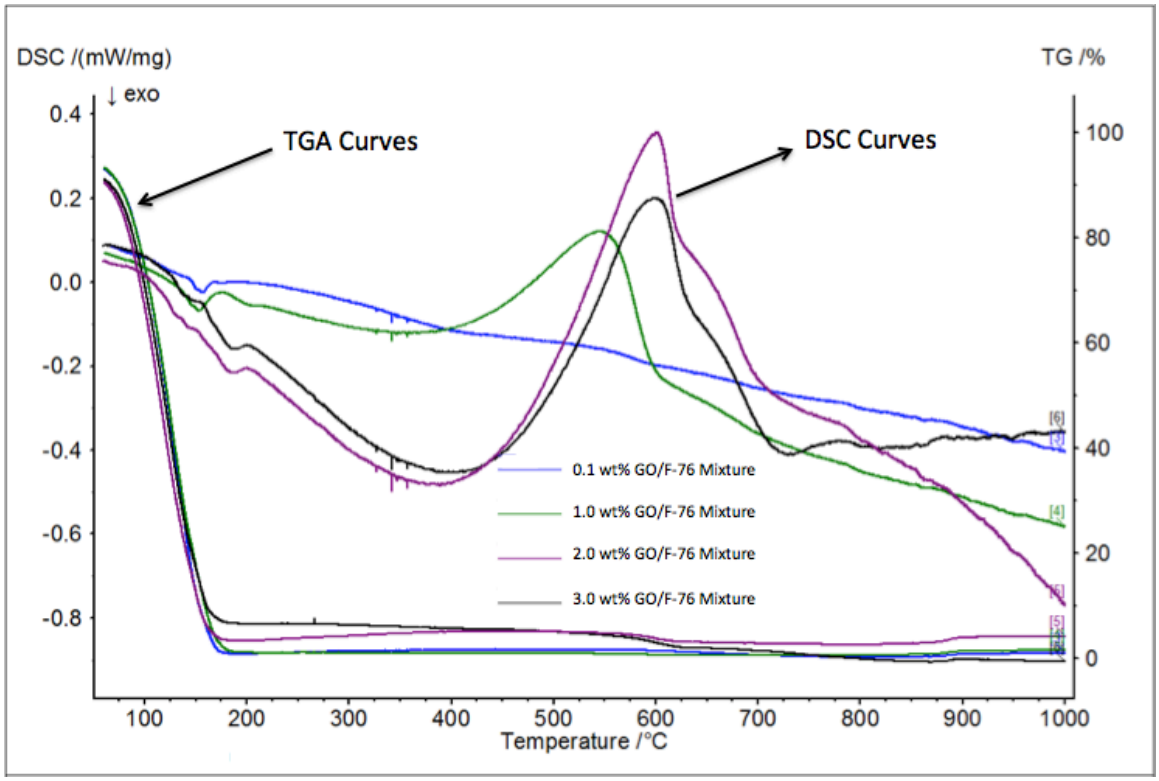


Figure 28. Complete DSC/TGA Analysis of GO-Mixed Fuel Samples

Zooming in on the exothermic reactions of the four mixtures, DSC analysis for all ratios of GO in F-76 revealed that the combustion took place at the same starting temperature of 110 °C as F-76, seen in Figure 29, with the exception of 3.0 wt% GO/F-76. While the entire combustion range occurred over roughly the same range, the heat flows in all cases increased when compared to F-76 listed in Table 5. It should be noted that these reactions occur over a slow burn rate, which might not be indicative of heat flows that would come from combustion inside a diesel engine. But, we do see the dramatic energy increases which paves the way to study their effects in a practical setting later on.

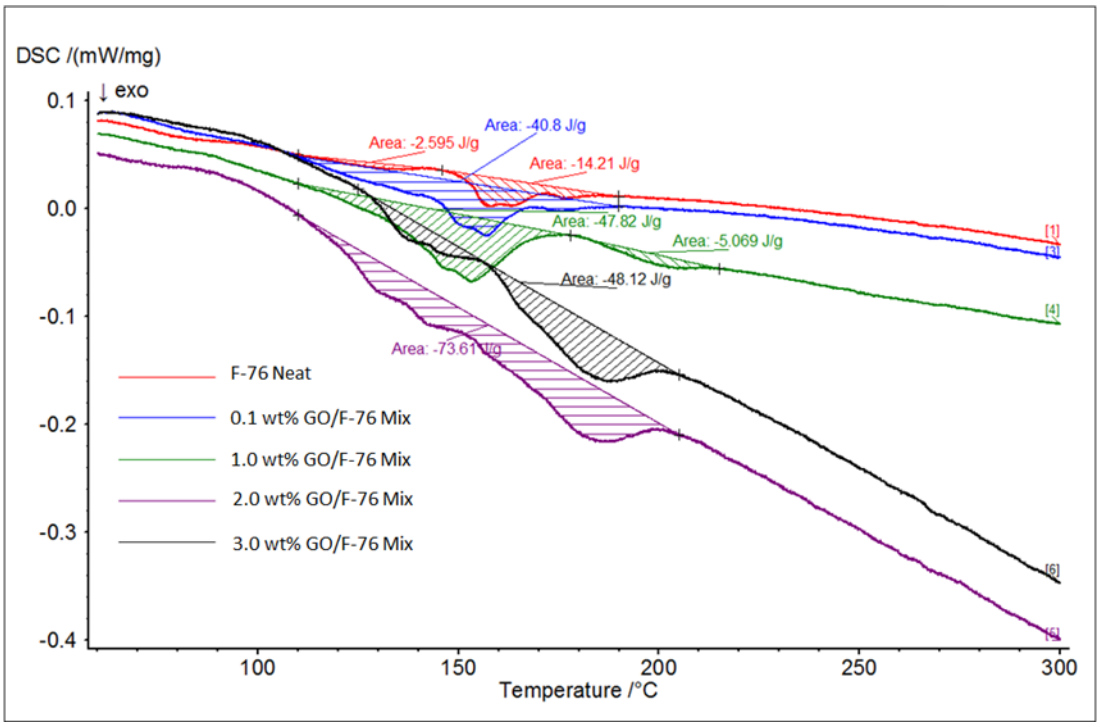


Figure 29. Differential Scanning Calorimetry for Graphite Oxide /F-76 Fuel Mixtures

Table 5. Comparison of Energy Output of F-76/GO Mixtures

| Propellant | Temperature Range of Energy Output [°C] | Energy Output [J/g] |
|---|---|---|
| F-76 | 110 - 190 | 16.805 |
| 0.1wt% GO Mixture | 110 - 190 | 40.8 |
| 1.0wt% GO Mixture | 110 - 215 | 52.889 |
| 2.0wt% GO Mixture | 110 - 205 | 73.61 |
| 3.0wt% GO Mixture | 125 - 205 | 48.12 |

Similar to the TGA data collected for F-76, each of the GO/F-76 mixtures had reductions in mass almost identical to F-76 (see Figure 28). That includes the temperature range of the mass reduction, but also the fact their masses were near zero around 180 ° C with no apparent solid residues left over after the run.

## 4. DSC for Graphene Mixtures

G fuel/additive mixtures were also subjected to the same conditions in the DSC prescribed in Table 2. In every mixture, endothermic reactions occur later in the DSC analysis. However, we considered that the area of heat absorption was relatively small in the 0.1 wt% G/F-76 compared the heavier mixtures, and thus, we would use this mixture as a basis to further study this G-based fuel in practical settings.

As we focus our attention to the exothermic regions of the four samples, Figure 30 illustrates that combustion took place over similar temperature ranges as with F-76 neat. Table 6 lists the ranges, and it also compares the heat flows apparent in the of the mixtures. It was quite interesting to see that only the 0.1 wt% and 2.0 wt% G/F-76 mixtures produced greater heat flows than F-76, while 1.0 wt% 3.0 wt% did not.

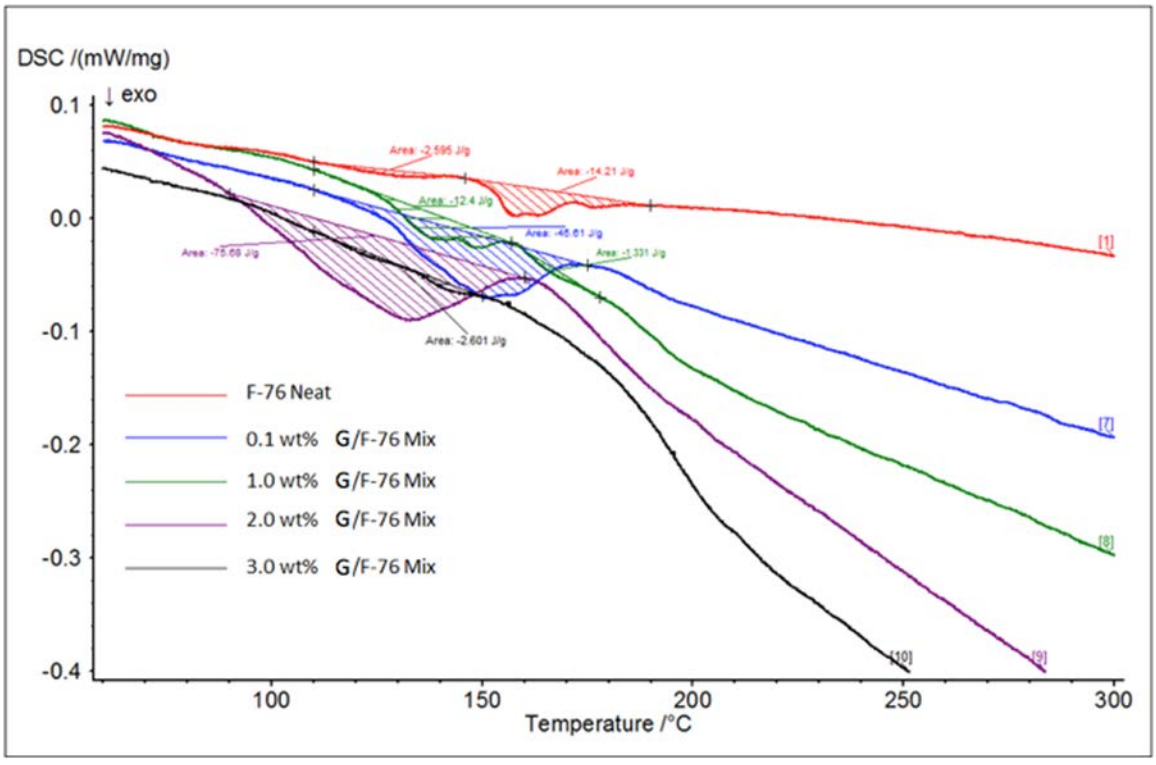


Figure 30. Differential Scanning Calorimetry for Graphene/F-76 Fuel Mixtures

Table 6. Comparison of Energy Output of F-76/Graphene Mixtures

| Propellant | Temperature Range of Energy Output [°C] | Energy Output [J/g] |
|---|---|---|
| F-76 | 110–190 | 16.805 |
| 0.1wt% Graphene Mixture | 110–175 | 45.61 |
| 1.0wt% Graphene Mixture | 110–178 | 13.731 |
| 2.0wt% Graphene Mixture | 90–160 | 75.68 |
| 3.0wt% Graphene Mixture | 110–150 | 2.601 |

TGA data in Figure 30 was nearly identical to F-76's and the GO/F-76 Mixture's analysis. The G/F-76 Mixtures has mass reduction in the same temperature range as the previous two analyses, their mass were nearly zero around $180\,^{\circ}\mathrm{C}$, and there was no apparent residues left over after the run was complete.

### 5. MS Data Analysis for F-76, GO Fuel Mixtures, and G Fuel Mixtures

While collecting DSC and TGA data, we simultaneously collected mass spectral (MS) data using the QMS. As is common knowledge with the chemical equation for the combustion of diesel fuel, a complete combustion of diesel fuel (which contained hydrocarbons) occurs when oxygen gas ($O_2$) is introduced and, after combustion, water ($H_2O$) and carbon dioxide ($CO_2$) are given off. The mass spectra separates molecular species. For example, a part of a peak for mass 44, for $CO_2$, when $CO_2$ is present, peaks for CO (mass 28), carbon (mass 12), and oxygen (mass 16). To aid the F-76 to create a more complete combustion, GO was added to which it was expected to introduce the oxygen groups that would enrich the fuel while G was added in order to increase combustive reactions. Therefore, we studied such chemical signatures as water, carbon dioxide, carbon monoxide, and others common in commercial diesel fuels like nitric oxide (NO), nitrogen dioxide ($NO_2$), sulfur dioxide ($SO_2$), and sulfur trioxide ($SO_3$).

### *a. Water*

Figures 31 and 32 show analyzed signatures analogous of water (mass of 18) after the F-76, GO/F-76 Mixtures, and G/F-76 Mixtures were exposed to conditions in Table 2. Water was produced starting below 100 ° C in the F-76 sample and G/F-76 mixtures; this was also the case for the GO/F-76 mixtures with the exception of the 2.0wt% sample. It appears that water is produced from the combustion reaction at about 270 ° C.

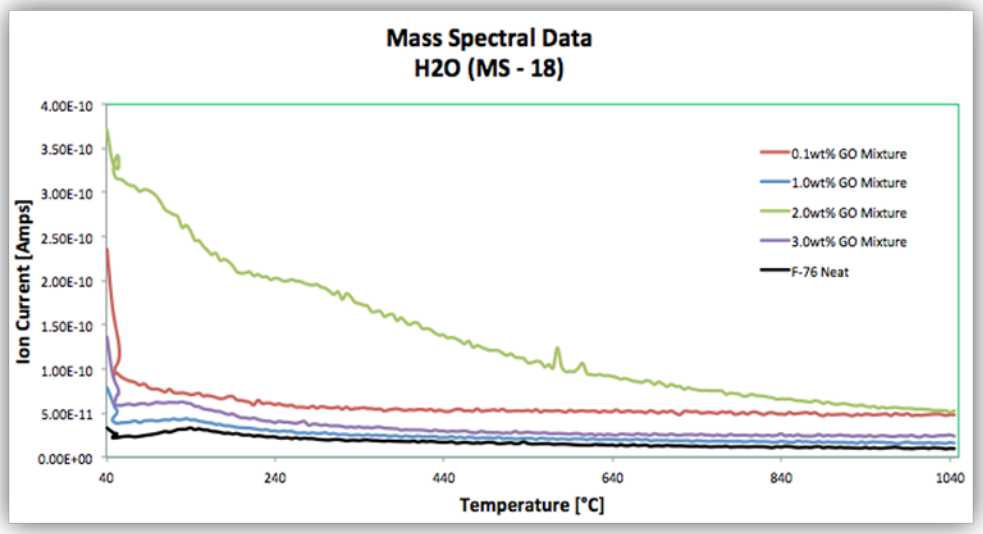


Figure 31. Mass Spectral Data for F-76 and the GO-Mixed Fuels for Water

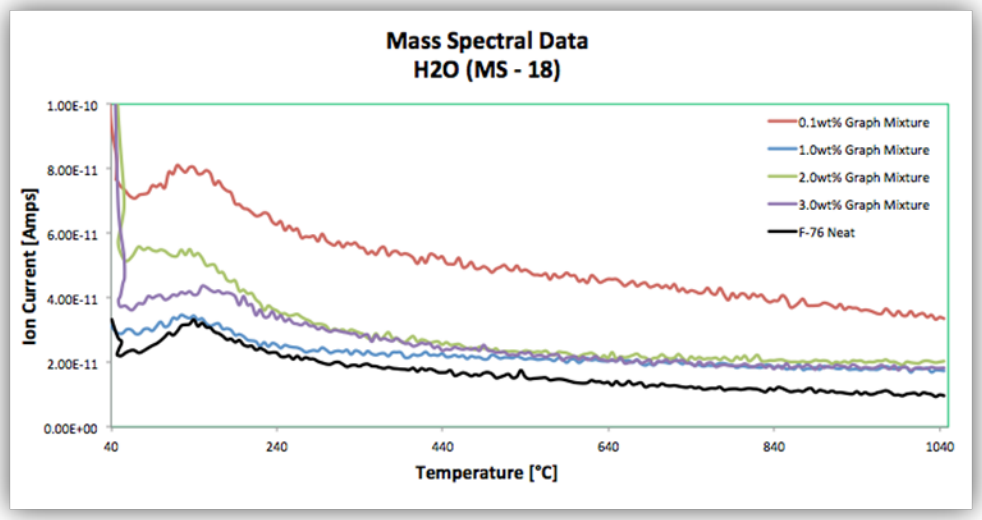


Figure 32. Mass spectral data for F-76 and the G-mixed fuels for water

### *b. Carbon Monoxide*

Figures 33 and 34 display signatures of CO (mass 28) for the F-76 sample, GO/F-76 Mixtures, and G/F-76 Mixtures. CO seems to be produced in an incremental way over the full combustion up to about 200 ° C in all cases.

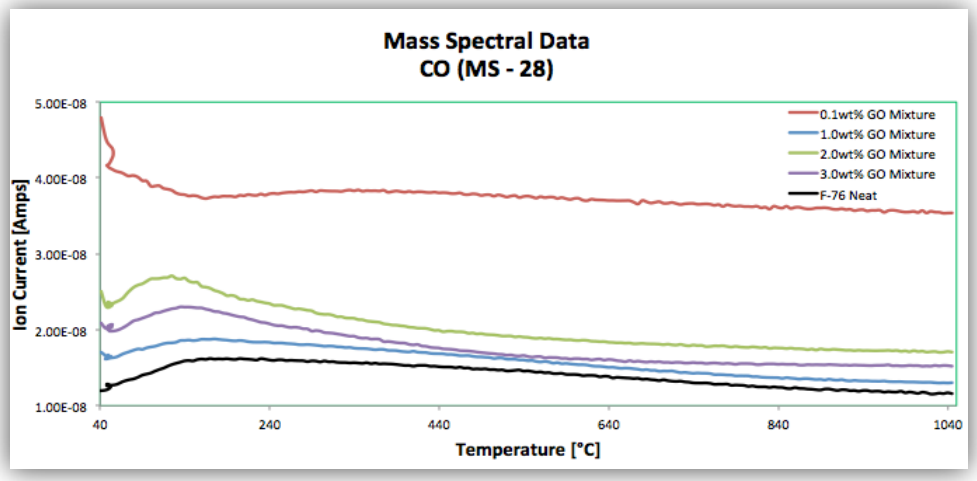


Figure 33. Mass Spectral Data for F-76 and the GO-Mixed Fuels for CO

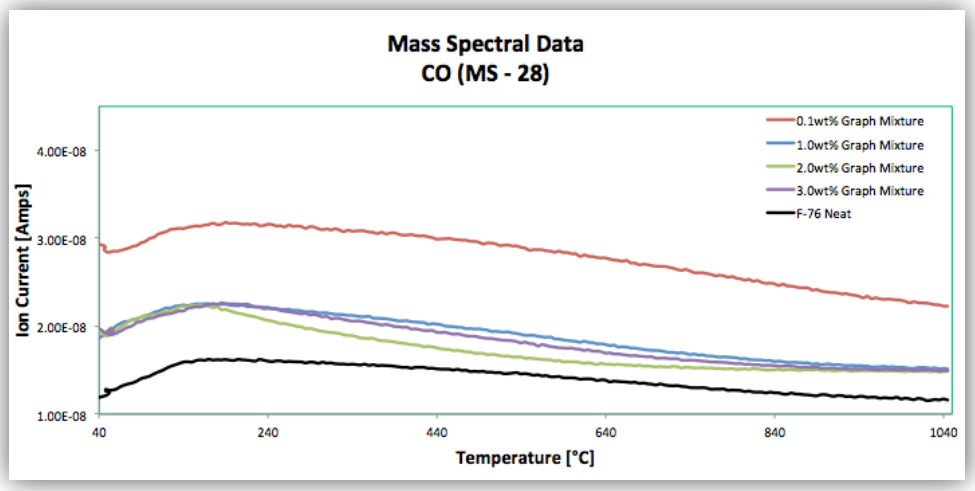


Figure 34. Mass Spectral Data for F-76 and the G-Mixed Fuels for CO

### *c. Carbon Dioxide*

$CO_2$ (mass 44) signatures were collected and plotted in Figures 35 and 36 for all samples analyzed. Every sample shows $CO_2$ signatures over the combustion of F-76 and for the burn off of solid byproducts up to ~660° C. All the GO-mixed and G-mixed fuels' signatures appear to be within the same range or higher (GO fuels) of the signature for F-76, indicating similar levels of combustion byproducts.

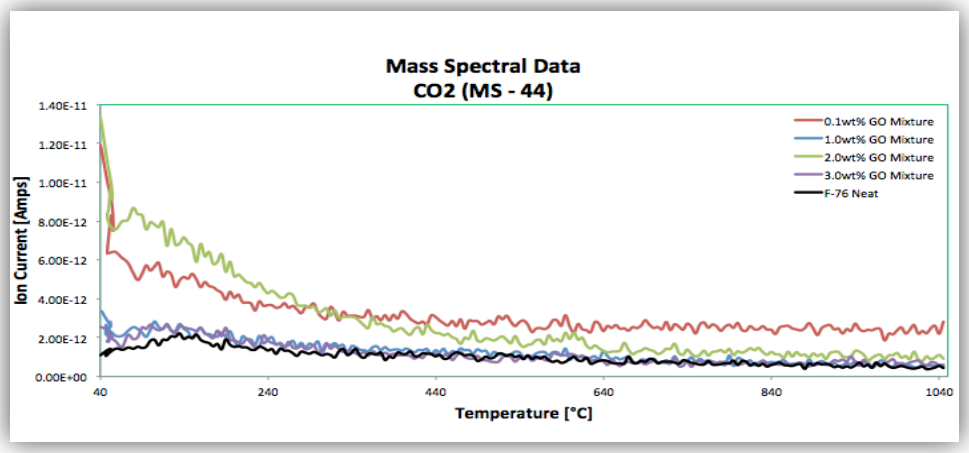


Figure 35. Mass Spectral Data for F-76 and the GO-Mixed Fuels for $CO_2$

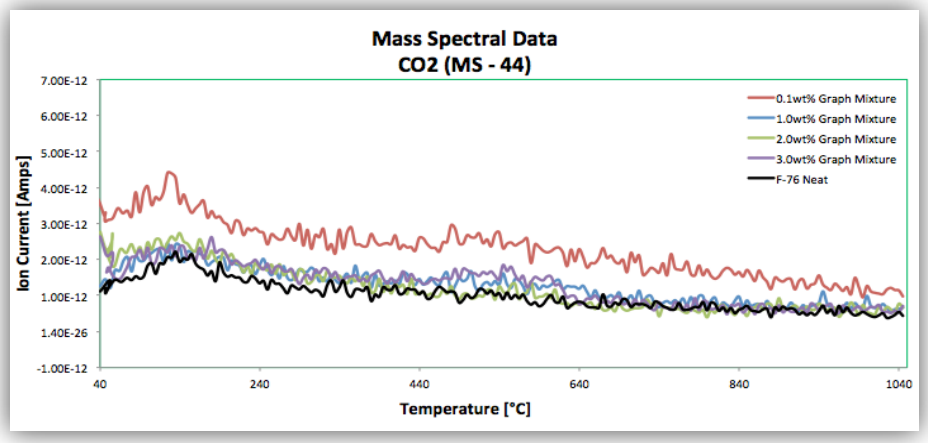


Figure 36. Mass Spectral Data for F-76 and the G-Mixed Fuels for $CO_2$

### *d. Other Gases Studied*

As mentioned at the beginning of this section, some commercial diesel fuels may contain contaminants like NO, $NO_2$, $SO_2$, or $SO_3$ (or any combination of these). It is mandated that F-76 not contain any of these set forth by the DON [31]. However, in the interest of thoroughness, we analyzed several samples of F-76 for each of these to ensure our F-76 was within regulation. Figure 37 displays signatures of NO, and there appeared to be no peaks or ion currents to indicate any contamination. Similarly, the F-76 was analyzed for each of the others contaminants with similar results.

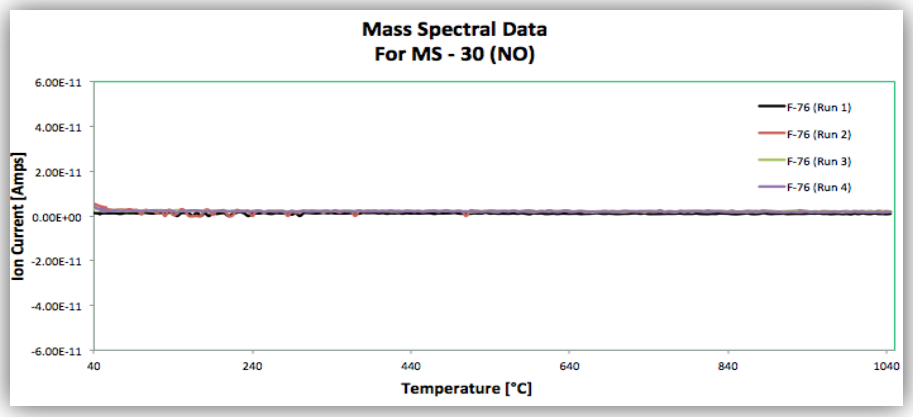


Figure 37. Mass Spectral Data of F-76 Runs for NO.

### 6. Cetane Number Testing

Southwest Research Institute collected several characteristics parameters from each of the fuel samples we mixed and shipped for analysis (see Table 7). These tests were conducted at high burn-rates that would be similar to practical settings. Across all samples, gross heat and net heat if combustion were equivalent. There also appeared to be no effect on cetane number with the addition of the GO and G. There was no conclusive evidence that these mixtures affected the F-76.

Table 7. Fuel Sample Characteristics Conducted by Southwest Research Institute

| Test [ASTM Reference] | | Units | F-76 | 0.1wt% GO/F-76 | 0.1wt% G/F-76 |
|---|---|---|---|---|---|
| Gross Heat Value [D240G] | MJ Heat | MJ/kg | 45.55 | 45.514 | 45.516 |
| | BTU Heat | BTU/lbf | 19583 | 19568 | 19568 |
| Net Heat of Combustion [D240N] | MJ Heat | MJ/kg | 43.122 | 42.702 | 42.709 |
| | BTU Heat | BTU/lbf | 18539 | 18358 | 18362 |
| Sulfur Content [D2622_07] | Sulfur Average | ppm | 1889.6 | 2758.2 | 1972.4 |
| Hydrogen Content [D3701] | Hydrogen | mass % | 11.45 | 13.25 | 13.23 |
| Cetane Assessment [D613] | Cetane Number | N/A | 48.6 | 48.5 | 49.9 |

### 7. Marine Diesel Testing

For the following section, we analyze data retrieved from the diesel engine for the three fuels mentioned in Chapter II, Section D. Specifically, we will compare pressure versus CAD, strain gauge versus CAD, and heat of release data of the GO-mixed and G-mixed fuels against that of F-76. We will also discuss any correlations with the information obtained from DSC and from Southwest Research Institute pertaining to the cetane numbers of the mixed fuels. It should be noted that the data found in this section was retrieved on the same day so that no variations of environmental parameters would

affect the data. The environmental parameters included the barometric pressure at 101456.2045 Pa (29.96 inHg) and the outside temperature at 16.6667 ° C (62.0 ° F).

### *a. Additive Injection inside Diesel Engine*

Before continuing into the data we obtained in the following paragraphs, we mixed the fuels in the same ratios as with the fuel samples we contracted out to Southwest Research Institute. However, when we pumped the fuels into the testing tank (see right-side image of Figure 16), we noticed that their colors were diluted and not consistent with the mixtures in Figure 38. We continued to run the fuels and collect data, and upon inspection after testing each fuel/additive mixture, we found that some of the additive (both GO and G) had been separated from the fuel inside the diesel's fuel/water separator. While we did see colorations for the additives in the fuel gauge on the tank, it is impossible to know just how much of the additives were collected by the separator. Therefore, we will continue to refer to the mixtures in this section by 0.1wt% GO/F-76 and 0.1wt% G/F-76.

Figure 38. (Left to Right) 2000 ml F-76, 2000 ml 0.1wt% GO/F-76 Mixture, and 1500 ml 0.1wt% G/F-76 Mixture

### *b. Pressure versus Crank Angle*

Figures 39–42 and 44–-47 show the pressure traces for 1100 rpm and 1700 RPM, respectively, and their respective loadings, with the three fuel types overlaid in each figure. Data was collected and complied using the MATLAB coding is included in Appendix C.

Peak pressures (PP) (Table 8) and the angles (AOP) at which those peak pressures occurred is shown in Table 9 for each of the three fuels at their respective speed/torque points. The angles are based on the position of the piston in its cycle. 360° refers to top dead center (TDC). 180° and 540° refer to the start and finish of the cylinder's cycle, respectively. In all cases, the AOP showed little to no variation as compared to F-76. There was a slight increase in peak pressure for the 1100 RPM / 162.6982 N-m (120 ft-lbf) speed load point for both the GO and graphene (see Figure 43).

Table 8. Peak Pressure Corresponding to Angle of Peak Pressure for Each Fuel in Diesel

| Peak Pressure [bars] | | | | |
|---|---|---|---|---|
| Speed [RPM] | Torque [ft-lbf] | F-76 | 0.1wt% GO/F-76 | 0.1wt% G/F-76 |
| 1100 | 50 | 44.6893 | 44.6158 | 45.0151 |
| | 75 | 45.3844 | 47.5412 | 47.2021 |
| | 95 | 50.6289 | 49.4053 | 48.7165 |
| | 120 | 51.6421 | 54.3333 | 55.1316 |
| 1700 | 50 | 46.5396 | 45.5293 | 45.413355 |
| | 75 | 48.2243 | 46.9498 | 46.9215 |
| | 95 | 50.6147 | 51.33855 | 51.7032 |
| | 120 | 54.5009 | 53.283 | 53.7791 |

Table 9. Angle of Peak Pressure for Each Fuel Testing in Diesel

| Angle of Peak Pressure [degrees] | | | | |
|---|---|---|---|---|
| Speed [RPM] | Torque [ft-lbf] | F-76 | 0.1wt% GO/F-76 | 0.1wt% G/F-76 |
| 1100 | 50 | 365.5 | 365.875 | 366.125 |
| | 75 | 366.375 | 366.375 | 366.875 |
| | 95 | 367.25 | 367.25 | 367.75 |
| | 120 | 367.875 | 368 | 368 |
| 1700 | 50 | 369 | 368.875 | 368.875 |
| | 75 | 369.275 | 369.25 | 369 |
| | 95 | 369.5 | 369.75 | 369.5 |
| | 120 | 369.875 | 369.625 | 370 |

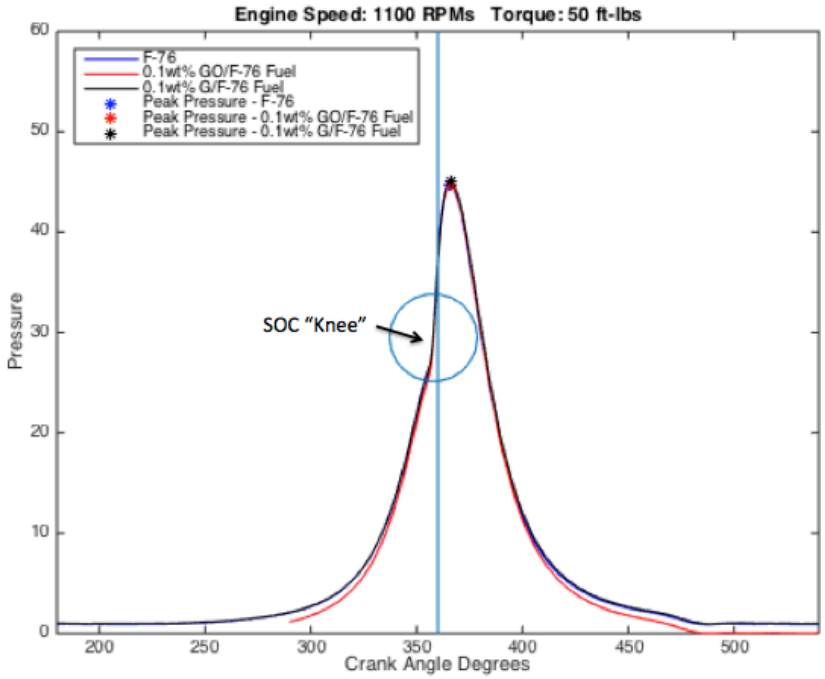


Figure 39. Pressure versus CAD for Engine at 1100 RPMs, 50 ft-lbf Torque

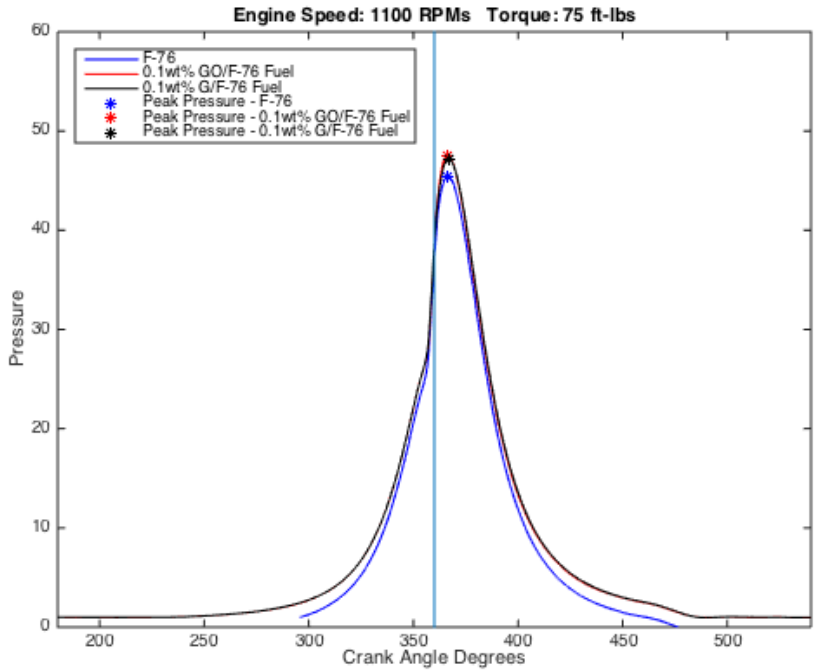


Figure 40. Pressure versus CAD for Engine at 1100 RPMs, 75 ft-lbf Torque

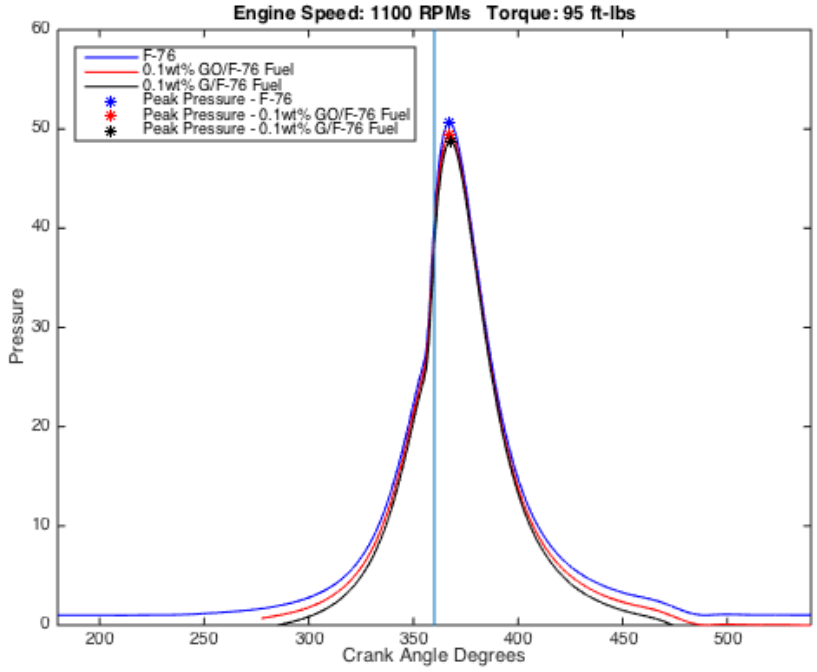


Figure 41. Pressure versus CAD for Engine at 1100 RPMs, 95 ft-lbf Torque

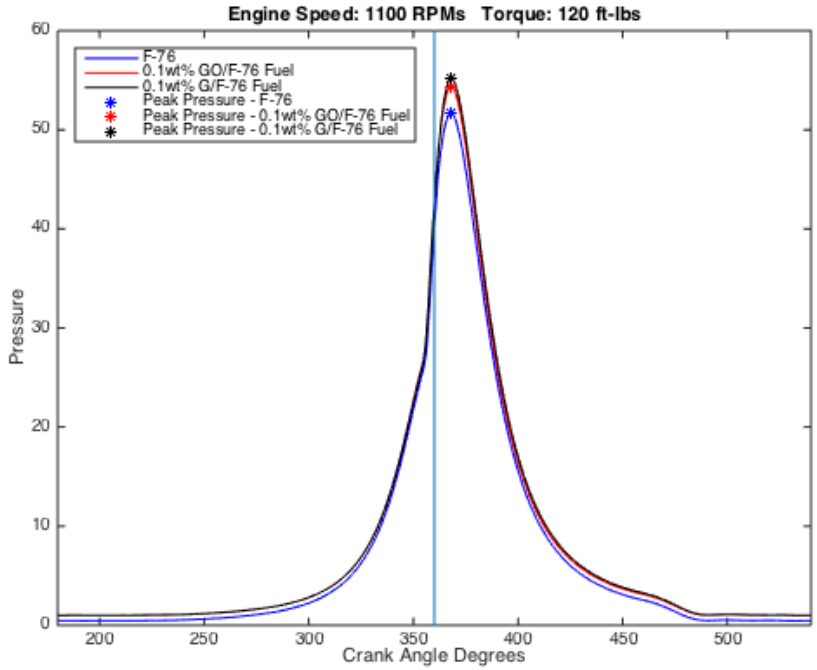


Figure 42. Pressure versus CAD for Engine at 1100 RPMs, 120 ft-lbf Torque

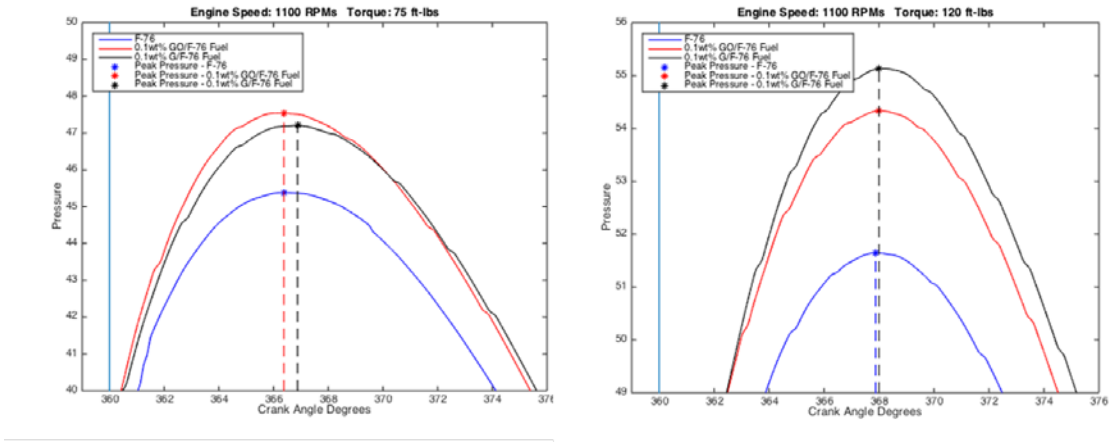


Figure 43. Expanded View of Press/CAD Data for Engine at 1100 RPMs for 75 and 120 ft-lbf of Torque

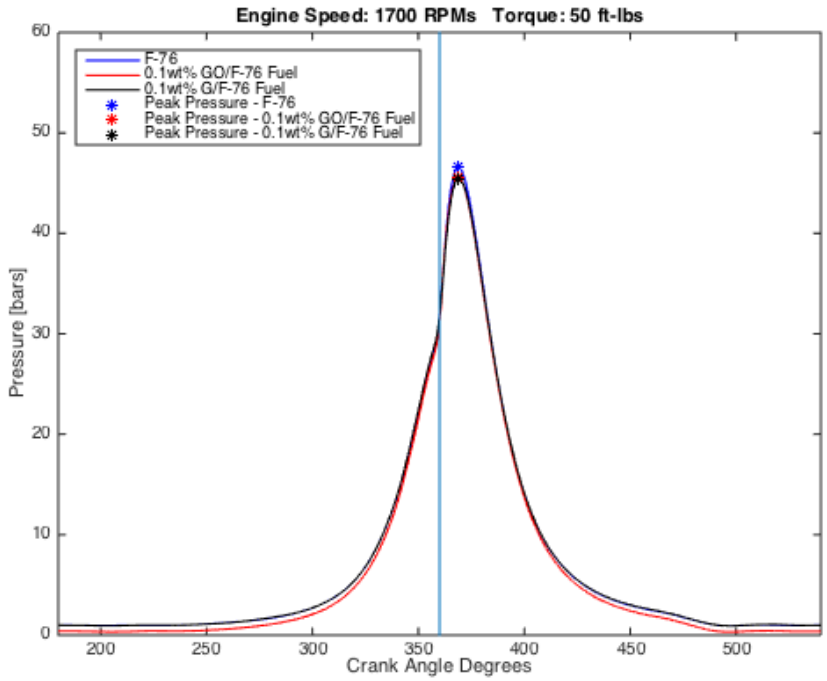


Figure 44. Pressure versus CAD for Engine at 1700 RPMs, 50 ft-lbf Torque

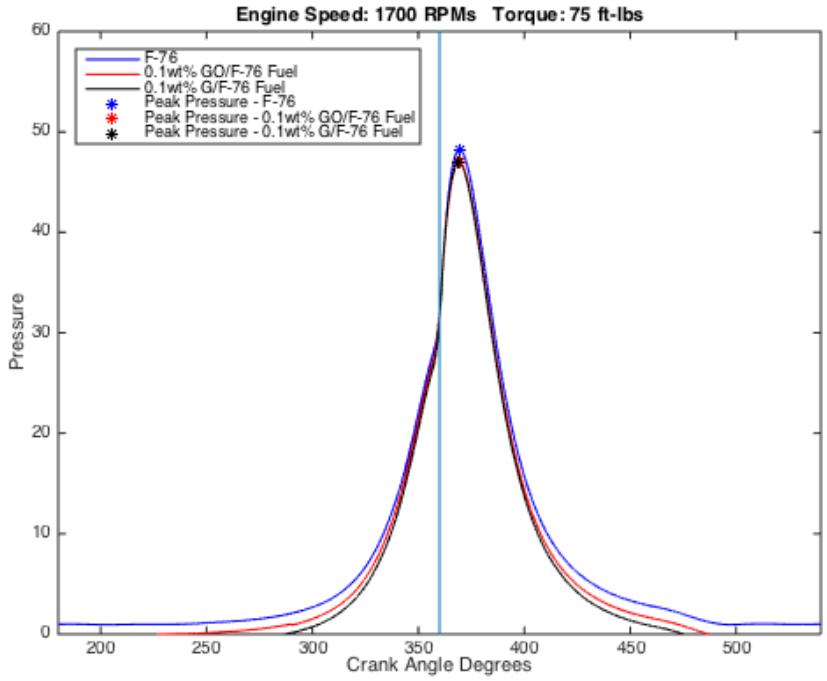


Figure 45. Pressure versus CAD for Engine at 1700 RPMs, 75 ft-lbf Torque

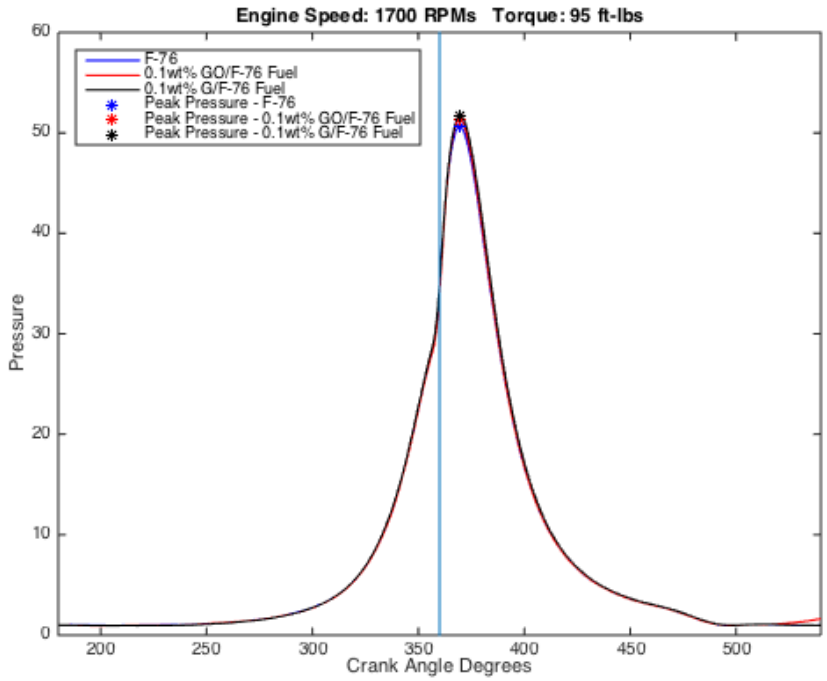


Figure 46. Pressure versus CAD for Engine at 1700 RPMs, 95 ft-lbf Torque

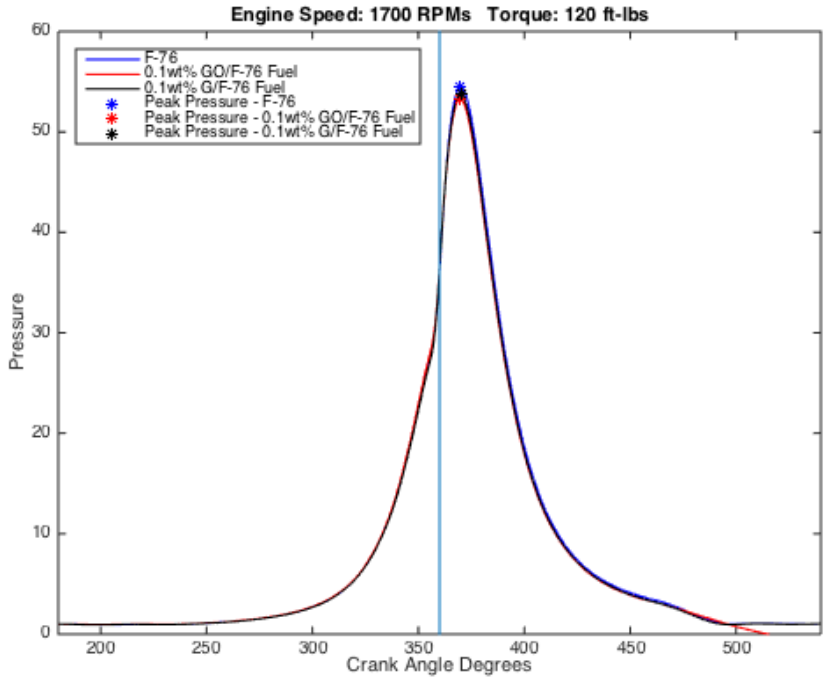


Figure 47. Pressure versus CAD for Engine at 1700 RPMs, 120 ft-lbf Torque

### *c. Maximum Rate Release*

Another indication that GO and G had effects on the combustion inside the diesel was the rate of release. A high rate of release can potentially be harmful to an engine, resulting in the possibility of engine knocking. Engine knocking occurs when pockets of fuel/air mixtures are detonated outside of the combustion cycle, causing shock waves inside the engine to occur which can be catastrophic to an engine.

Table 10 lists the maximum rate of release (MRR) values for the fuel samples ran through the diesel. These values were determined using the MATLAB coding in Appendix E by taking the derivative of the pressure data used to create those plots in and dividing those by the derivative of the CAD data used in the same plots. Table 10 provides the numerical data for the MRR and Figure 48 shows this data in a bar graph to show just how the additives affected the MRR. For 1100 RPM, MRR for GO appears to be lower than F-76 at lower torques, while G appears to be lower than F-76 at higher torques. At 1700 RPM, GO and G seem to lower the MRR except for the G-mixed fuel at 120 ft-lbf of torque.

Table 10. Maximum Rate of Release

| Maximum Rate of Release [Joules/CAD] | | | | |
|---|---|---|---|---|
| Speed [RPM] | Torque [ft-lbf] | F-76 | 0.1wt% GO/F-76 | 0.1wt% G/F-76 |
| 1100 | 50 | 7.5846 | 4.3615 | 7.8974 |
| | 75 | 8.0542 | 7.7228 | 8.1064 |
| | 95 | 6.0224 | 6.2125 | 5.4298 |
| | 120 | 6.1042 | 6.2894 | 5.3462 |
| 1700 | 50 | 6.9231 | 4.5869 | 5.2628 |
| | 75 | 8.8718 | 4.8205 | 7.7372 |
| | 95 | 9.2051 | 6.0192 | 8.7051 |
| | 120 | 6.5513 | 5.4564 | 10.1154 |

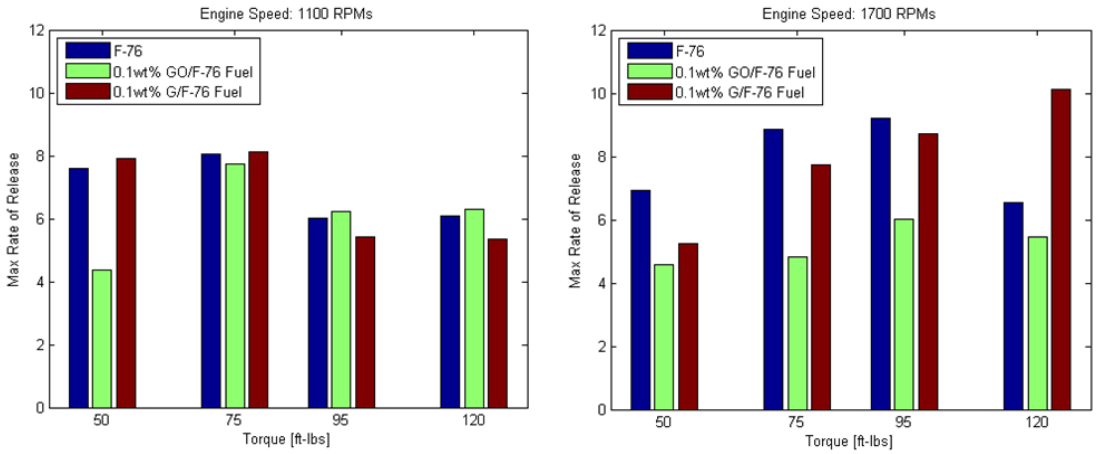


Figure 48. Bar Graph for Maximum Rate of Heat Release of F-76, 0.1wt% GO/F-76 Mixture, and 0.1wt% G/F-76 Mixture.

### *d. Strain Gauge versus Crank Angle Degrees*

As previously defined, IGD is the difference between SOC and SOI where both of these quantities must be determined. To characterize the start of injection for this engine, a strain gage was been mounted on the rocker arm of the fuel injector. The gage is arranged in a half-bridge configuration and its signal was amplified using an instrumentation amplifier. The resulting strain signals were analyzed to confirm previous results [44], specifically that SOI was independent of speed, load and fuel type.

Figures 49–56 (Figure 57 showing a close-up of the signal) show the strain gage signals versus CAD for various speeds and loadings. The raw signals suffered vertical drift as well as noise. A vertical bias was applied to best horizontally align the signals relative to the common initial increase of the signal. Overlap of the signals then was taken to signify SOI. Though this method does not definitively determine the exact SOI, it does provide a reasonable reference so that qualitative characteristics can be deduced.

According to Petersen *et al.,* SOI for F-76 should occur near 10° before TDC (BTC) [44]. Table 11 lists the angle at which SOI occurred in each of the fuel samples at the engine's speed/torque runs. Most of the additive fuels had injection around 14° BTC staying consistent with the SOI points for F-76, and there did not appear to be any differences in the strain gauge values of the fuel mixtures compared to F-76. For this thesis, 14° BTC was be used.

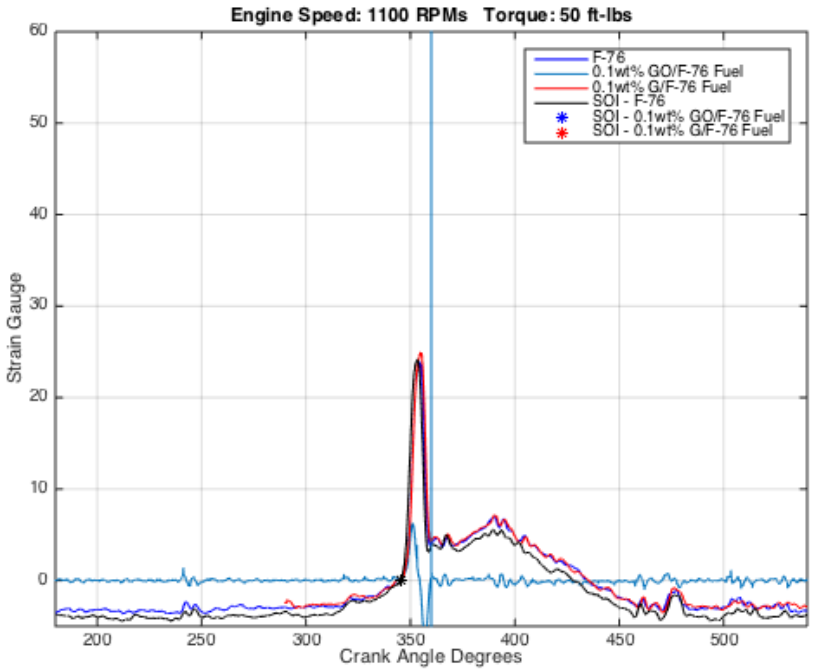


Figure 49. Strain Gauge versus CAD for Engine at 1100 RPM, 50 ft-lbf Torque

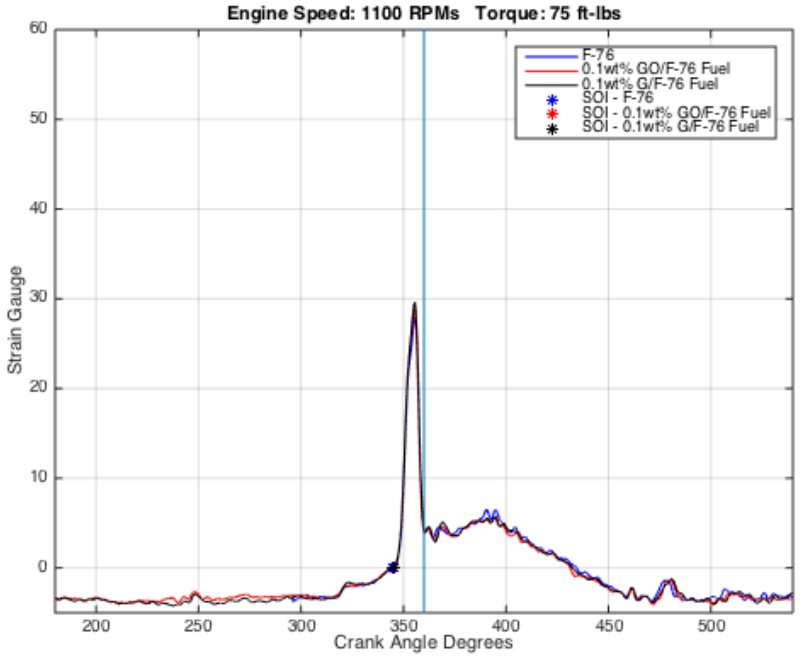


Figure 50. Strain Gauge versus CAD for Engine at 1100 RPM, 75 ft-lbf Torque

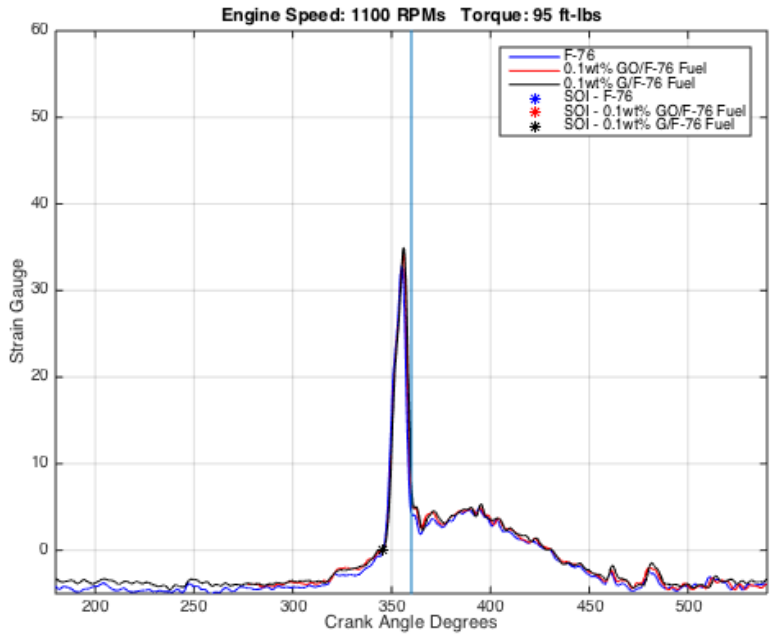


Figure 51. Strain Gauge versus CAD for Engine at 1100 RPM, 95 ft-lbf Torque

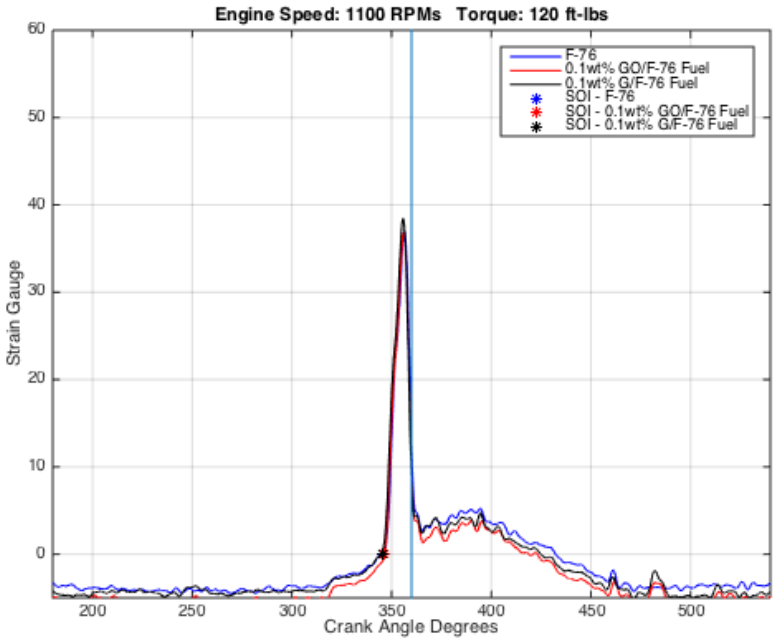


Figure 52. Strain Gauge versus CAD for Engine at 1100RPM, 120 ft-lbf Torque

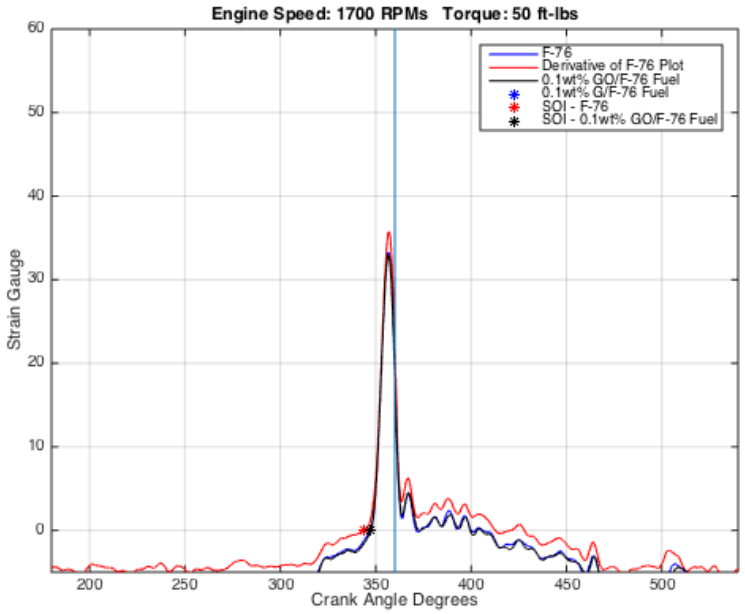


Figure 53. Strain Gauge versus CAD for Engine at 1700 RPM, 50 ft-lbs Torque

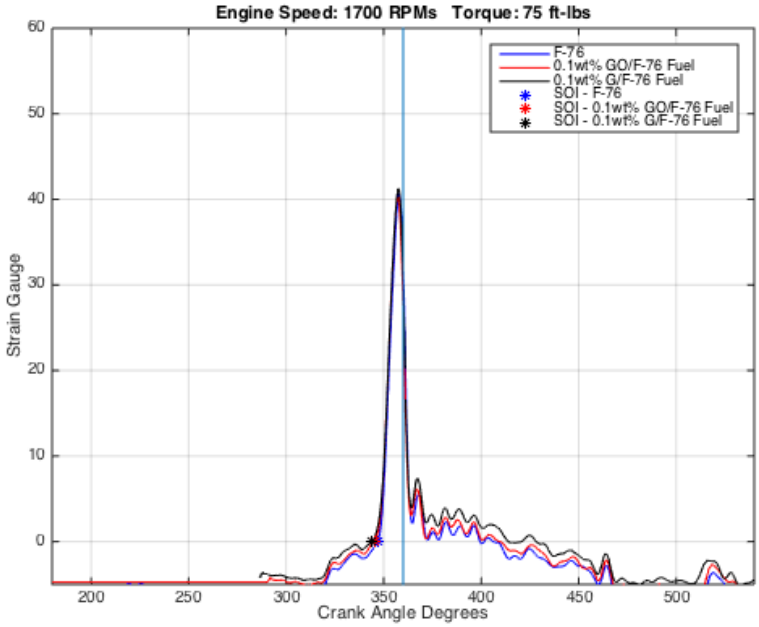


Figure 54. Strain Gauge versus CAD for Engine at 1700 RPM, 75 ft-lbs Torque

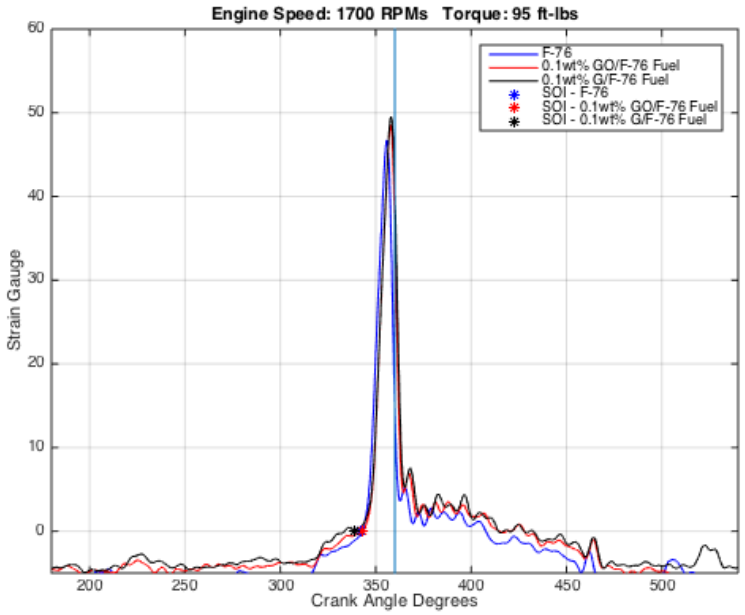


Figure 55. Strain Gauge versus CAD for Engine at 1700 RPM, 95 ft-lbf Torque

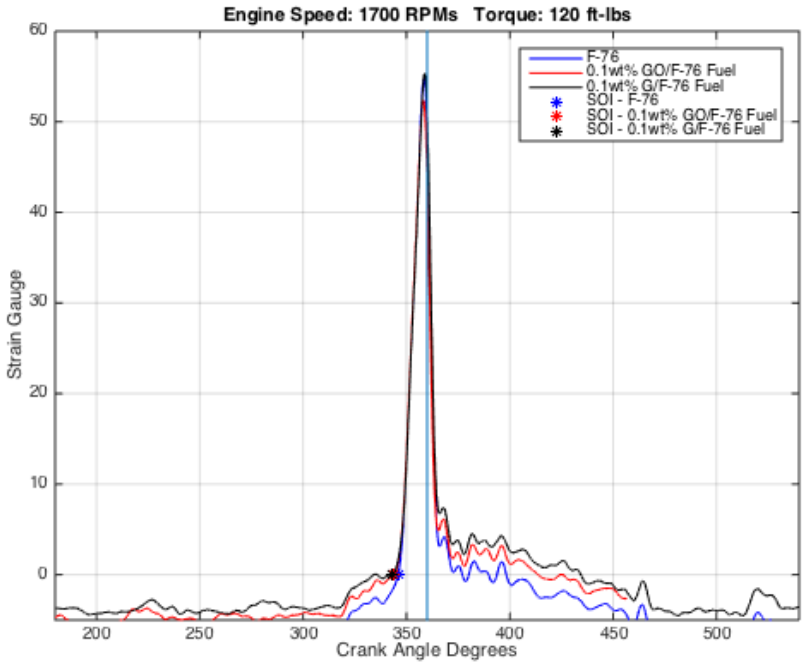


Figure 56. Strain Gauge versus CAD for Engine at 1700 RPM, 120 ft-lbf Torque

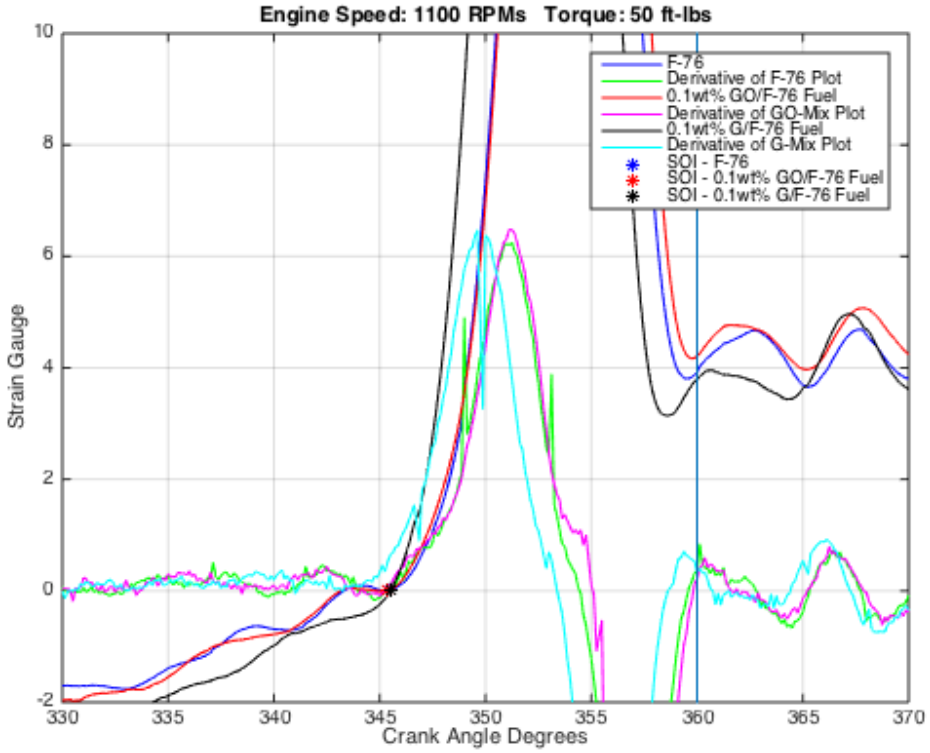


Figure 57. Expanded View of Strain Gauge/CAD Data for Engine at 1100 RPMs and 50 ft-lbf of Torque

Table 11. Start of Injection before Top Dead Center

| Start of Injection (BTC) [degrees] | | | | |
|---|---|---|---|---|
| Speed [RPM] | Torque [ft-lbf] | F-76 | 0.1wt% GO/F-76 | 0.1wt% G/F-76 |
| 1100 | 50 | 14.625 | 14.625 | 14.5 |
| | 75 | 15.75 | 14.5 | 14.875 |
| | 95 | 14.125 | 14.125 | 14.25 |
| | 120 | 13.875 | 13.5 | 14.75 |
| 1700 | 50 | 12.875 | 16 | 12.5 |
| | 75 | 13 | 14.875 | 15.875 |
| | 95 | 17.5 | 17.25 | 20.75 |
| | 120 | 14 | 16 | 16.625 |

### *e. Heat of Release*

Figure 58 shows a heat of release profile for F-76 at 1700 rpm and 120 ft-lbf torque. SOC is determined by finding the maximum slope of the curve and then projecting a line to the zero baseline. The intersection determines SOC. Similar analysis was done to determine SOC for GO and G data. From this analysis, the SOC for the GO and G were comparable to that of F-76, that is, no difference was determined.

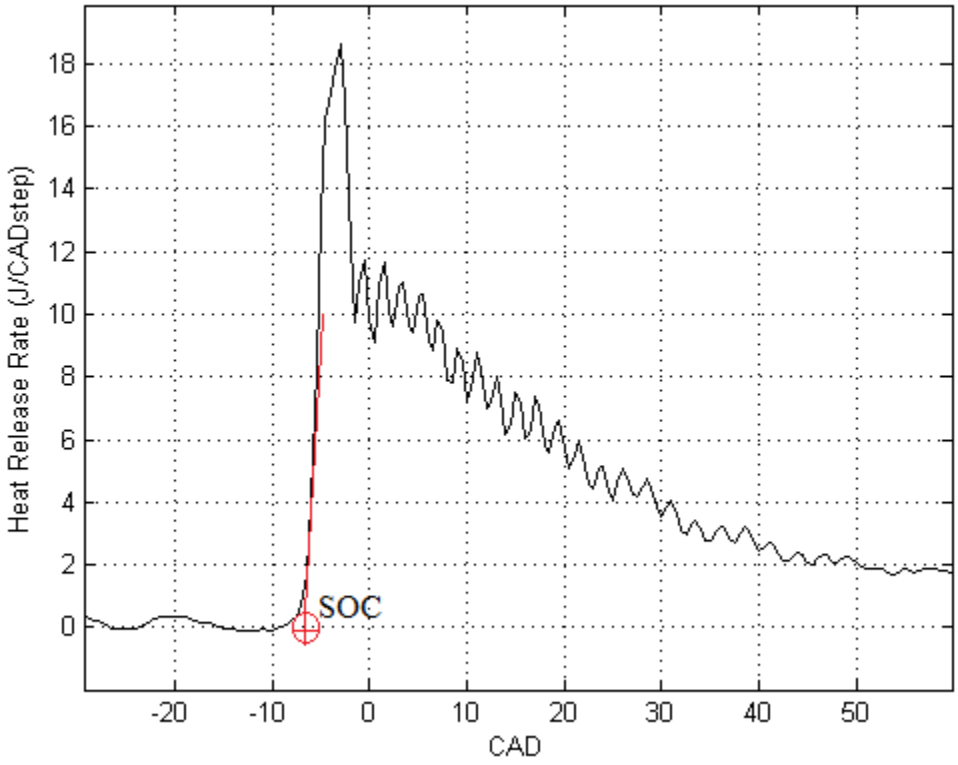


Figure 58. Heat of Release at 1700 rpm, 120 ft-lbf

### *f. Lambda Values of Diesel Exhaust*

Lambda values were collected from the exhaust gases of the diesel engine using the lambda meter in Figure 59. Lambda values are used to calculate the ratio between the amount of oxygen actually present in a combustion chamber versus the amount that should have been present for perfect combustion [48]. Thus, for perfect combustion the amount inside the chamber would be equal to the amount required, making for a one-to-one ratio. Ratios greater than 1:1 mean an overabundance of oxygen inside the chamber, and ratios less than that mean that not enough oxygen was present inside the chamber for complete combustion.


Figure 59. ETAS LA4-4.9 Lambda Meter

In Table 12, we collected lambda values for F-76, 0.1wt% GO/F-76 fuel, and 0.1wt% G/F-76 fuel at engine speeds of 1100 and 1700 RPM, at torques of 50, 75, 95, and 120 ft-lbf. As illustrated in Figure 60, the lambda values decreases as torque increased in each of the three fuels. Comparing the fuel/additive mixtures with that of F-76, one can also see that the additives decreased the lambda values at the same speed/torque runs. This could indicate that more complete combustion occurs inside the cylinders.

Table 12. Lambda Values for Fuel Samples in Diesel Engine

| Lambda Values | | | | |
|---|---|---|---|---|
| Speed [RPM] | Torque [ft-lbf] | F-76 | 0.1wt% GO/F-76 | 0.1wt% G/F-76 |
| 1100 | 50 | 6.55 | 6.37 | 4.89 |
| | 75 | 5.64 | 5.58 | 4.62 |
| | 95 | 5.01 | 5.11 | 4.31 |
| | 120 | 4.88 | 4.42 | 4.11 |
| 1700 | 50 | 5.55 | 5.37 | 5.63 |
| | 75 | 4.98 | 4.97 | 4.94 |
| | 95 | 4.60 | 4.53 | 4.60 |
| | 120 | 4.31 | 4.17 | 4.38 |

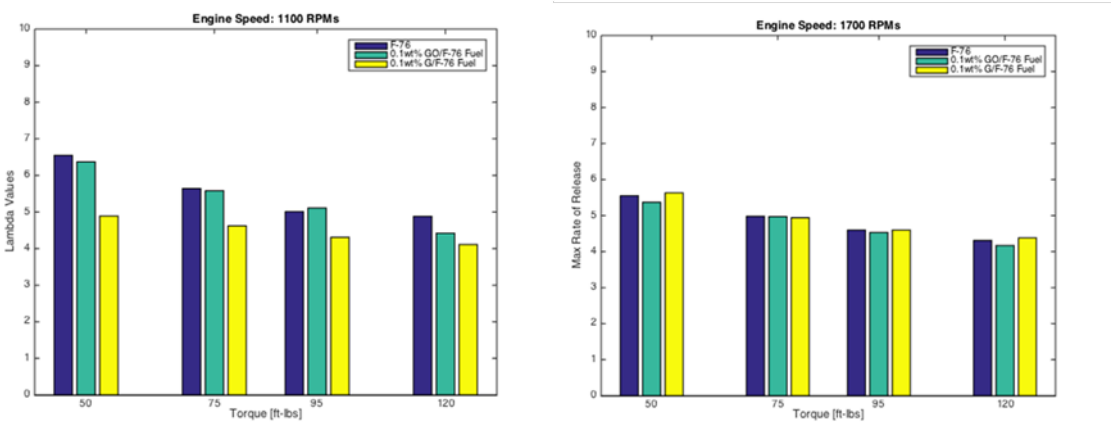


Figure 60. Bar Graph for Lambda Values of Diesel Exhaust for F-76, 0.1wt% GO/F-76 Mixture, and 0.1wt% G/F-76 Mixture

### *g. Ignition Delay*

Ignition delay difference, $IGD_{GO/GRAPH}$-$IGD_{F76}$, was calculated for both the GO and G mixtures. As mentioned previously for the SOC data, no discernible difference was found from that analysis. This translates further to the fact that no difference in ignition delay differences for GO and G were measured as compared to F-76.

THIS PAGE INTENTIONALLY LEFT BLANK

# IV. CONCLUSIONS AND FUTURE WORK

During the course of this thesis, several milestones were achieved, as well as several conclusions obtained that provided insight to our hypotheses.

Graphite oxide (GO) and graphene (G) were successfully prepared in our laboratory. We synthesized GO by oxidation of graphite, while we prepared G through thermal exfoliation of GO. XRD and SEM techniques were employed to verify their crystalline structures and their particle size and distribution, respectively. We also studied their calorimetric characteristics using the DSC and their mass reduction characteristic with TGA to illustrate these parameters as they were exposed to slow burning-rates in an air environment.

Using NATO F-76 diesel fuel as our basis fuel, we prepared GO and G as additives to be mixed with the fuel in quantities from 0.1 wt% up to 3.0 wt%. Comparing to F-76 neat, we studied their properties using DSC, TGA and MS. We found that in all GO-mixed fuels (0.1, 1, 2 and 3%), energy output during combustion at slow burn-rates improved over F-76. For the G-mixed fuels the results were less consistent, showing improved energy output only for samples with additives in 0.1 and 2%. TGA for all mixtures showed a complete weight loss in a single step for all samples. MS analysis studied such mass signature related to water, carbon dioxide, carbon monoxide, and other gases typical in fuels. We saw that water and carbon dioxide had similar burn off temperatures across all mixtures compared to F-76. Ultimately, we concluded that 0.1wt% GO and G mixtures should be studied further in practical combustive reactions settings and compared to F-76. Those samples contain the minimum amount of additive but still show an increase in the heat flows measured when compared to bare fuel.

We prepared 1.5-liter quantities of 0.1wt% GO/F-76, 0.1wt% G/F-76 mixtures, and F-76 neat to obtain analysis of cetane number, gross heat value, and net heat of combustion analysis with the assistance of Southwest Research Institute. Through a high burn-rate process, data showed there was no conclusive evidence of changes in any of these parameters against F-76.

We also prepared the same mixtures in the same quantities to study in a practical setting, namely, using a Detroit 3-53 marine diesel engine. Of note, we found that the fuel/water separator was separating an unknown amount of our additives in our fuel/additive mixtures, when directly pumped into our tank, although the fuel in the fuel gauge still contained some additive. We studied such parameters as pressure and strain versus crank angle of the pistons, maximum rate of release (MRR), oxygen content (lambda value) of exhaust gases, heat of release relating to energy output, and ignition delay, concluding that:

- Slight increases in peak pressure (PP) for both GO-mixed and G-mixed fuels over F-76, relating to the possibility of higher heat releases, while the any angle of peak pressure (AOP) changes were minimal.
- Decreased MRR for both GO-mixed and G-mixed fuel over F-76, relating to more complete combustion cycles and decreasing the likelihood of engine knocking.
- Consistent SOI points around 14° before TDC and consistent strain inside the cylinders for the enhanced fuels and F-76, relating to decreased likelihood of injection problems and thermal damage inside the cylinders.
- There were no differences found in the heat of releases or start of combustion points for either of the additive mixtures against F-76 at either 1100 or 1700 RPM.
- Decreased lambda values for both GO-mixed and G-mixed fuels over F-76 when compared at the same speeds and torques, and decreased lambda values as speed and torque increased overall. This relates the possibility of more complete combustion inside the cylinders.
- Consequentially, as there were no differences in heat of release or SOC, the ignition delay for both additive mixtures translated no difference against F-76.

Future work is recommended in two areas. The first is with the experimental setup. We had issues with the GO and G separating in the fuel/water separator. An evaluation of the diesel engine setup should be done to determine a more appropriate method of fuel injection to fully evaluate the potential of using these additives.

Second, the quantity of the fuel samples in which this study used was minimalistic. Larger quantities (gallons) should be created in order to obtain many cycles of data in the diesel engine to further develop data, which could better represent the potential of these additives.

THIS PAGE INTENTIONALLY LEFT BLANK

# APPENDIX A. COST ANALYSIS OF GRAPHITE OXIDE AND GRAPHENE IN HOUSE

Table 13 includes a list of each product used for the synthesis of GO with the prices of the bulk chemicals, as well as the price of the batch sizes taken at a percentage of the bulk price.

Table 13. Estimated Costs for In-house Synthesis of GO, after [49]–[51]

| GO Production | | | | | |
|---|---|---|---|---|---|
| | Units | Bulk | | Batch-Size | |
| Graphite Nanopowder | g | 25 | $41.10 | 0.75 | $1.23 |
| H2SO4 | ml | 500 | $48.00 | 90 | $8.64 |
| H3PO4 | ml | 500 | $79.00 | 10 | $1.58 |
| KMnO4 | g | 500 | $113.77 | 4.5 | $1.02 |
| H2O2 | ml | 500 | $90.10 | 1.5 | $0.27 |
| DI Water | ml | 18927.1 | $40.68 | 120 | $0.26 |
| HCl | ml | 500 | $61.90 | 360 | $44.57 |
| Ethanol | ml | 500 | $66.60 | 360 | $47.95 |
| Estimate Per Batch | | | | 1.4 | $105.53 |
| Estimate Per 1 gram | | | | 1 | $75.38 |

THIS PAGE INTENTIONALLY LEFT BLANK

# APPENDIX B. PARTICULATE ANALYSIS OF SCANNING ELECTRON MICROSCOPY IMAGES

Figures 61 shows particle areas GO using SEM imaging.

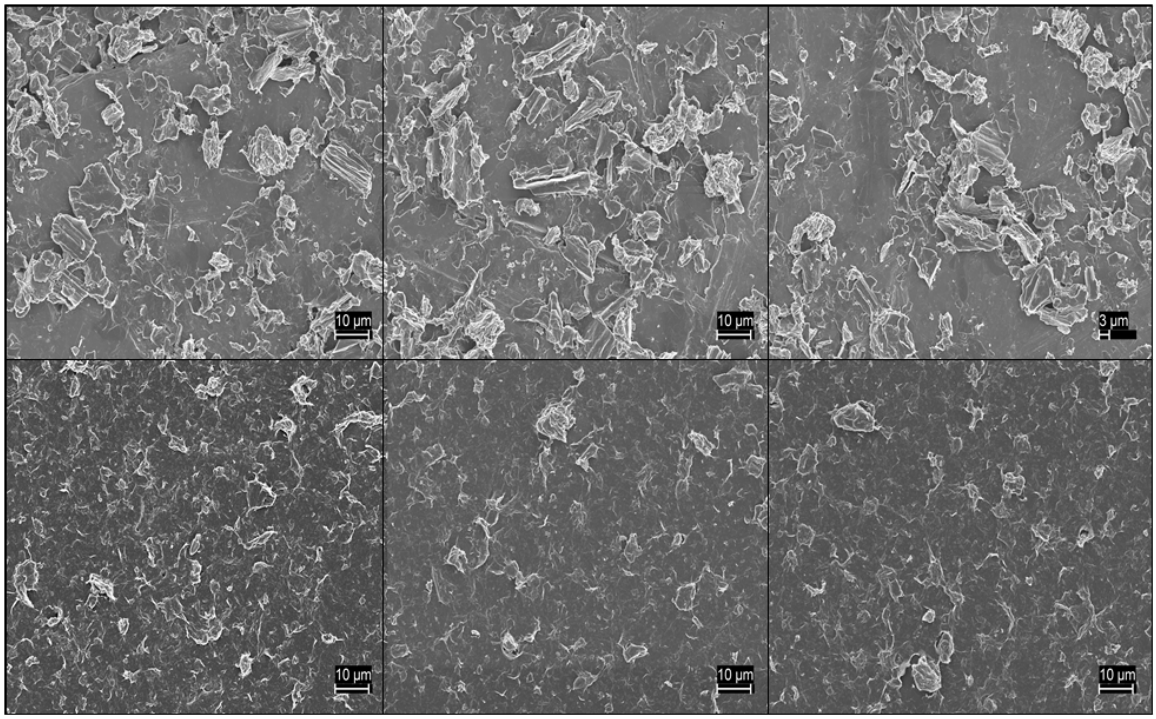


Figure 61. GO Particles after Five Minutes of Grinding (Top Row), GO Particles after Fifteen Minutes of Grinding (Bottom Row)

THIS PAGE INTENTIONALLY LEFT BLANK

# APPENDIX C. PRESSURE VERSUS CAD MATLAB CODING

```
clear all; close all; clc;

t = 180:0.0001:540;
%%%%%%%%%% 1700 RPMs @ 50 ft-lbs Torque %%%%%%%%%%
figure;
% Reads the excel spreadsheet and the specified sheet.
[v,Press,vt] = xlsread('DieselTests.xlsx',1);
% Pressure (bars) and CAD data pulled
Press = v(1:2:7051,1); CAD = v(1:2:7051,3);
% Plots Pressure (y-axis) versus CAD (x-axis)
plot(t,spline(CAD,Press,t),'b')
title('Engine Speed: 1700 RPMs   Torque: 50 ft-lbs')
ylabel('Pressure [bars]')
xlabel('Crank Angle Degrees')
% Specifies the range of data 360 = 0 degrees (CAD), 180 = -180 degrees,
  % and  540 = 180 degrees.
xlim([180 540]);
% Specifies the range for pressure duirng fuel cycle.
ylim([0 60]);
% Discovers the peak pressure and angle of peak pressure
[maxPress,I] = max(Press);
maxPress;
maxCAD = CAD(I);
% Defines the Max Rate of Heat Release
m = diff(Press)./diff(CAD);
MRR_1700_50_F76 = max(m);
hold on

[v,Press,vt] = xlsread('DieselTests.xlsx',3);
Press = v(1:2:3861,1); CAD = v(1:2:3861,3);
plot(t,spline(CAD,Press,t),'r')
% [maxPress,I] = max(Press);
% maxPress
% maxCAD = CAD(I)
m = diff(Press)./diff(CAD);
MRR_1700_50_GO = max(m);

[v,Press,vt] = xlsread('DieselTests.xlsx',5);
Press = v(1:2:6987,1); CAD = v(1:2:6987,3);
plot(t,spline(CAD,Press,t),'k')
% [maxPress,I] = max(Press);
% maxPress
% maxCAD = CAD(I)
m = diff(Press)./diff(CAD);
MRR_1700_50_G = max(m);

[v,Press,vt] = xlsread('DieselTests.xlsx',9);
Press = v(5,3:4:11); CAD = v(5,2:4:10);
plot(CAD(1),Press(1),'b*',CAD(2),Press(2),'r*',CAD(3),Press(3),'k*')

legend('F-76','0.1wt% GO/F-76 Fuel','0.1wt% G/F-76 Fuel','Peak Pressure
- F-76',...
    'Peak Pressure - 0.1wt% GO/F-76 Fuel','Peak Pressure - 0.1wt% G/F-76
Fuel',...
    'Location','northwest')

line([360 360], [0 60])
```

```
%%%%%%%%%% 1700 RPMs @ 75 ft-lbs Torque %%%%%%%%%%
figure;
[v,Press,vt] = xlsread('DieselTests.xlsx',1);
Press = v(1:2:6013,5); CAD = v(1:2:6013,7);
plot(t,spline(CAD,Press,t),'b')
title('Engine Speed: 1700 RPMs   Torque: 75 ft-lbs')
ylabel('Pressure')
xlabel('Crank Angle Degrees')
xlim([180 540]); ylim([0 60]);
% [maxPress,I] = max(Press);
% maxPress
% maxCAD = CAD(I)
m = diff(Press)./diff(CAD);
MRR_1700_75_F76 = max(m);
hold on

[v,Press,vt] = xlsread('DieselTests.xlsx',3);
Press = v(1:2:6455,5); CAD = v(1:2:6455,7);
plot(t,spline(CAD,Press,t),'r')
% [maxPress,I] = max(Press);
% maxPress
% maxCAD = CAD(I)
m = diff(Press)./diff(CAD);
MRR_1700_75_GO = max(m);

[v,Press,vt] = xlsread('DieselTests.xlsx',5);
Press = v(1:2:4291,5); CAD = v(1:2:4291,7);
plot(t,spline(CAD,Press,t),'k')
% [maxPress,I] = max(Press);
% maxPress
% maxCAD = CAD(I)
m = diff(Press)./diff(CAD);
MRR_1700_75_G = max(m);

[v,Press,vt] = xlsread('DieselTests.xlsx',9);
Press = v(6,3:4:11); CAD = v(6,2:4:10);
plot(CAD(1),Press(1),'b*',CAD(2),Press(2),'r*',CAD(3),Press(3),'k*')
legend('F-76','0.1wt% GO/F-76 Fuel','0.1wt% G/F-76 Fuel','Peak Pressure
- F-76',...
    'Peak Pressure - 0.1wt% GO/F-76 Fuel','Peak Pressure - 0.1wt% G/F-76
Fuel','Location','northwest')

line([360 360], [0 60])

%%%%%%%%%% 1700 RPMs @ 95 ft-lbs Torque %%%%%%%%%%
figure;
[v,Press,vt] = xlsread('DieselTests.xlsx',1);
Press = v(1:2:7245,9); CAD = v(1:2:7245,11);
plot(t,spline(CAD,Press,t),'b')
title('Engine Speed: 1700 RPMs   Torque: 95 ft-lbs')
ylabel('Pressure')
xlabel('Crank Angle Degrees')
xlim([180 540]); ylim([0 60]);
% [maxPress,I] = max(Press);
% maxPress
% maxCAD = CAD(I)
m = diff(Press)./diff(CAD);
MRR_1700_95_F76 = max(m);
hold on

[v,Press,vt] = xlsread('DieselTests.xlsx',3);
```

```
Press = v(1:2:5089,9); CAD = v(1:2:5089,11);
plot(t,pchip(CAD,Press,t),'r')
% [maxPress,I] = max(Press);
% maxPress
% maxCAD = CAD(I)
m = diff(Press)./diff(CAD);
MRR_1700_95_GO = max(m);

[v,Press,vt] = xlsread('DieselTests.xlsx',5);
Press = v(1:2:6917,9); CAD = v(1:2:6917,11);
plot(t,spline(CAD,Press,t),'k')
% [maxPress,I] = max(Press);
% maxPress
% maxCAD = CAD(I)
m = diff(Press)./diff(CAD);
MRR_1700_95_G = max(m);

[v,Press,vt] = xlsread('DieselTests.xlsx',9);
Press = v(7,3:4:11); CAD = v(7,2:4:10);
plot(CAD(1),Press(1),'b*',CAD(2),Press(2),'r*',CAD(3),Press(3),'k*')
legend('F-76','0.1wt% GO/F-76 Fuel','0.1wt% G/F-76 Fuel','Peak Pressure
- F-76',...
    'Peak Pressure - 0.1wt% GO/F-76 Fuel','Peak Pressure - 0.1wt% G/F-76
Fuel','Location','northwest')

line([360 360], [0 60])

%%%%%%%%%% 1700 RPMs @ 120 ft-lbs Torque %%%%%%%%%%
figure;
[v,Press,vt] = xlsread('DieselTests.xlsx',1);
Press = v(1:2:6133,13); CAD = v(1:2:6133,15);
plot(t,spline(CAD,Press,t),'b')
title('Engine Speed: 1700 RPMs   Torque: 120 ft-lbs')
ylabel('Pressure')
xlabel('Crank Angle Degrees')
xlim([180 540]); ylim([0 60]);
% [maxPress,I] = max(Press);
% maxPress
% maxCAD = CAD(I)
m = diff(Press)./diff(CAD);
MRR_1700_120_F76 = max(m);
hold on

[v,Press,vt] = xlsread('DieselTests.xlsx',3);
Press = v(1:2:4200,13); CAD = v(1:2:4200,15);
plot(t,pchip(CAD,Press,t),'r')
% [maxPress,I] = max(Press);
% maxPress
% maxCAD = CAD(I)
m = diff(Press)./diff(CAD);
MRR_1700_120_GO = max(m);

[v,Press,vt] = xlsread('DieselTests.xlsx',5);
Press = v(1:2:7235,13); CAD = v(1:2:7235,15);
plot(t,spline(CAD,Press,t),'k')
% [maxPress,I] = max(Press);
% maxPress
% maxCAD = CAD(I)
m = diff(Press)./diff(CAD);
MRR_1700_120_G = max(m);

[v,Press,vt] = xlsread('DieselTests.xlsx',9);
```

```
Press = v(8,3:4:11); CAD = v(8,2:4:10);
plot(CAD(1),Press(1),'b*',CAD(2),Press(2),'r*',CAD(3),Press(3),'k*')
legend('F-76','0.1wt% GO/F-76 Fuel','0.1wt% G/F-76 Fuel','Peak Pressure
- F-76',...
    'Peak Pressure - 0.1wt% GO/F-76 Fuel','Peak Pressure - 0.1wt% G/F-76
Fuel','Location','northwest')

line([360 360], [0 60])

%%%%%%%%%%%%%%%%%%%%%%%%%%%%%%%%%%%%%%%%%%%%%%%%%%%%%%%%%%%%%%%%%%%%%%%%
%%

%%%%%%%%%% 1100 RPMs @ 50 ft-lbs Torque %%%%%%%%%%
figure;
[v,Press,vt] = xlsread('DieselTests.xlsx',2);
Press = v(1:2:9927,1); CAD = v(1:2:9927,3);
plot(t,spline(CAD,Press,t),'b')
title('Engine Speed: 1100 RPMs   Torque: 50 ft-lbs')
ylabel('Pressure')
xlabel('Crank Angle Degrees')
xlim([180 540]); ylim([0 60]);
% [maxPress,I] = max(Press);
% maxPress
% maxCAD = CAD(I)
m = diff(Press)./diff(CAD);
MRR_1100_50_F76 = max(m);
hold on

[v,Press,vt] = xlsread('DieselTests.xlsx',4);
Press = v(1:2:3961,1); CAD = v(1:2:3961,3);
plot(CAD,Press,'r')
% plot(t,pchip(CAD,Press,t),'r')
% [maxPress,I] = max(Press);
% maxPress
% maxCAD = CAD(I)
m = diff(Press)./diff(CAD);
MRR_1100_50_GO = max(m);

[v,Press,vt] = xlsread('DieselTests.xlsx',6);
Press = v(1:2:10997,1); CAD = v(1:2:10997,3);
plot(t,spline(CAD,Press,t),'k')
% [maxPress,I] = max(Press);
% maxPress
% maxCAD = CAD(I)
m = diff(Press)./diff(CAD);
MRR_1100_50_G = max(m);

[v,Press,vt] = xlsread('DieselTests.xlsx',9);
Press = v(1,3:4:11); CAD = v(1,2:4:10);
plot(CAD(1),Press(1),'b*',CAD(2),Press(2),'r*',CAD(3),Press(3),'k*')

x = 356; y = 27;
plot(x,y,'o','MarkerSize',50)

legend('F-76','0.1wt% GO/F-76 Fuel','0.1wt% G/F-76 Fuel','Peak Pressure
- F-76',...
    'Peak Pressure - 0.1wt% GO/F-76 Fuel','Peak Pressure - 0.1wt% G/F-76
Fuel','Location','northwest')

line([360 360], [0 60])
```

```
%%%%%%%%%%% 1100 RPMs @ 75 ft-lbs Torque %%%%%%%%%%%
figure;
[v,Press,vt] = xlsread('DieselTests.xlsx',2);
Press = v(1:2:6885,5); CAD = v(1:2:6885,7);
% plot(t,pchip(CAD,Press,t),'b')
plot(CAD,Press,'b')
title('Engine Speed: 1100 RPMs   Torque: 75 ft-lbs')
ylabel('Pressure')
xlabel('Crank Angle Degrees')
xlim([180 540]); ylim([0 60]);
% [maxPress,I] = max(Press);
% maxPress
% maxCAD = CAD(I)
m = diff(Press)./diff(CAD);
MRR_1100_75_F76 = max(m);
hold on

[v,Press,vt] = xlsread('DieselTests.xlsx',4);
Press = v(1:2:10895,5); CAD = v(1:2:10895,7);
plot(t,spline(CAD,Press,t),'r')
% [maxPress,I] = max(Press);
% maxPress
% maxCAD = CAD(I)
m = diff(Press)./diff(CAD);
MRR_1100_75_GO = max(m);

[v,Press,vt] = xlsread('DieselTests.xlsx',6);
Press = v(1:2:10035,5); CAD = v(1:2:10035,7);
plot(t,spline(CAD,Press,t),'k')
% [maxPress,I] = max(Press);
% maxPress
% maxCAD = CAD(I)
m = diff(Press)./diff(CAD);
MRR_1100_75_G = max(m);

[v,Press,vt] = xlsread('DieselTests.xlsx',9);
Press = v(2,3:4:11); CAD = v(2,2:4:10);
plot(CAD(1),Press(1),'b*',CAD(2),Press(2),'r*',CAD(3),Press(3),'k*')
legend('F-76','0.1wt% GO/F-76 Fuel','0.1wt% G/F-76 Fuel','Peak Pressure
- F-76',...
    'Peak Pressure - 0.1wt% GO/F-76 Fuel','Peak Pressure - 0.1wt% G/F-76
Fuel','Location','northwest')

line([360 360], [0 60])

%%%%%%%%%%% 1100 RPMs @ 95 ft-lbs Torque %%%%%%%%%%%
figure;
[v,Press,vt] = xlsread('DieselTests.xlsx',2);
Press = v(1:2:10681,9); CAD = v(1:2:10681,11);
plot(t,spline(CAD,Press,t),'b')
title('Engine Speed: 1100 RPMs   Torque: 95 ft-lbs')
ylabel('Pressure')
xlabel('Crank Angle Degrees')
xlim([180 540]); ylim([0 60]);
% [maxPress,I] = max(Press);
% maxPress
% maxCAD = CAD(I)
m = diff(Press)./diff(CAD);
MRR_1100_95_F76 = max(m);
hold on

[v,Press,vt] = xlsread('DieselTests.xlsx',4);
```

```
Press = v(1:2:6535,9); CAD = v(1:2:6535,11);
% plot(t,spline(CAD,Press,t),'r')
plot(CAD,Press,'r')
% [maxPress,I] = max(Press);
% maxPress
% maxCAD = CAD(I)
m = diff(Press)./diff(CAD);
MRR_1100_95_GO = max(m);

[v,Press,vt] = xlsread('DieselTests.xlsx',6);
Press = v(1:2:7783,9); CAD = v(1:2:7783,11);
plot(t,spline(CAD,Press,t),'k')
% [maxPress,I] = max(Press);
% maxPress
% maxCAD = CAD(I)
m = diff(Press)./diff(CAD);
MRR_1100_95_G = max(m);

[v,Press,vt] = xlsread('DieselTests.xlsx',9);
Press = v(3,3:4:11); CAD = v(3,2:4:10);
plot(CAD(1),Press(1),'b*',CAD(2),Press(2),'r*',CAD(3),Press(3),'k*')
legend('F-76','0.1wt% GO/F-76 Fuel','0.1wt% G/F-76 Fuel','Peak Pressure
- F-76',...
    'Peak Pressure - 0.1wt% GO/F-76 Fuel','Peak Pressure - 0.1wt% G/F-76
Fuel','Location','northwest')

line([360 360], [0 60])

%%%%%%%%%% 1100 RPMs @ 120 ft-lbs Torque %%%%%%%%%%
figure;
[v,Press,vt] = xlsread('DieselTests.xlsx',2);
Press = v(1:2:8283,13); CAD = v(1:2:8283,15);
plot(t,spline(CAD,Press,t),'b')
title('Engine Speed: 1100 RPMs   Torque: 120 ft-lbs')
ylabel('Pressure')
xlabel('Crank Angle Degrees')
xlim([180 540]); ylim([0 60]);
% [maxPress,I] = max(Press);
% maxPress
% maxCAD = CAD(I)
m = diff(Press)./diff(CAD);
MRR_1100_120_F76 = max(m);
hold on

[v,Press,vt] = xlsread('DieselTests.xlsx',4);
Press = v(1:2:9591,13); CAD = v(1:2:9591,15);
plot(t,spline(CAD,Press,t),'r')
% [maxPress,I] = max(Press);
% maxPress
% maxCAD = CAD(I)
m = diff(Press)./diff(CAD);
MRR_1100_120_GO = max(m);

[v,Press,vt] = xlsread('DieselTests.xlsx',6);
Press = v(1:2:10343,13); CAD = v(1:2:10343,15);
plot(t,spline(CAD,Press,t),'k')
% [maxPress,I] = max(Press);
% maxPress
% maxCAD = CAD(I)
m = diff(Press)./diff(CAD);
MRR_1100_120_G = max(m);
```

```
[v,Press,vt] = xlsread('DieselTests.xlsx',9);
Press = v(4,3:4:11); CAD = v(4,2:4:10);
plot(CAD(1),Press(1),'b*',CAD(2),Press(2),'r*',CAD(3),Press(3),'k*')
legend('F-76','0.1wt% GO/F-76 Fuel','0.1wt% G/F-76 Fuel','Peak Pressure
- F-76',...
    'Peak Pressure - 0.1wt% GO/F-76 Fuel','Peak Pressure - 0.1wt% G/F-76
Fuel','Location','northwest')

line([360 360], [0 60])
```

THIS PAGE INTENTIONALLY LEFT BLANK

# APPENDIX D. STRAIN GAUGE VERSUS CAD MATLAB CODING

```
clear all; close all; clc;

t = 180:0.0001:540;
%%%%%%%%%% 1700 RPMs @ 50 ft-lbs Torque %%%%%%%%%%
%%% Data for F-76 %%%
figure;
% Reads the excel spreadsheet and the specified sheet.
[v,Strain,vt] = xlsread('DieselTests.xlsx',1);
% Strain Gauge and CAD data pulled
Strain = v(1:2:7051,4); CAD = v(1:2:7051,3);
% Plots Stain Gauge (y-axis) versus CAD (x-axis)
plot(t,spline(CAD,Strain-18.051276,t),'b')
title('Engine Speed: 1700 RPMs   Torque: 50 ft-lbs')
ylabel('Strain Gauge')
xlabel('Crank Angle Degrees')
% Specifies the range of data 360 = 0 degrees (CAD), 180 = -180 degrees,
  % and  540 = 180 degrees.
xlim([180 540])
% Specifies the range for strain (dimensionless value) during fuel
cycle.
ylim([-5 60]);
grid on
hold on

% Used to plot the derivative of the plot to determine the Start of
Injection.
% m = diff(Strain)./diff(CAD);
% plot(CAD(2:end),m,'g')

%%% Data for 0.1wt% GO/F-76 Fuel  %%%
[v,Strain,vt] = xlsread('DieselTests.xlsx',3);
Strain = v(1:2:3861,4); CAD = v(1:2:3861,3);
plot(t,spline(CAD,Strain-18.47363,t),'r')
% m = diff(Strain)./diff(CAD);
% plot(CAD(2:end),m,'c')

%%% Data for 0.1wt% GO/F-76 Fuel %%%
[v,Strain,vt] = xlsread('DieselTests.xlsx',5);
Strain = v(1:2:6987,4); CAD = v(1:2:6987,3);
plot(t,spline(CAD,Strain-19.998388,t),'k')
% m = diff(Strain)./diff(CAD);
% plot(CAD(2:end),m,'m')

%%% Start of Injection (SOI) Points %%%
[v,Strain,vt] = xlsread('DieselTests.xlsx',9);
Strain = 0; CAD = 360 - v(5,5:4:13);
plot(CAD(1),Strain,'b*',CAD(2),Strain,'r*',CAD(3),Strain,'k*')
legend('F-76','Derivative of F-76 Plot','0.1wt% GO/F-76 Fuel','0.1wt%
G/F-76 Fuel','SOI - F-76',...
    'SOI - 0.1wt% GO/F-76 Fuel','SOI - 0.1wt% G/F-76 Fuel')

% Plots vertical line at 360 (0 degrees) to show Top Dead Center
line([360 360], [-5 60])


%%%%%%%%%% 1700 RPMs @ 75 ft-lbs Torque %%%%%%%%%%
figure;
```

```
[v,Strain,vt] = xlsread('DieselTests.xlsx',1);
Strain = v(1:2:6013,8); CAD = v(1:2:6013,7);
plot(t,spline(CAD,Strain-23.98732,t),'b')
title('Engine Speed: 1700 RPMs   Torque: 75 ft-lbs')
ylabel('Strain Gauge')
xlabel('Crank Angle Degrees')
xlim([180 540]); ylim([-5 60]);
grid on
hold on
% m = diff(Strain)./diff(CAD);
% plot(CAD(2:end),m)

[v,Strain,vt] = xlsread('DieselTests.xlsx',3);
Strain = v(1:2:4233,8); CAD = v(1:2:4233,7);
plot(t,pchip(CAD,Strain-13.14215,t),'r')
% m = diff(Strain)./diff(CAD);
% plot(CAD(2:end),m)


[v,Strain,vt] = xlsread('DieselTests.xlsx',5);
Strain = v(1:2:4291,8); CAD = v(1:2:4291,7);
plot(CAD,Strain-20.80007,'k')
% m = diff(Strain)./diff(CAD);
% plot(CAD(2:end),m)

[v,Strain,vt] = xlsread('DieselTests.xlsx',9);
Strain = 0; CAD = 360 - v(6,5:4:13);
plot(CAD(1),Strain,'b*',CAD(2),Strain,'r*',CAD(3),Strain,'k*')
legend('F-76','0.1wt% GO/F-76 Fuel','0.1wt% G/F-76 Fuel','SOI - F-
76',...
    'SOI - 0.1wt% GO/F-76 Fuel','SOI - 0.1wt% G/F-76 Fuel')

line([360 360], [-5 60])

%%%%%%%%%% 1700 RPMs @ 95 ft-lbs Torque %%%%%%%%%%%
figure;
[v,Strain,vt] = xlsread('DieselTests.xlsx',1);
Strain = v(1:2:7245,12); CAD = v(1:2:7245,11);
plot(t,spline(CAD,Strain-23.9824,t),'b')
title('Engine Speed: 1700 RPMs   Torque: 95 ft-lbs')
ylabel('Strain Gauge')
xlabel('Crank Angle Degrees')
xlim([180 540]); ylim([-5 60]);
grid on
hold on
% m = diff(Strain)./diff(CAD);
% plot(CAD(2:end),m)


[v,Strain,vt] = xlsread('DieselTests.xlsx',3);
Strain = v(1:2:5089,12); CAD = v(1:2:5089,11);
plot(CAD,Strain-11.99684,'r')
% m = diff(Strain)./diff(CAD);
% plot(CAD(2:end),m)

[v,Strain,vt] = xlsread('DieselTests.xlsx',5);
Strain = v(1:2:6917,12); CAD = v(1:2:6917,11);
plot(t,spline(CAD,Strain-21.761726,t),'k')
% m = diff(Strain)./diff(CAD);
% plot(CAD(2:end),m)
```

```
[v,Strain,vt] = xlsread('DieselTests.xlsx',9);
Strain = 0; CAD = 360 - v(7,5:4:13);
plot(CAD(1),Strain,'b*',CAD(2),Strain,'r*',CAD(3),Strain,'k*')
legend('F-76','0.1wt% GO/F-76 Fuel','0.1wt% G/F-76 Fuel','SOI - F-
76',...
    'SOI - 0.1wt% GO/F-76 Fuel','SOI - 0.1wt% G/F-76 Fuel')

line([360 360], [-5 60])

%%%%%%%%%% 1700 RPMs @ 120 ft-lbs Torque %%%%%%%%%%
figure;
[v,Strain,vt] = xlsread('DieselTests.xlsx',1);
Strain = v(1:2:6133,16); CAD = v(1:2:6133,15);
plot(t,spline(CAD,Strain-16.28205,t),'b')
title('Engine Speed: 1700 RPMs   Torque: 120 ft-lbs')
ylabel('Strain Gauge')
xlabel('Crank Angle Degrees')
xlim([180 540]); ylim([-5 60]);
grid on
hold on
% m = diff(Strain)./diff(CAD);
% plot(CAD(2:end),m)


[v,Strain,vt] = xlsread('DieselTests.xlsx',3);
Strain = v(1:2:4200,16); CAD = v(1:2:4200,15);
plot(CAD,Strain-16.47796,'r')
% m = diff(Strain)./diff(CAD);
% plot(CAD(2:end),m)

[v,Strain,vt] = xlsread('DieselTests.xlsx',5);
Strain = v(1:2:7235,16); CAD = v(1:2:7235,15);
plot(t,spline(CAD,Strain-21.996702,t),'k')
% m = diff(Strain)./diff(CAD);
% plot(CAD(2:end),m)

[v,Strain,vt] = xlsread('DieselTests.xlsx',9);
Strain = 0; CAD = 360 - v(8,5:4:13);
plot(CAD(1),Strain,'b*',CAD(2),Strain,'r*',CAD(3),Strain,'k*')
legend('F-76','0.1wt% GO/F-76 Fuel','0.1wt% G/F-76 Fuel','SOI - F-
76',...
    'SOI - 0.1wt% GO/F-76 Fuel','SOI - 0.1wt% G/F-76 Fuel')

line([360 360], [-5 60])

%%%%%%%%%%%%%%%%%%%%%%%%%%%%%%%%%%%%%%%%%%%%%%%%%%%%%%%%%%%%%%%%%%%%%%%%%%%%%%%

%%%%%%%%%% 1100 RPMs @ 50 ft-lbs Torque %%%%%%%%%%
figure;
[v,Strain,vt] = xlsread('DieselTests.xlsx',2);
Strain = v(1:2:9927,4); CAD = v(1:2:9927,3);
plot(t,spline(CAD,Strain-16.64707,t),'b')
title('Engine Speed: 1100 RPMs   Torque: 50 ft-lbs')
ylabel('Strain Gauge')
xlabel('Crank Angle Degrees')
xlim([180 540]); ylim([-5 60]);
grid on
hold on
m = diff(Strain)./diff(CAD);
plot(CAD(2:end),m)
```

```
[v,Strain,vt] = xlsread('DieselTests.xlsx',4);
Strain = v(1:2:3961,4); CAD = v(1:2:3961,3);
plot(CAD,Strain-15.593468,'r')
% m = diff(Strain)./diff(CAD);
% plot(CAD(2:end),m)

[v,Strain,vt] = xlsread('DieselTests.xlsx',6);
Strain = v(1:2:10997,4); CAD = v(1:2:10997,3);
plot(t,spline(CAD,Strain-27.422533,t),'k')
% m = diff(Strain)./diff(CAD);
% plot(CAD(2:end),m)

[v,Strain,vt] = xlsread('DieselTests.xlsx',9);
Strain = 0; CAD = 360 - v(1,5:4:13);
plot(CAD(1),Strain,'b*',CAD(2),Strain,'r*',CAD(3),Strain,'k*')
legend('F-76','0.1wt% GO/F-76 Fuel','0.1wt% G/F-76 Fuel','SOI - F-
76',...
    'SOI - 0.1wt% GO/F-76 Fuel','SOI - 0.1wt% G/F-76 Fuel')

line([360 360], [-5 60])

%%%%%%%%%%% 1100 RPMs @ 75 ft-lbs Torque %%%%%%%%%%%
figure;
[v,Strain,vt] = xlsread('DieselTests.xlsx',2);
Strain = v(1:2:6885,8); CAD = v(1:2:6885,7);
% plot(t,pchip(CAD,Press,t),'b')
plot(CAD,Strain-23.51281,'b')
title('Engine Speed: 1100 RPMs   Torque: 75 ft-lbs')
ylabel('Strain Gauge')
xlabel('Crank Angle Degrees')
xlim([180 540]); ylim([-5 60]);
grid on
hold on
% m = diff(Strain)./diff(CAD);
% plot(CAD(2:end),m)

[v,Strain,vt] = xlsread('DieselTests.xlsx',4);
Strain = v(1:2:10895,8); CAD = v(1:2:10895,7);
plot(t,spline(CAD,Strain-11.897199,t),'r')
% m = diff(Strain)./diff(CAD);
% plot(CAD(2:end),m)

[v,Strain,vt] = xlsread('DieselTests.xlsx',6);
Strain = v(1:2:10035,8); CAD = v(1:2:10035,7);
plot(t,spline(CAD,Strain-31.030337,t),'k')
% m = diff(Strain)./diff(CAD);
% plot(CAD(2:end),m)

[v,Strain,vt] = xlsread('DieselTests.xlsx',9);
Strain = 0; CAD = 360 - v(2,5:4:13);
plot(CAD(1),Strain,'b*',CAD(2),Strain,'r*',CAD(3),Strain,'k*')
legend('F-76','0.1wt% GO/F-76 Fuel','0.1wt% G/F-76 Fuel','SOI - F-
76',...
    'SOI - 0.1wt% GO/F-76 Fuel','SOI - 0.1wt% G/F-76 Fuel')

line([360 360], [-5 60])

%%%%%%%%%%% 1100 RPMs @ 95 ft-lbs Torque %%%%%%%%%%%
figure;
[v,Strain,vt] = xlsread('DieselTests.xlsx',2);
Strain = v(1:2:10681,12); CAD = v(1:2:10681,11);
```

```
plot(t,spline(CAD,Strain-27.54128,t),'b')
title('Engine Speed: 1100 RPMs   Torque: 95 ft-lbs')
ylabel('Strain Gauge')
xlabel('Crank Angle Degrees')
xlim([180 540]); ylim([-5 60]);
grid on
hold on
% m = diff(Strain)./diff(CAD);
% plot(CAD(2:end),m)

[v,Strain,vt] = xlsread('DieselTests.xlsx',4);
Strain = v(1:2:6535,12); CAD = v(1:2:6535,11);
plot(CAD,Strain-17.104163,'r')
% m = diff(Strain)./diff(CAD);
% plot(CAD(2:end),m)

[v,Strain,vt] = xlsread('DieselTests.xlsx',6);
Strain = v(1:2:7783,12); CAD = v(1:2:7783,11);
plot(t,spline(CAD,Strain-31.590552,t),'k')
% m = diff(Strain)./diff(CAD);
% plot(CAD(2:end),m)

[v,Strain,vt] = xlsread('DieselTests.xlsx',9);
Strain = 0; CAD = 360 - v(3,5:4:13);
plot(CAD(1),Strain,'b*',CAD(2),Strain,'r*',CAD(3),Strain,'k*')
legend('F-76','0.1wt% GO/F-76 Fuel','0.1wt% G/F-76 Fuel','SOI - F-
76',...
    'SOI - 0.1wt% GO/F-76 Fuel','SOI - 0.1wt% G/F-76 Fuel')

line([360 360], [-5 60])

%%%%%%%%%% 1100 RPMs @ 120 ft-lbs Torque %%%%%%%%%%
figure;
[v,Strain,vt] = xlsread('DieselTests.xlsx',2);
Strain = v(1:2:8283,16); CAD = v(1:2:8283,15);
plot(t,spline(CAD,Strain-29.42998,t),'b')
title('Engine Speed: 1100 RPMs   Torque: 120 ft-lbs')
ylabel('Strain Gauge')
xlabel('Crank Angle Degrees')
xlim([180 540]); ylim([-5 60]);
grid on
hold on
% m = diff(Strain)./diff(CAD);
% plot(CAD(2:end),m)

[v,Strain,vt] = xlsread('DieselTests.xlsx',4);
Strain = v(1:2:9591,16); CAD = v(1:2:9591,15);
plot(t,spline(CAD,Strain-20.058725,t),'r')
% m = diff(Strain)./diff(CAD);
% plot(CAD(2:end),m)

[v,Strain,vt] = xlsread('DieselTests.xlsx',6);
Strain = v(1:2:10343,16); CAD = v(1:2:10343,15);
plot(t,spline(CAD,Strain-29.394644,t),'k')
% m = diff(Strain)./diff(CAD);
% plot(CAD(2:end),m)

[v,Strain,vt] = xlsread('DieselTests.xlsx',9);
Strain = 0; CAD = 360 - v(4,5:4:13);
plot(CAD(1),Strain,'b*',CAD(2),Strain,'r*',CAD(3),Strain,'k*')
legend('F-76','0.1wt% GO/F-76 Fuel','0.1wt% G/F-76 Fuel','SOI - F-
```

```
76',...
    'SOI - 0.1wt% GO/F-76 Fuel','SOI - 0.1wt% G/F-76 Fuel')

line([360 360], [-5 60])
```

# APPENDIX E. MAX RATE OF RELEASE MATLAB CODING

```
%% Max Rate of Release
clear all; close all; clc;
[v,LAM,vt] = xlsread('DieselTests.xlsx',9);
LAM = v(:,4:4:12);
LAM_1100 = [LAM(1,1) LAM(1,2) LAM(1,3);
            LAM(2,1) LAM(2,2) LAM(2,3);
            LAM(3,1) LAM(3,2) LAM(3,3);
            LAM(4,1) LAM(4,2) LAM(4,3);]
LAM_1700 = [LAM(5,1) LAM(5,2) LAM(5,3);
            LAM(6,1) LAM(6,2) LAM(6,3);
            LAM(7,1) LAM(7,2) LAM(7,3);
            LAM(8,1) LAM(8,2) LAM(8,3);]
T = [50, 75, 95, 120];

figure;
bar(T,LAM_1100);
title('Engine Speed: 1100 RPMs')
xlabel('Torque [ft-lbs]'); ylabel('Max Rate of Release');
legend('F-76','0.1wt% GO/F-76 Fuel','0.1wt% G/F-76
Fuel','Location','northwest')
ylim([0 12])

figure;
bar(T,LAM_1700)
title('Engine Speed: 1700 RPMs')
xlabel('Torque [ft-lbs]'); ylabel('Max Rate of Release');
legend('F-76','0.1wt% GO/F-76 Fuel','0.1wt% G/F-76
Fuel','Location','northwest')
```

THIS PAGE INTENTIONALLY LEFT BLANK

# APPENDIX F. LAMBDA VALUE MATLAB CODING

```
%% Lambda Values

clear all; close all; clc;
[v,LAM,vt] = xlsread('DieselTests.xlsx',10);
LAM = v(:,2:4);
LAM_1100 = [LAM(1,1) LAM(1,2) LAM(1,3);
            LAM(2,1) LAM(2,2) LAM(2,3);
            LAM(3,1) LAM(3,2) LAM(3,3);
            LAM(4,1) LAM(4,2) LAM(4,3);]
LAM_1700 = [LAM(5,1) LAM(5,2) LAM(5,3);
            LAM(6,1) LAM(6,2) LAM(6,3);
            LAM(7,1) LAM(7,2) LAM(7,3);
            LAM(8,1) LAM(8,2) LAM(8,3);]
T = [50, 75, 95, 120];

figure;
bar(T,LAM_1100);
title('Engine Speed: 1100 RPMs')
xlabel('Torque [ft-lbs]'); ylabel('Lambda Values');
legend('F-76','0.1wt% GO/F-76 Fuel','0.1wt% G/F-76
Fuel','Location','northeast')
ylim([0 10])

figure;
bar(T,LAM_1700)
title('Engine Speed: 1700 RPMs')
xlabel('Torque [ft-lbs]'); ylabel('Max Rate of Release');
legend('F-76','0.1wt% GO/F-76 Fuel','0.1wt% G/F-76
Fuel','Location','northeast')
ylim([0 10])
```

THIS PAGE INTENTIONALLY LEFT BLANK

# APPENDIX G. HEAT OF RELEASE MATLAB CODING

The following coding was developed by Professor Patrick Caton, Mechanical Engineering professor at the United States Naval Academy. It was used in the determination of the heat of release data for this research.

```
% basic_data_analysis
% --------------------
% This is where you start to analyze engine data. After setting all
initial
% conditions and parameters in the init_cond_param function, establish
the
% data file name or the range of data files to analyze in the header
lines
% of this function, then call it from the command line.
%
% 2/19/10: modified for use with new diesel CFR data acquisition system,
% utilizing 360 CAD encoder, similar to HMMWV system (Caton)
%
% 3/1/10: determination of premixed fraction and plot output added
% (Mathes/Ries)
%
% 3/15/10: premixed fraction calculation modified; SOI determination
corrected (Caton)
%
% 3/18/10: edited energy_release function and moved PF calculation into
it;
% the problem was that only the final cycle's energy release profile was
% being used to calculate PF metrics.
clear all;
close all;

for file_index = 22:22
    filename = num2str(file_index);

    % Establish initial conditions and parameters
    [icp] = init_cond_param();

    % Read in raw data
    data = dlmread(filename);
    disp(sprintf('Data read from file %s.', filename));

    % Extract data vectors
    rawP = data(:,icp.Pcol);
    rawCAD = data(:,icp.CADcol);
    rawINJ = data(:,icp.INJcol);

    % Analyze pressure data
    cycle_num = 0;
    [cycle_data, avg_data] = raw_data_analysis(rawP, rawCAD, rawINJ,
cycle_num, icp);
    disp(sprintf('Analyzed raw data for file %s.', filename));

    % Calculate energy release metrics
    valid_indices = [];
    for k=1:length(cycle_data)
```

```
        disp(sprintf('Energy release calculations for cycle #%d.', k));
        cycle = cycle_data{k};
        [energy_release] = energy_release_analysis(cycle(:,1),
cycle(:,3), cycle(:,2), avg_data.speed(k), avg_data.SOI(k), icp);
        if energy_release.err==1
            continue;
        end
        ign_delay(k) = energy_release.ign_delay;
        comb_dur(k) = energy_release.comb_dur;
        SOC(k) = energy_release.SOC;
        CAD5(k) = energy_release.CAD5;
        CAD10(k) = energy_release.CAD10;
        CAD50(k) = energy_release.CAD50;
        CAD90(k) = energy_release.CAD90;
        PF_time(k) = energy_release.PF_time;
        PF_energy(k) = energy_release.PF_energy;
        delta_Qch(k) = energy_release.delta_Qch;
        valid_indices(length(valid_indices)+1) = k;
        dQch{k} = energy_release.dQch_avg;
    end

    % Calculate average energy release data
    ign_delay_avg = careful_avg(ign_delay(valid_indices));
    comb_dur_avg = careful_avg(comb_dur(valid_indices));
    SOCavg = careful_avg(SOC(valid_indices));
    CAD5avg = careful_avg(CAD5(valid_indices));
    CAD10avg = careful_avg(CAD10(valid_indices));
    CAD50avg = careful_avg(CAD50(valid_indices));
    CAD90avg = careful_avg(CAD90(valid_indices));
    delta_Qch_avg = careful_avg(delta_Qch(valid_indices));
    PF_time_avg = careful_avg(PF_time(valid_indices));
    PF_energy_avg = careful_avg(PF_energy(valid_indices));

    % Shift combustion metrics by 360 CAD
    SOCavg_new = SOCavg-360;
    SOIavg_new = avg_data.SOIavg -360;
    CAD10avg_new = CAD10avg-360;
    CAD50avg_new = CAD50avg-360;
    CAD90avg_new = CAD90avg-360;
    CAD_new = energy_release.CAD-360;

    % Find indices corresponding to SOC, CAD10/50/90, and SOI
    SOC_index = fdvec(CAD_new, SOCavg_new);
    CAD10_index = fdvec(CAD_new, CAD10avg_new);
    CAD50_index = fdvec(CAD_new, CAD50avg_new);
    CAD90_index = fdvec(CAD_new, CAD90avg_new);
    SOI_index = fdvec(CAD_new, SOIavg_new);

    % Record compiled data
    compiled_data(file_index,:) = [avg_data.GMEPavg avg_data.peakpavg
avg_data.aopavg avg_data.maxrravg SOIavg_new SOCavg_new CAD10avg_new
CAD50avg_new CAD90avg_new PF_time_avg PF_energy_avg ign_delay_avg];

    % Save data arrays as they are built in case loop breaks down
    save data_backup
end
```

# LIST OF REFERENCES


[1] Energy, environment, and climate change. (n.d.). Department of the Navy. [Online]. Available: http://greenfleet.dodlive.mil,. Accessed 1 May 2015.

[2] NDW host energy management course. (n.d.). Department of the Navy. [Online]. Available: http://www.navy.mil/submit/display.asp?story_id=87104. Accessed 25 May 2015.

[3] Task force energy. (n.d.). Department of the Navy. [Online]. Available: http://greenfleet.dodlive.mil/energy/task-force-energy/. Accessed 25 May 2015.

[4] Marines enforce energy warrior ethos. (n.d.). Department of the Navy. [Online]. Available: https://www.dvidshub.net/news/156116/marines-enforce-energy-warrior-ethos#.VWP2tmCaFby. Accessed 6 Mar 2015.

[5] The Department of the Navy's energy goals. (n.d.). Department of the Navy. [Online]. Available: http://www.navy.mil/features/Navy_EnergySecurity.pdf;. Accessed 1 May 2015.

[6] Great green fleet. (n.d.). Department of the Navy. [Online]. Available: http://greenfleet.dodlive.mil/energy/great-green-fleet/. Accessed 25 May 2015.

[7] Department of the Navy's Energy Program for Security and Independence. (n.d.). Department of the Navy. [Online]. Available: http://greenfleet.dodlive.mil/files/2010/04/Naval_Energy_Strategic_Roadmap_100710.pdf. Accessed 1 May 2015.

[8] Navy tests biofuel-powered "green hornet." (n.d.). Department of the Navy. [Online]. Available: http://www.navy.mil/submit/display.asp?story_id=52768. Accessed 1 Mar 2015.

[9] N. F. Vilardi, "Graphitic oxide and graphene as enhancers for combustible mixtures," M.S. thesis, Dept. of Mech and Aerosp. Eng. Naval Postgraduate School, Monterey, CA, 2014.

[10] H. He *et al.*, "Solid-state NMR studies of the structure of graphite oxide," *J. Phys. Chem.*, vol. 100, Sep. 1996.

[11] A. Lerf *et al.*, "C and H HAS NMR studies of graphite oxide and its chemically modified derivatives," *Solid State Ionics*, vol. 101–103, pp. 857–863, 1997.

[12] A. Bannov *et al.*, "Synthesis and studies of properties of graphite oxide and thermally expanded graphite," *Pleiades Pub. Ltd.*, vol. 50, pp. 183–190, 2014.

[13] H. Jeong *et al.*, "Tailoring the characteristics of graphite oxides by different oxidation times," *J. Phys. D. Appl. Phys.*, vol. 42, Mar. 2009.

[14] G. Titelman *et al.*, "Characteristics and microstructure of aqueous colloidal dispersions of graphite oxide," *Science Direct*, vol. 43, pp. 641–649, 2004.

[15] W. Gao *et al.*, "Engineering graphite oxide materials for application in water purification," *ACS Appl. Mater. Interf.*, vol. 3, Jun. 2011.

[16] S. Sarkar *et al.*, "Magnetic properties of graphite oxide and reduced graphene oxide," *Physica*, vol. 64, pp. 78–82, Nov. 2014.

[17] C. Gomez-Navarro *et al.*, "Electronic transport properties of individual chemically reduced graphene oxide sheets," *Nano Lett.*, vol. 7, pp. 3499–3503, Nov. 2007.

[18] A. R. Maxson, "Novel synthesis and characterization of inorganic fullerene type WS2 and graphene hybrids," M.S. thesis, Dept. of Mech and Aerosp. Eng. Naval Postgraduate School, Monterey, CA, 2013.

[19] T. Lambert *et al.*, "Graphite oxide as a precursor for the synthesis of disordered graphenes using the aerosol-through-plasma method," *Carbon*, vol. 48, pp. 4081–4089, 2010.

[20] J. Sabourin *et al.*, "Functionalized graphene sheet colloids for enhanced fuel/propellant combustion," *ACS Nano*, vol. 3, pp. 3945–3954, 2009.

[21] J. Li *et al.*, "The preparation of graphene oxide and its derivatives and their application in bio-tribological systems," *Lubricants*, vol. 2, pp. 137–161, 2014.

[22] T. Chen *et al.*, "High throughput exfoliation of graphene oxide from expanded graphite with assistance of strong oxidant in modified Hummers method," in *8th China Intl. Nanoscience and Technol. Symp.*, vol. 188, 2009.

[23] J. Pyun, "Graphene oxide as catalyst: Application of carbon materials beyond nanotechnology," *Angew. Chem. Int. Edit.*, vol. 50, pp. 46–48, 2011.

[24] M. Stoller *et al.*, "Graphene-based ultracapacitors," *Nano Lett.*, vol. 8, pp. 3498–3502, 2008.

[25] Y. Lin *et al.*"Dual-gate graphene FETs with f(T) of 50 Ghz," *IEEE Electron Device Lett.*, vol. 31, pp. 68–70, 2010.

[26] V. Yong and J. Tour, "Theoretical efficiency of nanostructured graphene-based photovoltaics," *Small*, vol. 6, pp. 313–318, 2010.

[27] M. Liang and L. Zhi, “Graphene-based electrode materials for rechargeable lithium batteries,” *J. Mater. Chem.*, vol. 19, pp. 5871–5878, 2009.

[28] S. Guo *et al.*, “Three-dimensional Pt-on-Pt bimetallic nanodendrites supported on graphene nanosheets: Facile synthesis and used as an advanced nanoelectrocatalyst for methanol oxidation,” *ACS Nano*, vol. 4, pp. 547–555, 2010.

[29] Z. Liu *et al.*, “Organic photovoltaic devices based on a novel acceptor material: Graphene,” *Adv Mater*, vol. 20, pp. 3924, 2008.

[30] A. Balandin, “Thermal properties of graphene and nanostructured carbon materials,” *Nature Materials*, vol. 10, pp. 569–581, 2011.

[31] Fuel, Naval Distillate, 14 Aug 2012. Naval Sea Systems Command. [Online] Available: https://www.wbdg.org/ccb/FEDMIL/dtl16884m.pdf.

[32] F-76 Military Diesel Material Safety Data Sheet, 28 May 2015. CITGO. [Online]. Available: http://www.docs.citgo.com/msds_pi/13176.pdf.

[33] N. Ladommatos *et al.*, “The effect of fuel cetane improver on diesel pollutant emissions,” *ELSEVIER*, vol. 75, pp. 8–14, 1996, 1995.

[34] V. Hosseini *et al.*, “Effects of different cetane number enhancement strategies on HCCl combustion and emissions,” *SAGE*, vol. 12, pp. 89–108, 2011.

[35] A. Rode *et al.*, “Synthesis and evaluation of stearic acid derivatives as cetane number improvers,” *Korean Chemical Society*, vol. 32, pp. 1965–1969, 2011.

[36] X. Lü *et al.*, “Improving the combustion and emissions of direct injection compression ignition engines using oxygenated fuel additives combined with a cetane number improver,” *Energy & Fuels*, vol. 19, pp. 1879–1888, 2005.

[37] Piston (Reciprocating) Engine Power Plants. (n.d.). Woodbank Communications Ltd. [Online]. Available: http://www.mpoweruk.com/piston_engines.htm. Accessed 25 May 2015.

[38] Graphite Oxide. (n.d.). ACS Material. [Online]. Available: http://www.acsmaterial.com/product.asp?cid=27&id=16. Accessed 6 May 2015.

[39] Single Layer Graphene. (n.d.). ACS Material. [Online]. Available: http://www.acsmaterial.com/product.asp?cid=25&id=20. Accessed 6 May 2015.

[40] W. Hummers and R. Offeman, “Preparation of graphite oxide,” *J. Am. Chem. Soc.*, vol. 80, p. 1339, Mar. 1958.

[41] D. Marcano *et al.*, "Improved synthesis of graphene oxide," ACSNano, vol. 4, pp. 4806–4814, 2010.

[42] Nitrogen 601(E200) 20 PSIG. (n.d.). Matheson. [Online]. Available: http://www.mathesongas.com/pdfs/flowchart/601%20%28E200%29/NITROGEN%20601%28E200%29%20GLASS%2020%20PSIG.pdf. Accessed 6 May 2015.

[43] S. Menon, "Thermal analysis," presented at NPS, MS4312 Characterization of Advanced Materials, Monterey, CA, Nov. 2014.

[44] J. Petersen *et al.*, "Combustion characterization and ignition delay modeling of low- and high-cetane alternative diesel fuels in a marine diesel engine," *Energy & Fuels*, vol. 28, pp. 5463–5471, 2014.

[45] T. Blanton and D. Majundar, "X-ray diffraction characterization of polymer intercalated graphite oxide," *ICDD-JCPDS*, pp. 186–193, 2014.

[46] M. Mowry *et al.*, "In situ raman spectroscopy and thermal analysis of the formation of nitrogen-doped graphene from urea and graphite oxide," *Rsc Advances*, vol. 3, pp. 21763–21775, 2013.

[47] S. Wakeland *et al.*, "Production of graphene from graphite oxide using urea as expansion-reduction agent," *Carbon*, vol. 48, pp. 3463–3470, 2010.

[48] Lambda as a Diagnostic Tool. (n.d.). Austin Community College. [Online]. Available: http://www.austincc.edu/wkibbe/lambda.htm. Accessed 25 May 2015.

[49] Sigma-Aldrich Material Pricing. (n.d.). Signma-Aldrich. [Online]. Available: http://www.sigmaaldrich.com/united-states.html. Accessed 6 May 2015.

[50] J. T. Baker Analyzed ACS Reagent Material Pricing. (n.d.). Capitol Scientific. [Online]. Available: http://www.capitolscientific.com/. Accessed 6 May 2015.

[51] Essential Wholesale & Labs Material Pricing. (n.d.). Essential Wholesale & Labs. [Online]. Available: http://www.essentialwholesale.com/. Accessed 6 May 2015.

# INITIAL DISTRIBUTION LIST

1. Defense Technical Information Center
   Ft. Belvoir, Virginia

2. Dudley Knox Library
   Naval Postgraduate School
   Monterey, California
   1.